Review

Metals in Neurobiology: Probing Their Chemistry and Biology with Molecular Imaging

Emily L. Que, Dylan W. Domaille, and Christopher J. Chang

Chem. Rev., **2008**, 108 (5), 1517-1549 • DOI: 10.1021/cr078203u • Publication Date (Web): 22 April 2008

Metals in Neurobiology: Probing Their Chemistry and Biology with Molecular Imaging

Emily L. Que, Dylan W. Domaille, and Christopher J. Chang*

Department of Chemistry, University of California, Berkeley, California 94720

Received October 26, 2007

Contents

* To whom correspondence should be addressed. Phone: (510)642-4704. Fax: (510)642-7301. E-mail: chrischang@berkeley.edu.

1. Introduction

The brain is a singular organ of unique biological complexity that serves as the command center for cognitive and motor function. As such, this specialized system also possesses a unique chemical composition and reactivity at the molecular level. In this regard, two vital distinguishing features of the brain are its requirements for the highest concentrations of metal ions in the body[1,2] and the highest per-weight consumption of body oxygen.[3] In humans, the brain accounts for only 2% of total body mass but consumes 20% of the oxygen that is taken in through respiration.[3] As a consequence of high oxygen demand and cell complexity, distinctly high metal levels pervade all regions of the brain and central nervous system. Structural roles for metal ions in the brain and the body include the stabilization of biomolecules in static (e.g., Mg^{2+} for nucleic acid folds, Zn^{2+} in zinc-finger transcription factors) or dynamic (e.g., Na^+ and K^+ in ion channels, Ca^{2+} in neuronal cell signaling) modes, and catalytic roles for brain metal ions are also numerous and often of special demand.[1,4]

Because of the intimate connection between its unique composition and function, the inorganic chemistry of the brain is inherently rich and remains an open frontier for study. Traditional studies of metals in neurobiology have focused on the chemistry and structural biology of redox-active s-block metal ions, including Na^+, K^+, Mg^{2+}, and Ca^{2+}. Na^+ and K^+ are present in high concentrations in the body (~0.1 M) and possess distinct compartmentalizations, with resting Na^+ levels higher in the extracellular space and K^+ levels higher inside cells.[5] The dynamic partitioning of these metal ions is controlled by ion-specific channels that selectively allow passage of either Na^+ or K^+ in and out of cells. In the brain, the uneven distribution of these metal ions across a given cell membrane creates a potential that enables transmission of information through action of electric currents down the axons of neurons. Along these lines, Ca^{2+} and Mg^{2+} are also key modulators of molecular information transfer within and between cells during neurotransmission.[2] Specific roles that these metal ions play in the brain will not be discussed further in this review, and the reader is referred to other excellent sources regarding the neurobiology of these metal ions.[6–12]

10.1021/cr078203u CCC: $71.00
Published on Web 04/22/2008

Emily L. Que was born in Ithaca, New York, in 1982 and grew up in St. Paul, Minnesota. She attended the University of Minnesota, Twin Cities (B.S. 2004), where she was an undergraduate researcher in the laboratories of Professor Lawrence Que, Jr., and Professor Andreas Stein. Emily was awarded a Barry M. Goldwater scholarship for her accomplishments in undergraduate research. Emily is currently a fourth-year graduate student in the laboratory of Professor Chris Chang at the University of California, Berkeley. Her general research interests lie in the field of bioinorganic chemistry, and her doctoral research concerns the development of "smart" MRI contrast agents for sensing applications.

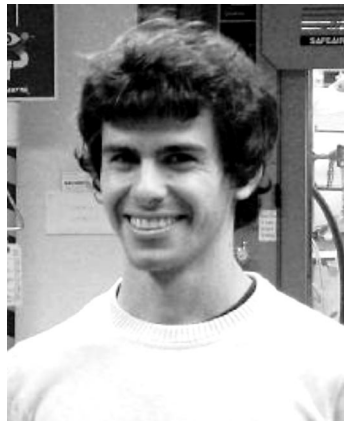

Dylan W. Domaille received his undergraduate education at the University of Oregon and performed research under the guidance of Professor James E. Hutchison with an interlude in the laboratory of Professor James R. Williamson at the Scripps Research Institute. He entered the chemical biology Ph.D program at the University of California, Berkeley, in 2005 and joined the laboratory of Professor Chris Chang. His graduate studies are focused on the design, synthesis, characterization, and applications of copper-responsive fluorophores for investigating the role of copper in biological processes, with a particular emphasis on neuronal systems.

Christopher J. Chang was born in Ames, Iowa, in 1974 and grew up in Indiana and California. He received his B.S. and M.S. degrees from Caltech in 1997, working with Prof. Harry Gray on the electronic structures of metal−nitrido and metal−oxo salen complexes. After spending a year as a Fulbright scholar in Strasbourg, France, with Dr. Jean-Pierre Sauvage in the area of chemical topology, Chris was a NSF and Merck predoctoral fellow at MIT and received his Ph.D. in 2002 under the supervision of Prof. Dan Nocera, where his thesis focused on the application of proton-coupled electron transfer as a mechanistic platform for developing catalytic oxygen reduction and evolution reactions. He stayed at MIT as a Jane Coffins Childs postdoctoral fellow with Prof. Steve Lippard from 2002 to 2004, working on zinc sensing for neuroscience applications, and then began his independent career at UC Berkeley in July 2004. Chris' research laboratory currently uses inorganic chemistry, organic chemistry, and chemical biology approaches to study problems in neuroscience and energy research.

Less thoroughly studied are the roles of d-block metals in the brain. Zinc, iron, copper, and related d-block metals are emerging as significant players in both neurophysiology and neuropathology, particularly with regard to aging and neurodegenerative diseases. Because the concentrations of these d-block metals in brain tissue are up to 10 000-fold higher than common neurotransmitters and neuropeptides, referring to these essential brain nutrients as trace elements is a clear misnomer.[1] Not only do these metals serve as components of various proteins and enzymes essential for normal brain function, but their labile forms, particularly those of Zn^{2+} and $Cu^{+/2+}$, are also connected to specialized brain activities. In this context, labile metal ion pools can possess protein or small molecule ligands or both that can be readily exchanged between different ligand sets.

The far-reaching connections of inorganic chemistry to unexplored aspects of brain function, aging, and disease have prompted demand for new methods to study metal ion function, misregulation, or both within intact, living samples. In this regard, molecular imaging with metal-responsive small-molecule probes coupled to optical fluorescence imaging (OI) and magnetic resonance imaging (MRI) modalities is emerging as a powerful approach to interrogating metal ion chemistry from the subcellular to the organismal level. These methods offer the potential for real-time detection in living systems with high spatial resolution, oxidation state specificity, and bioavailability information that is difficult or impossible to obtain using conventional techniques such as atomic absorption spectroscopy, radioisotope labeling, histochemical techniques, and inductively coupled plasma mass spectrometry. Seminal work in fluorescent Ca^{2+} sensors by Tsien[13] and MR (magnetic resonance)-based enzyme reporters by Meade and co-workers[14] provide success stories that presage the potential impact of applying molecular imaging approaches to studies at the inorganic chemistry/neurobiology interface.

In this review, we will provide a brief overview of the field of transition metals in neurobiology, focusing on the contributions of d-block metals zinc, iron, and copper to neurophysiology, aging, and neuropathology, as well as progress in the development of molecular probes for visualizing zinc, iron, and copper ion pools in living environments by fluorescence or magnetic resonance imaging. We note that other essential d-block metals (e.g., Cr, Mn, Co, Ni) not covered by this review are also worthy of further investigation. We will limit our discussion to small-molecule synthetic reagents that have been or can be potentially applied to probe Zn^{2+}, $Fe^{2+/3+}$, and $Cu^{+/2+}$ in biological settings, noting that other platforms such as peptides/proteins, nucleic acids, and materials can provide viable and complementary alternatives for these purposes as well. Tables 1−3 provide a list of properties for selected small-molecule probes for Zn, Fe, and Cu ions.

Table 1. Properties of Fluorescent Zn^{2+} Sensors

probe	K_d for Zn^{2+}	λ_{ex}, nm,[b] free (Zn^{2+})	λ_{em}, nm[a,b] free (Zn^{2+})	Φ free (Zn^{2+})	cellular/membrane partition
1, TSQ		334	495	(0.1)	permeable
2, Zinquin A	0.2 nM	370	490		impermeable, permeable ester
4, TFLZn		360	498		permeable
5	0.55 pM	330	553 (528)	0.03 (0.11)	permeable
6		345	448	(0.26)	permeable
7	0.5 μM	343	450	0.038 (0.88)	
Eu-**8**		262	700 τ = 0.62 (0.62)		
Tb-**8**	0.6 μM	262	545 τ = 1.82 (1.82)		
Tb-**9**	2.6 nM	260	490, 546, 587 τ = (1.45)		
Eu-**10**	59 nM	249, 318, 330 (253, 320)	579, 593, 614 τ = 0.52 (0.58)	0.009 (0.074)	impermeable
Eu-**11**		280	616 τ = 0.99 (0.40)		
12, ZP1	0.7 nM	515 (507)	531 (527)	0.38 (0.87)	permeable
13, ZP2	0.5 nM	498 (490)	522 (517)	0.25 (0.92)	permeable
14, ZP3	0.7 nM	502 (492)	521 (516)	0.15 (0.92)	permeable
15, ZP4	0.65 nM	506 (495)	521 (515)	0.06 (0.34)	permeable
16, ZP5	0.5 nM	504 (495)	520 (517)	0.29 (0.48)	impermeable
17, ZP6	0.5 nM	506 (495)	519 (517)	0.10 (0.34)	impermeable
18, ZP7	0.5 nM	505 (495)	521 (517)	0.04 (0.05)	impermeable
19, ZP8	0.6 nM	500 (489)	516 (510)	0.03 (0.35)	impermeable
20, ZnAF-1	0.78 nM	489 (492)	514	0.022 (0.23)	
21, ZnAF-2	2.7 nM	490 (492)	514	0.023 (0.36)	impermeable, permeable ester
22, ZnAF-1F	2.2 nM	489 (492)	514	0.004 (0.17)	
23, ZnAF-2F	5.5 nM	490 (492)	514	0.006 (0.24)	impermeable, permeable ester
24, FluoZin-3	15 nM	488	515		impermeable, permeable ester
25, RhodZin-3	65 nM	545	575		impermeable, permeable ester
26, BDA	0.1 nM	491	509	0.077 (0.857)	permeable
27, WZS	0.62 nM	449	~550	0.03 (0.19)	permeable
28, NG-DCF	1 μM	492	521		impermeable, permeable ester
29, NG-PDX	30−40 μM	491	520		impermeable, permeable ester
30, FluoZin-1	7.8 μM	491	520		impermeable, permeable ester
31, FluoZin-2	2.1 μM	492	521		impermeable, permeable ester
32, RhodZin-1	23 μM	548	589		impermeable, permeable ester
33, X-RhodZin-1	11 μM	575	604		impermeable, permeable ester
34, ZS5	1.5 μM	497 (490)	522 (517)	0.36 (0.80)	permeable
35, ZP9	0.69 μM	505 (495)	526 (521)	0.02 (0.41)	permeable
36, ZP10	1.9 μM	506 (497)	523 (516)	0.08 (0.33)	permeable
37, QZ1	33 μM	505 (498)	524 (524)	0.024 (0.78)	permeable
38, QZ2	41 μM	499 (489)	520 (518)	0.005 (0.70)	permeable
39, ZnAF-2M	38 nM	490 (492)	514	0.034 (0.27)	
40, ZnAF-2MM	3.9 μM	490 (493)	514	0.006 (0.10)	
41, ZnAF-3	0.79 μM	490 (493)	514	0.029 (0.38)	impermeable, permeable ester
42, ZnAF-4	25 μM	490 (492)	514	0.012 (0.22)	
43, ZnAF-5	0.69 mM	490 (492)	514	0.004 (0.21)	
44, DPA-Cy	63 nM	730	780	0.02 (0.41)	permeable
45, FuraZin	3.4 μM	378 (330) R_{max}/R_{min} > 150	510 (510)		impermeable, permeable ester
46, IndoZin	3.0 μM	350 (350)	480 (395) R_{max}/R_{min} > 100		impermeable, permeable ester
47, ZnAF-R1	0.79 nM	359 (329)	532 (528)	0.088 (0.031)	
48, ZnAF-R2	2.8 nM	365 (335) R_{max}/R_{min} = 4	495 (495)	0.17 (0.10)	impermeable, permeable ester
49, CZ1	0.25 nM	445, 505	488, 534 R_{max}/R_{min} > 8	0.04 (apo CZ1) 0.21 (0.64) ZP fragment free (Zn^{2+})	permeable
51	32 μM	299 (406)	460 (406) R_{max}/R_{min} = 19	0.23 (0.22)	
52	0.6 nM	305 (297)	471 (415) R_{max}/R_{min} = 30	0.28 (0.17)	
53	0.8 pM	305 (334)	460 (406) R_{max}/R_{min} = 82	0.09 (0.21)	
54, Zinbo-5	2.2 nM	337 (376)	407 (433) R_{max}/R_{min} > 30	0.02 (0.10)	permeable
55, ZNP1	0.55 nM	503, 539 (547)	528, 604 (545, 624) R_{max}/R_{min} = 18	0.02 (0.05)	impermeable, permeable ester
56, DIPCY	98 nM	627 (671) R_{max}/R_{min} = 5	758 (765)	0.02 (0.02)	

[a] For luminescent lanthanide sensors (**8**−**11**), excited-state lifetime values (τ) in H_2O are listed with the emission wavelengths. [b] For ratiometric sensors (**45**−**56**), the relative fluorescence excitation or emission ratio change (R_{max}/R_{min}) is listed with the excitation or emission wavelengths.

2. Zinc in Neurobiology

2.1. Basic Aspects of Zinc in the Brain

2.1.1. Tissue Concentrations and Distributions

Zinc is the second most abundant transition metal in the body and its highest concentrations occur in the brain.[15] Levels of zinc in the gray matter, the region of the brain containing neuron cell bodies (~0.5 mM), are on the order of magnesium[1] and are up to 10 000-fold higher in concentration than common organic neurotransmitters. Within brain tissue, zinc is nonuniformly distributed and is most abundant in the hippocampus, amygdala, neocortex, and olfactory bulb regions.[15] Neuronal zinc is partitioned into two main classes: a static Zn^{2+} pool that is tightly bound to various metalloproteins and a labile Zn^{2+} pool that is mobile.[16] Over 90% of the Zn^{2+} found in the brain and the body is classified as static, playing structural roles in transcription factors and

Table 2. Properties of Fluorescent $Fe^{2+/3+}$ Probes

probe	K_d for Fe^{n+}	λ_{ex}, nm, free (Fe^{n+})	λ_{em}, nm,[a] free (Fe^{n+})	Φ free (Fe^{n+})	cellular/membrane partition
			Fe^{2+} Probes		
62, Calcein	~10 fM	486	517		impermeable, permeable ester
63, Phen Green SK	<1 μM	507	532		impermeable, permeable ester
75		358	430		
			Fe^{3+} Probes		
64, Azotobactin	8×10^{-29} M	380	490		
65, FL-DFO		485	535		
66, FL-NBD		475	548		
67		474	538		endocytosed
68		432	470	0.01	permeable
69		416	474		permeable
70		323	464	0.28	permeable
71	6.7 μM	336	412		
72	100 μM	506 (508)	508, 634 (512) $R_{max}/R_{min} = 11$	0.026	
73	316 μM	510	575		
74, FDI	43 μM	510	583		permeable

[a] For ratiometric sensor **72**, the relative fluorescence excitation or emission ratio change (R_{max}/R_{min}) is listed with the excitation or emission wavelengths.

Table 3. Properties of Fluorescent $Cu^{+/2+}$ Probes

probe	K_d for Cu^{n+}	λ_{ex}, nm, free (Cu^{n+})	λ_{em}, nm,[a] free (Cu^{n+})	Φ free (Cu^{n+})	cellular/membrane partition
			Cu^{+} Probes		
76, CTAP-1	40 pM	365	485	0.03 (0.14)	permeable
77, CS1	3.6 pM	540	566 (561)	0.016 (0.13)	permeable
78		325 (328)	388 (415)	0.014 (0.25)	
Eu−**79**		(350)	(615)		
			Cu^{2+} Probes		
80	4.1 μM	497 (501)	509 (513)	(0.0001) 0.25	
81	14.5 μM	520	573 (585)		
82	0.7 μM	451	525 (475) $R_{max}/R_{min} = 14$	0.112 (0.114)	
83		420 (510)	518 (592) $R_{max}/R_{min} = 20$	0.0054 (0.0046)	
84, Rhodamine B hydrazide		(510)	(578)	(0.31)	
85		(495)	(516)	<0.02 (0.95)	
86		(489)	(513)	(0.95)	

[a] For ratiometric sensors (**82** and **83**), the relative fluorescence excitation or emission ratio change (R_{max}/R_{min}) is listed with the excitation or emission wavelengths.

related proteins as well as structural and catalytic roles in enzymes.[16–20] In addition to these tightly bound stores, labile pools of Zn^{2+} are present throughout the brain and central nervous system and are largely localized within the vesicles of zinc-dependent glutamatergic neurons. For example, in the hippocampus, a region of the brain essential for learning and long-term memory storage, Zn^{2+} concentrations can reach up to 300 μM in the mossy fiber boutons of neurons that extend from the dentate gyrus to neurons in the hilar and CA3 fields.[15] Similar input−output systems in the cortex, amygdala, and olfactory bulb also require such "zinc-containing neurons". The abundance and unique cellular localizations of neuronal zinc have stimulated interest in deciphering its contributions to neurophysiology, particularly as a calcium surrogate in specialized brain circuits.

2.1.2. Brain Zinc Homeostasis

The high concentrations and mobility of zinc in the brain necessitate a tightly orchestrated and regulated homeostasis for Zn^{2+} uptake, accumulation, trafficking, and efflux. An overview of homeostatic zinc pathways in brain neurons is summarized in Figure 1. For example, many plausible routes for neuronal Zn^{2+} uptake are available and overlap with Ca^{2+} entry pathways. Included are voltage-gated Ca^{2+} channels, Na^{+}/Ca^{2+} exchangers, *N*-methyl-D-aspartate (NMDA) receptor-gated channels, and channels gated by kainate or 2-amino-5-methyl-4-isoaxazolylpropionate (AMPA) receptors.[19] Moreover, zrt/irt-like (ZIP) proteins can also transport Zn^{2+} and other divalent metal ions (e.g., Fe^{2+}, Mn^{2+}, and Cd^{2+}) across plasma membranes.[21] There are at least 15 of these ZIP transporters present in human cells.

Once inside the neuron, Zn^{2+} ions are shuttled to various subcellular locales. The major class of proteins that direct intracellular Zn^{2+} accumulation and trafficking is the zinc transporter family (ZnTs).[21] These integral membrane proteins are members of the solute carrier 30 family (SLC30) and help maintain intracellular Zn^{2+} homeostasis by promoting Zn^{2+} translocation from the cytosol to organelles or back to the extracellular environment. At least 10 ZnTs have been identified in human cells so far, and each exhibits tissue-specific expression and differential responses to dietary zinc and physiological stimuli.[21] Of these isoforms, ZnT1, -3, and -6 are abundant in the brain and central nervous system, whereas ZnT2, -4, -5, -7, -8, -9, and -10 are largely localized to other tissues. ZnT1 is widely expressed throughout the body and responds to dietary zinc uptake; its mRNA expression is down-regulated in situations of zinc deficiency and up-regulated in times of zinc excess.[22,23] This protein is the only zinc transporter localized to the plasma membrane, where it controls the efflux of Zn^{2+} from the cytosol to the extracellular environment.[21] ZnT2 transports Zn^{2+} into late endosomes,[24,25] and ZnT-5,[26] -6,[27] and -7[28] are associated with Golgi Zn^{2+} transport. ZnT4[29] and ZnT8[30] are involved in trafficking of Zn^{2+} to intracellular vesicles and the functions of ZnT9[31] and ZnT10[32] remain elusive. Of particular importance to zinc neurobiology is ZnT3, which

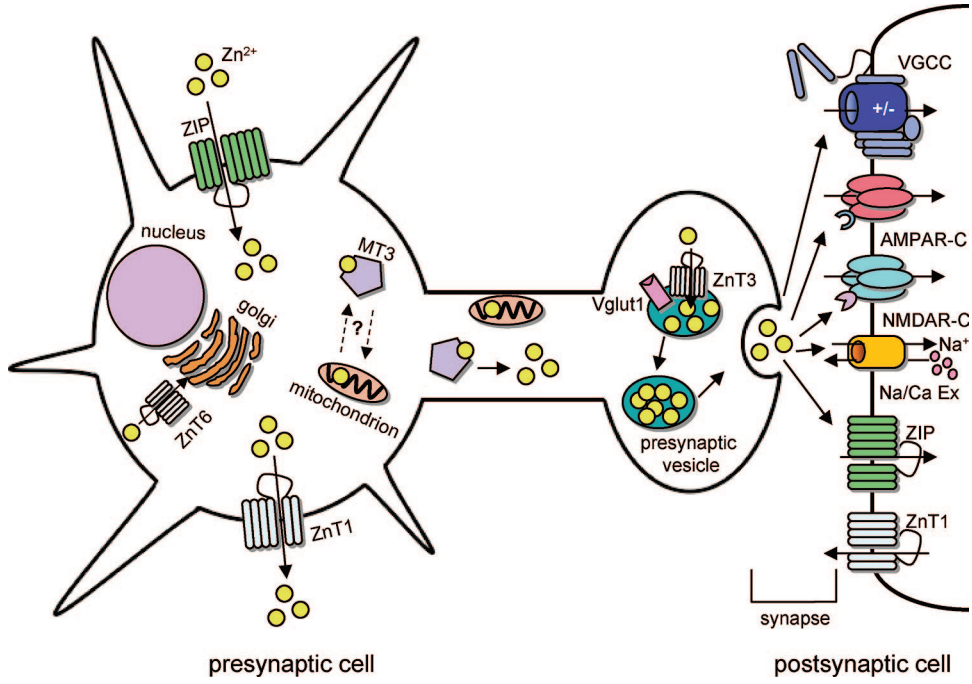

Figure 1. A schematic model for neuronal Zn^{2+} homeostasis. List of abbreviations: AMPAR-C, AMPA receptor-gated channel; MT3, metallothionein-3; Na/Ca Ex, Na^{+}/Ca^{2+} exchanger; NMDAR-C, NMDA receptor-gated channel; VGCC, voltage-gated calcium channel; Vglut1, vesicular glutamate transporter-1; ZIP, zrt/irt-like proteins; ZnT, zinc transporter protein.

is expressed exclusively in the brain and testis. Electron microscopy experiments reveal that this isoform is particularly abundant in brain regions that possess high levels of labile, chelatable Zn^{2+}, including the hippocampus, amygdala, neocortex, and olfactory bulb.[33] The strong spatial correlation between ZnT3 and vesicular pools of labile Zn^{2+}, coupled with the fact that ZnT3 knockout mice show no evidence for chelatable zinc in these regions, suggests a plausible function for ZnT3 in controlling the loading of ionic Zn^{2+} into presynaptic vesicles.[34] In addition to ZnT3, the vesicular glutamate transporter (Vglut1) is also present on Zn^{2+}-containing presynaptic vesicles. These two transporters are functionally coupled; increased Vglut1 expression leads to higher vesicular Zn^{2+} levels, and increased ZnT3 expression leads to higher vesicular glutamate levels in a zinc-dependent fashion.[35]

Another family of proteins that are critical for maintaining neuronal Zn^{2+} homeostasis are the metallothioneins (MTs).[36–38] These cysteine-rich peptides play multiple roles in the brain ranging from the removal of heavy-metal contaminants[17,38,39] to the detoxification of reactive oxygen species (ROS).[37,40–42] More pertinent to the present discussion is that MTs can also serve as cytosolic buffers for neuronal Zn^{2+} by formation of zinc−thiolate clusters. Four major MT isoforms (MT1−4) have been identified in mammals. MT1 and MT2 are widely expressed in all mammalian tissues. MT4 is localized to the stratified squamous epithelium, but little is known about its function.[43] MT3 is a brain-specific metallothionein that is especially abundant in zinc-containing glutamatergic neurons.[44] MT3 and related isoforms typically coordinate seven Zn^{2+} ions, but under conditions of cytosolic zinc excess, MT3 can accommodate up to nine Zn^{2+} ions.[45] MTs bind Zn^{2+}centers with high affinity ($K_d \approx 0.1$ pM)[37] while allowing facile exchanges of Zn^{2+} ions with proteins having lower Zn^{2+} affinities.[37,46,47] This useful combination of high thermodynamic stability and kinetic lability supports the notion that MTs act as cytosolic zinc buffers in all human cells.[37,38,48]

In addition to redox-neutral ligand exchange pathways, MTs can also provide ionic Zn^{2+} to the cytosol through oxidative pathways. For example, oxidation of low-reduction potential MTs by various ROS and other cellular oxidants, including glutathione disulfide,[42,49] hydrogen peroxide,[50] nitric oxide (NO), and NO-derived nitrosothiols,[51–54] can lead to subsequent release of MT-bound Zn^{2+} ions. Of particular interest is the emerging synergistic relationship between neuronal Zn^{2+} and NO.[4,55,56] Specifically, Zn^{2+} release from MT3 in neurons can be induced by endogenous NO, an observation that implicates a potential role for MT3 in converting NO signals to Zn^{2+} signals in the brain.[4,52,54]

Finally, the expression of genes essential to Zn^{2+} homeostasis and protection against metal ion and ROS toxicity is regulated by the zinc finger protein metal response element binding transcription factor-1 (MTF1).[57] MTF1 controls the cellular production of ZnTs and MTs as well as γ-glutamylcysteine synthetase (γ-GCS), an enzyme that is essential for glutathione synthesis and is selectively activated by Zn^{2+}.[57]

2.2. Physiological and Pathological Functions of Brain Zinc

2.2.1. Zinc Neurophysiology

Zinc is important to the body as a cofactor in an extensive number of proteins and enzymes. Zinc finger proteins (ZFPs), transcription factors that bind to specific DNA sequences, encompass 1% of the human proteome. Furthermore, zinc is the only metal that is a cofactor in all six classes of enzymes. Enzymes of particular interest to the brain include Cu/Zn superoxide dismutase (SOD1), various peptidases (e.g., dipeptidyl aminopeptidase), enzymes involved in myelination (e.g., serum alkaline phosphatase), etc.

In addition to these protein-bound zinc pools, interest in the specialized roles of labile zinc in the brain has grown since Maske originally used histochemical diphenylthiocarbazone (dithizone) staining to first identify pools of ex-

changeable neuronal Zn^{2+} over 50 years ago,[58] with subsequent experiments showing that this Zn^{2+} was associated with the mossy fiber axons in the hippocampus.[59] The high concentrations of vesicular Zn^{2+} observed in the mossy fibers and at the tips of specific types of axons in other regions of the brain has garnered much interest, but the exact roles of Zn^{2+} remain elusive and the mechanisms of how zinc mediates neuronal processes is a topic of current debate.[59–62] One current model for synaptic zinc function proposes that Zn^{2+} is a modulator of synaptic transmission and thus plays a key role in synaptic plasticity.[59,60,63,64] Several studies with live hippocampal slices support the idea that Zn^{2+} is released from the presynaptic mossy fiber boutons[65–72] and that this release can be dependent on a variety of factors, including the presence of Ca^{2+},[65,67] K^+,[65,69] or kainate[65] or membrane depolarization.[66–68] In addition, Zn^{2+} released into the synaptic cleft can potentially enter the postsynaptic neuron, a phenomenon not observed with other neurotransmitters or neuromodulators.[71]

Despite indications of synaptic Zn^{2+} release by many laboratories, the precise roles for these mobile zinc stores remain speculative at this time. One proposal is that zinc could act as a conventional, transmitter-like signal between presynaptic and postsynaptic neurons. Studies regarding the interactions between Zn^{2+} and NMDA receptors (NMDARs) have shed some light on the potential role(s) for synaptic Zn^{2+}. Zinc is a known antagonist of NMDARs, acting via a high-affinity (nanomolar) voltage-independent pathway and a low-affinity (submicromolar) voltage-dependent pathway.[73–80] This range of affinities for Zn^{2+} suggest that Zn^{2+} can modulate both the baseline activity of NMDARs via the high-affinity receptors and the activity of NMDARs in times of high activity to prevent overstimulation via the low-affinity receptors.[81] NMDARs, in turn, can reduce the neurotoxicity of excess Zn^{2+} stores by blocking their entry into postsynaptic dendrites.[82] Zn^{2+} can also modulate the inhibitory postsynaptic currents (IPSCs) of γ-aminobutyric acid (GABA) receptors (GABARs).[83] Another mode by which zinc could potentially act as a signaling agent is by entering the postsynaptic neuron through various ion channels. In addition to ZIP proteins, Ca^{2+} channels linked with AMPA or kainate receptors are Zn^{2+} permeable,[84] so entry into the postsynaptic neuron could occur via several pathways. An intracellular Zn^{2+} signal is also possible, with analogous signaling events observed in the case of Ca^{2+}. There are several Ca^{2+} storage sites that have been identified in the cell (e.g., sarcoplasmic or smooth endoplasmic reticulum) that can rapidly release this cation when necessary;[85] no organelle-based storage pool for labile intracellular Zn^{2+} has been identified as of yet, but because NO can promote the release of Zn^{2+} from MT3,[4,52,54] this protein may provide a source for intracellular zinc signals.[60] Once released, cytosolic Zn^{2+} can potentially interact with a variety of proteins to modulate their functions, including protein kinase C (PKC),[86] calcium/calmodulin-dependent protein kinase II (CaMKII),[87] and the Src kinase family.[88] In addition, intracellular Zn^{2+} signals have been proposed to move between the cytosol and mitochondria and influence mitochondrial function.[89,90] Frederickson has classified these potential Zn^{2+} signals as Zn^{2+}-SYN, Zn^{2+}-TRANS, and Zn^{2+}-INT.[60]

The most convincing evidence for a functional role for labile synaptic zinc comes from recent *in vivo* results using knockin mice carrying the mutation D80A in the glycine receptor (GlyR) α1 subunit gene Gira1.[91] Remarkably, this point mutation eliminates zinc potentiation of α1-containing GlyR currents while leaving GlyR expression, synaptic localization, and basal glycinergic transmission unchanged. Because the potentiations of their spontaneous glycinergic currents by Zn^{2+} are impaired, the D80A mutant mice develop a severe neuromotor disorder that resembles human hyperekplexia (startle disease). Paradoxically, this first direct *in vivo* proof of zinc as a neuromodulator is not with the zinc-enriched glutamatergic neurons but rather with glycinergic ones. Thus, the fascinating question of why a neuroactivator (glutamate) and neuroinhibitor (zinc) are colocalized in the same neuronal vesicles in specific regions in the brain remains unresolved.

The roles of Zn^{2+} in neurotransmission are still controversial, as other models challenge proposals of labile synaptic Zn^{2+} release. In particular, Kay has suggested that Zn^{2+} detected in the extracellular space subsequent to neuronal stimulation may in fact be bound to biomacromolecules found in synaptic vesicles.[62,92] These biomacromolecule–Zn^{2+} complexes are proposed to possess open coordination sites on the Zn^{2+} center, allowing for ternary complex formation with sensor molecules. Another proposal is that Zn^{2+} modulates the release of other neurotransmitters through its interaction with pores or other biomolecules.[93] Finally, given the coexpression of ZnT3 and Vglut1 in presynaptic vesicles, Zn^{2+} may act as a regulator of levels of the neurotransmitter glutamate.[35]

2.2.2. Zinc Neuropathology

Although mounting evidence suggests that ionic zinc is an endogenous modulator of synaptic activity and neural function, exposure to uncontrolled pools of labile Zn^{2+} can lead to excitotoxic neuronal death. Neurons are most susceptible to this type of cell death during epileptic seizures, head trauma, cerebral ischemia and reperfusion, and related situations of overintense neural activity.[94–96] Experiments utilizing a variety of imaging techniques show that after brain injury, the levels of labile Zn^{2+} in the vesicles of mossy fiber boutons decrease with concomitant increases in labile Zn^{2+} in the corresponding postsynaptic neurons.[15] Following transient global ischemia, excess pools of labile Zn^{2+} can be detected in the hilar and CA1 regions of the hippocampus, as well as in the cerebral cortex, thalamus, striatum, and amygdala.[97–99] Moreover, the deleterious effects of this uncontrolled Zn^{2+} release can be minimized if synthetic Zn^{2+} chelators or Zn^{2+}-binding proteins are administered either before or immediately after the excitotoxic event.[100–102] The precise origin(s) of this excess zinc remains elusive, but three potential sources of Zn^{2+} are plausible: (i) Zn^{2+} in presynaptic vesicles, (ii) Zn^{2+} bound to proteins in the neuronal cytosol, and (iii) mitochondrial Zn^{2+} in postsynaptic neurons.[103,104] In this regard, a likely protein source of Zn^{2+} is MT3, which releases Zn^{2+} upon exposure to NO.[4,52,54] Excitotoxic Zn^{2+} can trigger cell death via several mechanisms, including cytotoxic upregulation of glutamate receptor activity,[84] downstream generation of reactive oxygen species,[105,106] and cross-talk with and overstimulation of nitric oxide signaling pathways.[37,52,56,89,107,108] Furthermore, recent work links mitochondrial dysfunction to elevated Zn^{2+} levels.[89,90]

In addition to these relatively rapid excitotoxic events, long-term disturbances in Zn^{2+} homeostasis have also been implicated in aging and age-related neurodegenerative dis-

eases, including Alzheimer's disease (AD).[59] One prominent pathological characteristic of AD is the accumulation of β-amyloid (Aβ) plaques in the extracellular milieu,[109] and misregulated Zn^{2+} may contribute to the deposition of these protein aggregates in the brain.[110] Aβ peptides are common cleavage products of the amyloid precursor protein (APP), an abundant protein of unknown function at the plasma membrane of neurons. Interestingly, APP contains a cysteine-rich region in its ectodomain that possesses a high affinity for Zn^{2+} (K_d = 750 nM).[111,112] Moreover, binding of Zn^{2+} to APP can inhibit the proteolytic cleavage of APP by α-secretase, a protease that generates nonamyloidogenic peptide products instead of Aβ.[113] The relative reduction in α-secretase activity compared with its β- and γ-secretase counterparts can, in turn, lead to excess formation of amyloidogenic Aβ peptides. In support of this model, the addition of Zn^{2+} in concentrations greater than 300 nM can precipitate Aβ in extracellular fluids,[113,114] and elevated levels of chelatable Zn^{2+} have been identified in amyloid plaques from the brains of both human and murine subjects.[110,115,116] More lines of evidence that point to disruption of labile zinc homeostasis in amyloid pathology are the facts that ZnT3 knockout mice show diminished susceptibility toward plaque formation[117] and that administration of the copper−zinc chelator clioquinol inhibits or reverses Aβ aggregation.[118,119] Taken together, these observations suggest a connection between zinc misregulation and neurodegeneration that is worthy of further investigation.

2.3. Molecular Imaging of Brain Zinc

2.3.1. Overview of Traditional Zinc Detection Methods

The growing contributions of zinc homeostasis to neurophysiology and neuropathology have prompted interest in devising new ways to detect Zn^{2+} in biological samples. Zn^{2+} is a difficult analyte to monitor owing to its closed-shell $4s^23d^{10}$ electronic configuration and absence of oxidation−reduction activity within biological environments. As such, conventional techniques (e.g., NMR, EPR, and electronic absorption spectroscopy) are largely ineffective for this spectroscopically silent metal ion. Atomic absorption spectroscopy (AA) provides a sensitive and selective method for zinc detection and has been used to track release of zinc into extracellular fluid after neuronal stimulation,[65] but this technique has limited spatial resolution and is destructive to the sample. Zinc also possesses a γ-emitting radioactive isotope, ^{65}Zn, that can be monitored using various methods, including autoradiography. Radioactive tracing experiments have been used to show release and uptake of Zn^{2+} upon neuronal stimulation[66] and to identify brain tumors,[120] but they carry the disadvantage of exposing samples to ionizing and potentially toxic γ-radiation and are ineffective for applications that require subcellular resolution. Furthermore, both AA and radioactive tracing techniques are incapable of distinguishing between labile and tightly bound zinc pools.

Because of these factors, the most prominent methods for identifying zinc in biological samples have relied traditionally on invasive histochemical procedures. As mentioned in a previous section, Maske pioneered the use of dithizone as a colorimetric indicator for labile Zn^{2+} in various tissues throughout the body, including the first evidence for exchangeable zinc pools in the brain.[58,121,122] When combined with optimized washing and chelation protocols, dithizone is a zinc-selective stain but is sensitive to environmental factors such as light, solvent, and heat. An alternative to colorimetry with greater sensitivity to Zn^{2+} in biological samples is Timm's staining, a silver amplification method in which metals are precipitated using sulfide and subsequently visualized using a silver development process. The original method is not metal-selective, but modified protocols have been developed by Danscher and others to furnish Zn^{2+} specificity.[123–128] The optical properties of the silver development product make Timm's staining compatible with both light and electron microscopy visualization techniques.

2.3.2. Criteria for Molecular Imaging of Zinc in Living Systems

Although the aforementioned methods have provided very useful snapshots of zinc biology, they are invasive and restricted to postmortem samples. As a result, devising alternative ways to track zinc in living biological samples is important for understanding dynamic changes that influence the effects of zinc on the brain in healthy and diseased states. Ideal tools for studying zinc neurobiology would enable the selective monitoring of Zn^{2+} pools with high spatial and temporal resolution in live samples ranging from dissociated cell cultures to intact tissue specimens to entire organisms. In this respect, two valuable techniques that have the potential to provide this type of information are optical imaging (OI) and magnetic resonance imaging (MRI). These modalities can provide a platform for real-time molecular imaging when combined with sensors or contrast agents that can respond to different levels of Zn^{2+} ions. In particular, optical imaging with fluorescent sensors has already proven useful for probing Zn^{2+} neurobiology in live hippocampal slices and neurons.[129–135] Magnetic resonance imaging with "smart" (i.e., analyte-responsive) contrast agents provides a complementary method for anatomical imaging in whole organisms to furnish *in vivo* information on dynamic zinc pools.[136–139]

Effective reagents for molecular imaging of Zn^{2+} ions in living systems must meet several requirements. The most important criterion is that a sensor should be selective for Zn^{2+} over other biologically abundant cations, including Ca^{2+} and Mg^{2+}. Zn^{2+}-sensor binding events should also be rapid and reversible, with dissociation constants (K_d) for Zn^{2+} that are matched to the particular application of interest. In this regard, a homologous series of probes with varying K_d values, ranging from subnanomolar to millimolar concentrations, are valuable for studying zinc in a variety of biological settings. For example, zinc probes with subnanomolar affinity would be useful in applications where only trace amounts of Zn^{2+} are expected but would be unsuitable for imaging dynamic changes in Zn^{2+} levels in firing neurons where Zn^{2+} concentrations may reach 0.3 mM.[15] In these cases, lower affinity probes would be required to ensure that Zn^{2+} binding would be reversible on relevant time scales. Biological compatibility is also essential, because useful zinc sensors should be water-soluble and nontoxic, be relatively insensitive to shifts in pH or ionic strength, and provide the ability to probe extracellular, intracellular, or subcellular regions.

In addition to these general considerations, specific optical requirements for fluorescent sensors include excitation and emission profiles in the visible range or lower energy, because this window minimizes photodamage to cells and tissue and helps circumvent native cellular autofluorescence; near-infrared (NIR) profiles are particularly useful for penetrating through skin and thicker specimens. Alternatively, multiphoton measurements or

Chart 1. UV-Excitable, Intensity-Based Fluorescent Zn^{2+} Sensors

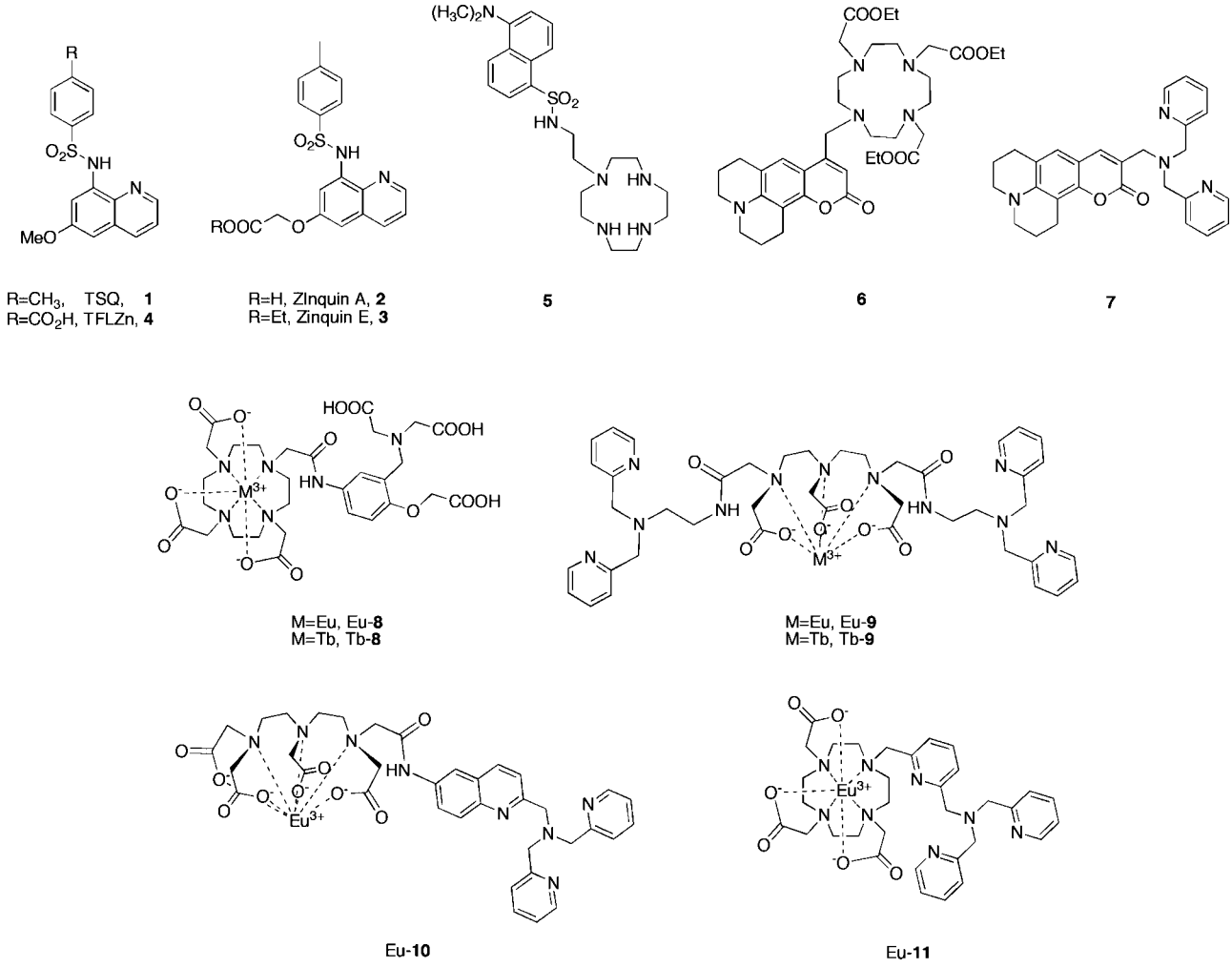

the use of luminescent reporters with longer excited-state lifetimes (e.g., lanthanides) can also mitigate sample damage and autofluorescence events associated with ultraviolet excitation. Another important consideration for biological imaging is choosing fluorescent reporters with large extinction coefficients (ε) and quantum yields (Φ), which will maximize optical brightness values ($\varepsilon \times \Phi$). Finally, fluorescent probes that give a turn-on increase or ratiometric response to Zn^{2+} are preferred because these types of readouts provide superior spatial and temporal resolution compared with their corresponding turn-off counterparts. Ratiometric sensors are particularly valued for their potential to quantitate Zn^{2+} concentrations by minimizing correction factors associated with variations in excitation source, emission collection efficiency, and sample thickness. For MR-based sensors, Zn^{2+}-responsive readouts can be manifested by modulations in the longitudinal (T_1) or the transverse (T_2) relaxivity or both. The main requirement for an effective MR sensor is maximizing the relaxivity change in response to analyte. The remainder of this section will provide a survey of synthetic chemical tools for molecular imaging of zinc in biological systems. This list is not meant to be comprehensive but instead is meant to provide the reader with a general flavor of the types of small-molecule tools and tactics that are currently available. Table 1 provides data on these various Zn^{2+} indicators.

2.3.3. Survey of Fluorescent and MRI Zinc Sensors

2.3.3.1. UV-Excitable, Intensity-Based Fluorescent Zinc Sensors. Chart 1 provides a selection of intensity-based fluorescent Zn^{2+} sensors with UV excitation. The first and most widely used fluorescent sensor for imaging Zn^{2+} in biological samples is 6-methoxy-8-*p*-toluenesulfonamidoquinoline (TSQ, **1**),[140] an aryl sulfonamide derivative of 8-aminoquinoline.[141,142] TSQ is nontoxic and membrane-permeable and exhibits a 100-fold increase in fluorescence intensity in response to Zn^{2+} in ethanol solution ($\lambda_{ex} = 380$ nm; $\lambda_{em} = 495$ nm).[140] Because of its utility in identifying labile zinc stores in the brain and other parts of the body, many derivatives of TSQ, including Zinquin A (**2**),[143,144] Zinquin E (**3**),[143] and TFLZn (**4**),[67] have been prepared in the past 20 years in attempts to improve water solubility, membrane permeability, or both. These quinoline dyes have been invaluable for live-cell imaging of zinc ions in many contexts[15,63,145] but are limited by their optical brightness ($\varepsilon \times \Phi \approx 10^3$ M^{-1} cm^{-1}), unstable partition coefficients, and propensity to form mixed 1:1 or 2:1 fluorophore/Zn^{2+} complexes.[63,144,146] Other UV-excitable fluorophore platforms, including dansyl (**5**)[147,148] and coumarin (**6** and **7**),[149,150] have also been utilized for biological Zn^{2+} detection. Finally, several lanthanide-based Zn^{2+} sensors (**8**−**11**) have been reported recently but most have not been applied successfully for live-cell imaging.[151−155] However, these types of compounds are promising for high-sensitivity

Chart 2. Visible-Excitable, Intensity-Based Fluorescent Sensors with High Zn^{2+} Affinities.

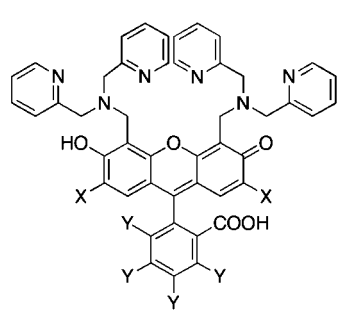

X=Cl, Y=H, ZP1, **12**
X=H, Y=H, ZP2, **13**
X=F, Y=H, ZP3, **14**

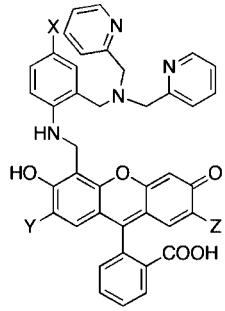

X=H, Y=H, Z=Cl, ZP4, **15**
X=F, Y=H, Z=Cl, ZP5, **16**
X=Cl, Y=H, Z=Cl, ZP6, **17**
X=OMe, Y=H, Z=Cl, ZP7, **18**
X=H, Y=F, Z=F, ZP8, **19**

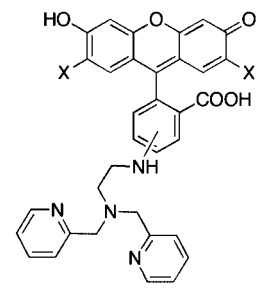

5-sub, X=H, ZnAF-1, **20**
6-sub, X=H, ZnAF-2, **21**
5-sub, X=F, ZnAF-1F, **22**
6-sub, X=F, ZnAF-2F, **23**

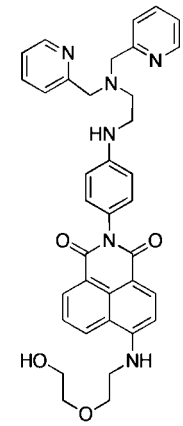

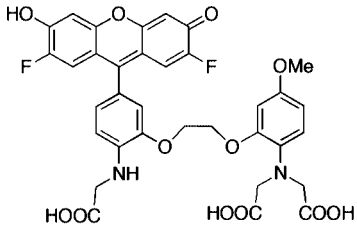

FluoZin-3, **24**

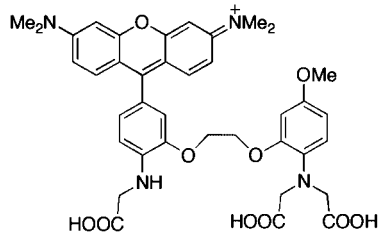

RhodZin-3, **25**

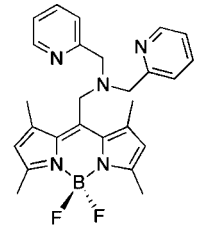

BDA, **26**

WZS, **27**

imaging applications owing to their long excited-state lifetimes that extend beyond native cellular autofluorescence and scattered light events. In this way, removal of virtually all background signals from biological samples can be achieved by gating the detector collection window. Eu^{3+}-based **10** has been used to image Zn^{2+} in cells, though this was achieved by injection of the complex into cells instead of by incubation.[155]

2.3.3.2. Visible-Excitable, Intensity-Based Fluorescent Sensors with High Zinc Affinities. The ability to minimize sample damage and native autofluorescence events associated with ultraviolet excitation coupled with the rising use of laser-based optical microscopy systems has spurred a rapid growth in the number of turn-on, zinc-specific fluorescent sensors that utilize visible excitation profiles (Chart 2). The fluorescein-based Zinpyr (ZP) family represents a prominent class of Zn^{2+} sensors in this regard, offering optical brightness values that are up to 50-fold greater than their quinoline counterparts. The ZP probes and related fluorogenic reagents utilize a photoinduced electron transfer (PET) mechanism for metal ion detection. In the absence of the metal ion analyte, the electron-rich receptor quenches the fluorescence of the dye reporter. Metal ion binding stops PET quenching and restores fluorescence from the dye. The first member of the ZP series, Zinpyr-1 (ZP1, **12**), combines a dichlorofluorescein core with two appended di-2-picolylamine (DPA) moieties; the pyridyl ligands provide selectivity for Zn^{2+} over hard metal ions Ca^{2+} and Mg^{2+} that are abundant in cellular systems.[156,157] Upon addition of up to 1 equiv of Zn^{2+}, the quantum yield of ZP1 undergoes a modest 2.2-fold increase from $\Phi = 0.39$ to 0.87 with characteristic fluorescein excitation and emission profiles in the range of 500 to 530 nm. A tight 1:1 Zn^{2+}/sensor complex ($K_d = 0.7$ nM) is responsible for the observed fluorescence increase, whereas binding of a second Zn^{2+} ion occurs with much lower affinity ($K_d = 85\ \mu M$) and no apparent fluorescence change. Zinpyr-2 (ZP2, **13**) is a parent fluorescein version of ZP1 that exhibits similar optical properties. Both sensors are capable of detecting changes in labile Zn^{2+} concentrations in living cells due to introduction of exogenous Zn^{2+}.

Although ZP1 and ZP2 are effective tools for live-cell zinc imaging, a limitation of these first-generation probes is that they possess relatively high pK_a values for the tertiary nitrogen atoms responsible for PET switching and, as a consequence, display background fluorescence in their apo states (p$K_a = 8.4$ and $\Phi = 0.38$ for ZP1, p$K_a = 9.4$ and $\Phi = 0.25$ for ZP2). This type of behavior is a general issue for metal ion sensing in water via PET, because proton-induced fluorescence turn-on events can interfere with or give false positives for metal ion binding. As a result, several approaches have been pursued to tune the pK_a values of receptor nitrogen switches for optimized Zn^{2+} responses. One such strategy is the introduction of electron-withdrawing groups into the fluorescein scaffold.[158] The most useful of these probes, Zinpyr-3 (ZP3, **14**), incorporates two fluorine atoms into the fluorescein backbone. This substitution reduces the pK_a of the benzylic PET amine to 6.8 and lowers the quantum yield of the apo probe to $\Phi = 0.15$. Zn^{2+} binding affords a 6-fold increase in fluorescence with high brightness ($\Phi = 0.92$). Like other members of the ZP family, ZP3 is selective for Zn^{2+} over other biologically relevant cations. Moreover, this bright dye is cell-permeable and capable of imaging endogenous Zn^{2+} pools in brain systems ranging from dissociated neurons to live tissue slices from the hippocampus. An alternative tactic is to switch from an aliphatic amine to an aromatic one, because anilines generally possess lower pK_a values. ZP4 (**15**) is a representative dye of this type.[159] Apo ZP4 has a quantum yield of $\Phi = 0.06$, which increases by ca. 6-fold upon binding Zn^{2+} ($\Phi = 0.34$). This probe has been used to selectively stain Zn^{2+}-damaged neurons in

tissue slices.[160] Other members of the ZP family have been synthesized to tune receptor electronics (ZP5−8, **16**−**19**)[161,162] and cell-permeability and retention (ZP1-ester or acid derivatives).[163]

A complementary class of fluorescein-based zinc probes that has been developed in parallel is the ZnAF family. Like the ZP series, the ZnAFs utilize a fluorescein reporter and DPA receptor for Zn^{2+} detection, but the main strategic difference is that the ZP sensors feature DPA units appended to the top ring xanthenone core, whereas the ZnAFs possess DPA groups linked to the bottom aromatic ring in either the 5 (ZnAF-1, **20**) or 6 (ZnAF-2, **21**) position.[164] Owing to their aniline PET switches, the ZnAF sensors display lower background fluorescence values ($\Phi = 0.02$) and larger turn-on responses (17- to 51-fold) compared with their ZP counterparts ($\Phi = 0.03-0.38$, 3−11-fold), but their Zn^{2+}-bound forms are not as bright. Fluorination produces improved ZnAF-1F (**22**) and ZnAF-2F (**23**) probes with almost no background fluorescence ($\Phi = 0.004$ for ZnAF-1F, $\Phi = 0.006$ for ZnAF-2F) and enhanced turn-on responses (60−69-fold).[165] The diacetyl version of ZnAF-2F is membrane-permeable and can image labile Zn^{2+} pools in acute rat hippocampal slices,[165] whereas the membrane-impermeable ZnAF-2 has been employed to monitor release of Zn^{2+} upon neuronal stimulation.[166]

Adaptation of commercial Ca^{2+} sensors provides another approach to biological Zn^{2+} sensing. For example, Ca^{2+} sensors Fluo-3 and Fluo-4 utilize the well-studied Ca^{2+} chelator bis(*o*-aminophenoxy)-ethane-*N*,*N*,*N*′,*N*′-tetraacetic acid (BAPTA), but these receptors actually possess higher affinities for Zn^{2+} than for Ca^{2+}.[167,168] To reduce the Ca^{2+} affinity of these probes beyond cellular concentration ranges while maintaining their affinity toward Zn^{2+}, removal of one of the acetate arms of BAPTA provides FluoZin-3 (**24**).[169] This sensor binds Zn^{2+} with high affinity ($K_d = 15$ nM) and a large fluorescence increase (over 200-fold). Because of its hard acetate ligands, FluoZin-3 responds slightly to Fe^{2+} and Ca^{2+} and displays less overall Zn^{2+} selectivity compared with DPA congeners, but the platform is selective and sensitive enough for many useful applications. For example, in part because of its large dynamic range, this probe can detect local bursts of endogenous Zn^{2+} excreted by pancreatic β-cells as far as 15 μm away from the cell (Figure 2). A rhodamine version of FluoZin-3, RhodZin-3 (**25**), has also been prepared and features a selective 75-fold increase in fluorescence in response to Zn^{2+} ions with high affinity ($K_d = 65$ nM).[170] The acetoxymethyl ester version of this sensor is cell-permeable and can be used to study mitochondrial Zn^{2+} homeostasis.[90]

Finally, high-affinity zinc sensors have also been developed using DPA ligands in conjunction with other visible-wavelength dyes. The two examples provided here are valued for their insensitivity to changes in pH. BDA (**26**) is a Zn^{2+} sensor based on the boron dipyrromethene (BODIPY) framework that exhibits a 7-fold increase in integrated emission upon Zn^{2+} binding with a high quantum efficiency ($\Phi_{apo} = 0.08$; $\Phi_{bound} = 0.86$), desirable optical properties ($\lambda_{ex} = 491$ nm; $\lambda_{em} = 509$ nm), and nanomolar Zn^{2+} affinity ($K_d = 1.0$ nM).[171] Moreover, the BODIPY-based probe is cell-permeable and can detect changes in labile Zn^{2+} concentrations in live TCA and PC12 cells incubated with $ZnCl_2$. WZS (**27**) combines a 4-aminonaphthalimide fluorophore and a DPA receptor for Zn^{2+} detection.[172] This probe also displays high Zn^{2+} affinity ($K_d = 0.62$ nM) and a visible excitation profile ($\lambda_{ex} = 449$ nm). The quantum yield of Zn^{2+}-bound WZS is within useful ranges ($\Phi = 0.19$) and the dye can report increases in intracellular Zn^{2+} within Zn^{2+}-incubated HeLa cells.

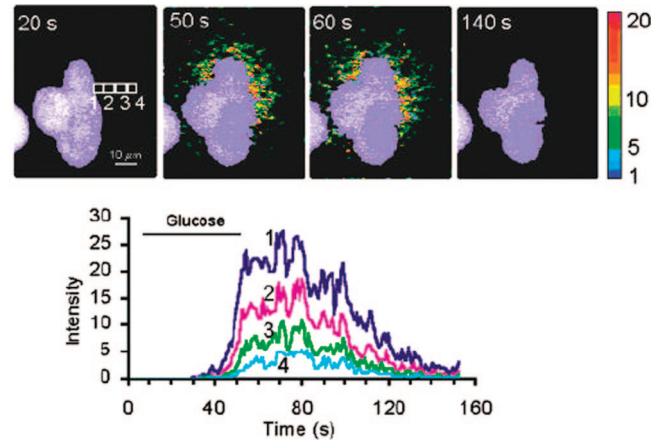

Figure 2. Imaging of Zn^{2+} secretion from pancreatic β-cells using FluoZin-3 (**24**). Images are shown in ratios of fluorescence intensities against a reference image collected in the beginning of the sequence. Images were acquired at 20, 50, 60, and 140 s. The temporal responses of Zn^{2+} secretion were analyzed using the four regions of interest (ROI, 4 μm^2) indicated as 1, 2, 3, and 4 in the first image. The traces from top to bottom correspond to the ROI 1, 2, 3, and 4, respectively. Cells were incubated in Krebs−Ringer buffer containing 2 μM FluoZin-3 and stimulated to secrete by the application of 20 mM glucose. The bar on top of the traces indicates the application of stimulation. Reprinted with permission from ref 169. Copyright 2002 American Chemical Society.

2.3.3.3. Visible-Excitable, Intensity-Based Fluorescent Sensors with Moderate Zinc Affinities. Many molecular imaging applications that involve changes in zinc concentrations when basal Zn^{2+} levels are high, for example, for zinc-containing vesicles in the mossy fiber boutons, require complementary Zn^{2+}-responsive sensors with micromolar to millimolar affinities. Chart 3 depicts a representative set of probes designed to meet this goal. The fluorescein-like Newport Green dyes NG-DCF (**28**)[173] and NG-PDX (**29**)[174] utilize aniline-fused DPA binding units to furnish probes with reduced binding affinity ($K_d = 1$ μM for NG-DCF, $K_d = 30-40$ μM for NG-PDX). The diacetate form of NG-DCF has been used to image cytosolic entry of Zn^{2+} through voltage- or glutamate-gated ion channels.[175,176]

Phenyliminodiacetate (PIDA) is another low-affinity zinc chelator used for fluorescence detection of Zn^{2+}. FluoZin-1 (**30**) and FluoZin-2 (**31**) are representative Zn^{2+}-sensing analogs to the calcium sensors Fluo-4 and Calcium Green.[174] FluoZin-1 displays a 200-fold increase in fluorescence in response to Zn^{2+} addition with a K_d of 7.8 μM. FluoZin-2 exhibits a 12-fold turn-on to Zn^{2+} with a K_d of 2.1 μM. Rhodamine analogs RhodZin-1 (**32**) and X-RhodZin-1 (**33**) have also been elaborated.[174] Because these probes are similar to their Ca^{2+} counterparts, they exhibit some sensitivity to millimolar concentrations of Ca^{2+}.

Lippard and co-workers have pursued several avenues to obtain fluorescein-based zinc sensors with moderate Zn^{2+} dissociation constants. For example, substitution of a DPA pyridine donor with a thioether or thiophene donor affords the Zinspy (ZS) family of probes.[177,178] ZS5 (**34**) is the most useful of the series, exhibiting a 4-fold fluorescence turn-on upon Zn^{2+}-binding with a high Zn^{2+}-bound quantum yield ($\Phi = 0.80$) and micromolar Zn^{2+} affinity ($K_d = 1.5$ μM). Interestingly, imaging experiments reveal not only that ZS5

Chart 3. Visible-Excitable, Intensity-Based Fluorescent Sensors with Moderate Zn^{2+} Affinities

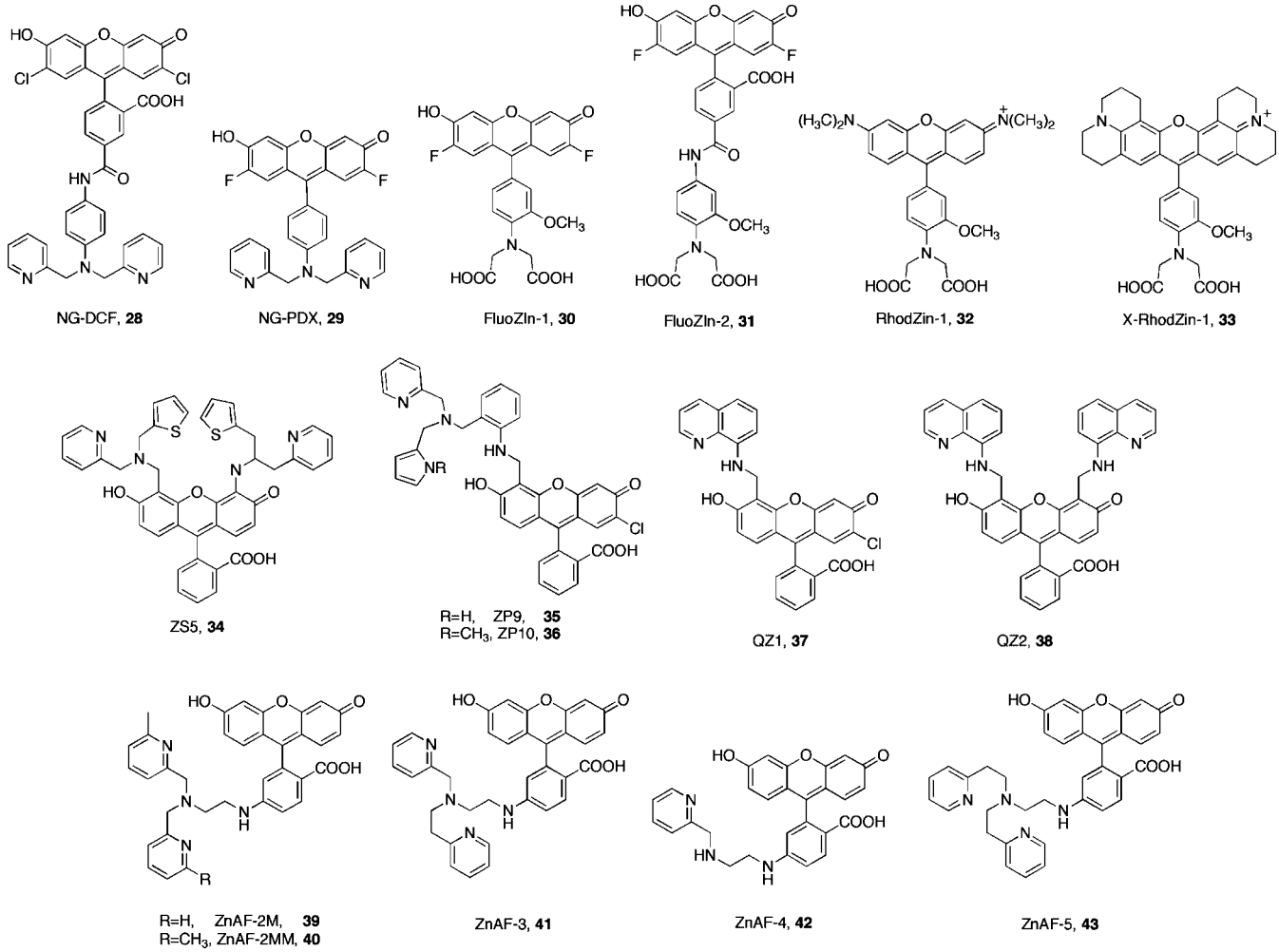

responds to Zn^{2+} in live cells but that this dye colocalizes with mitochondria in HeLa cells. This probe is capable of imaging glutamate-induced Zn^{2+} intake in embryonic hippocampal neurons and *S*-nitrosocysteine (SNOC)-induced Zn^{2+} release from native protein stores in dentate gyrus neurons (Figure 3). Substitution of a DPA picolyl arm with a pyrrole affords ZP9 (**35**) and ZP10 (**36**).[179] ZP9 binds Zn^{2+} with moderate affinity (K_d = 0.69 μM), exhibits a 12-fold turn-on response, and can image endogenous Zn^{2+} stores in adult rat hippocampal slices. Finally, the Quinozin (QZ) family of sensors combines versatile aldehyde fluorescein starting materials with quinoline receptors.[180] Cell-permeable QZ1 (**37**), with one aminoquinoline unit for metal chelation, binds zinc with micromolar affinity (K_d = 33 μM) and exhibits a 44-fold increase in fluorescence in response to Zn^{2+}(Φ_{apo} = 0.024; Φ_{bound} = 0.78). QZ2 (**38**), with two aminoquinoline units for metal chelation, has a higher turn-on response to Zn^{2+} (Φ_{apo} = 0.005; Φ_{bound} = 0.70) with similar Zn^{2+}-binding characteristics (K_d = 41 μM). Imaging experiments in HeLa cells were used to compare the abilities of low-affinity QZ2 and high-affinity ZP3 (K_d = 0.7 nM) to sense varying levels of Zn^{2+} in the cell. Cells were incubated with a range of Zn^{2+} concentrations (0 to 200 μM); ZP3 displayed saturation behavior beginning at 50 μM, whereas QZ2 was not yet saturated at 200 μM.

Lower affinity Zn^{2+} sensors are also available from the modular ZnAF platform developed by Nagano and coworkers.[181] In particular, a series of ZnAF derivatives (**39**−**43**) were prepared that systematically probed the factors of zinc-chelator denticity, sterics, and chelate ring size, resulting in a family of Zn^{2+}-responsive sensors that can detect Zn^{2+} concentrations from 10^{-10} to 10^{-3} M. The

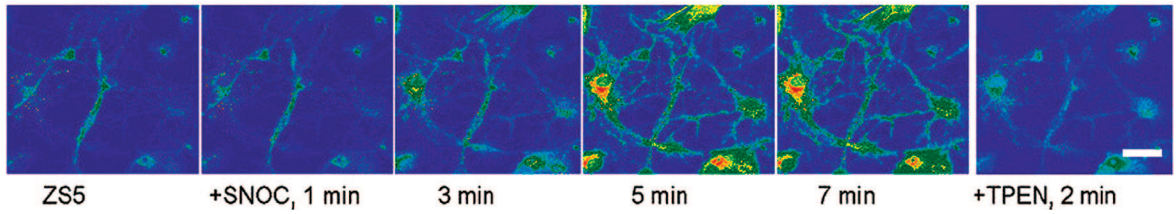

Figure 3. Imaging endogenous Zn^{2+} release in primary dentate gyrus neuronal cultures following nitrosative stress with ZS5 (**34**). The cells were treated with 10 μM ZS5 (30 min, 37 °C, 5% CO_2), washed, and imaged. An aliquot of SNOC was added (final concentration = 1.5 mM), and the fluorescence change was recorded at 1-min intervals. Time points for 0, 1, 3, 5, and 7 min are shown. The right-most panel shows the fluorescence decrease that occurred 2 min after addition of 200 μM *N*,*N*,*N*′,*N*′-tetrakis-(2-pyridylmethyl)-ethylenediamine (TPEN). The scale bar indicates 25 μm. Reprinted with permission from ref 177. Copyright 2006 American Chemical Society.

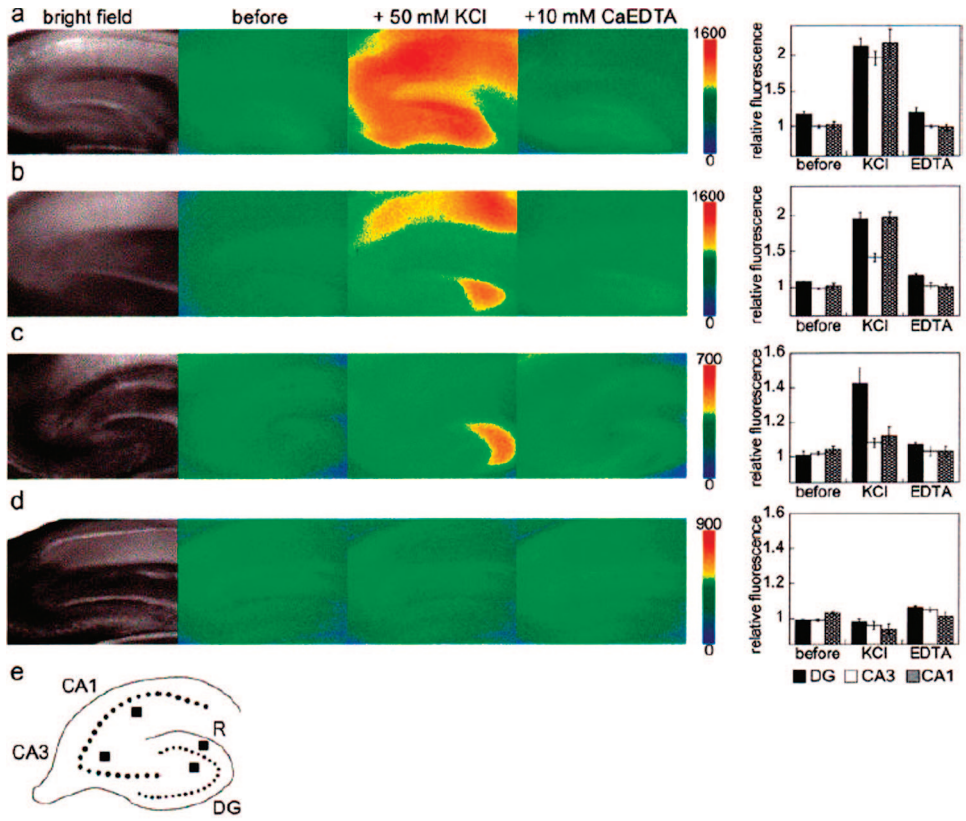

Figure 4. Fluorescence response of ZnAFs detecting extracellularly released Zn^{2+} in hippocampal slices. Fluorescence excited at 470−490 nm was measured soon after rat hippocampal slices were loaded with 1 μM ZnAF-2 (**21**, K_d = 2.7 nM) (a), ZnAF-2M (**38**, K_d = 38 nM) (b), ZnAF-3 (**40**, K_d = 0.79 μM) (c), or ZnAF-4 (**41**, K_d = 25 μM) (d). Then, 50 mM KCl (at 1 min) and 10 mM CaEDTA (at 10 min) were added to the imaging solution. Bright field images and fluorescence images at 0 min (before), at 3 min (+50 mM KCl), and at 15 min (+10 mM CaEDTA) are shown in each row. Relative fluorescence intensities of DG, CA3, and CA1 are shown in the bar graph, expressed as mean ± SE (n = 3 for ZnAF-2, ZnAF-3, and ZnAF-4 and n = 5 for ZnAF-2M). The bottom schematic (e) shows the approximate positions used for measurements of fluorescence intensity in the dentate gyrus (DG), CA3, CA1, and R (as a reference) region. Reprinted with permission from ref 181. Copyright 2005 American Chemical Society.

modified ZnAFs are membrane-impermeable, whereas their diacetate versions are permeable. Moreover, these dyes can monitor, in real time, Zn^{2+} release in hippocampal slices provoked by potassium-induced neuronal depolarization; the differences in observed localized fluorescence intensities using sensors with varying K_d values elegantly establishes the value of sensors with tunable binding affinities (Figure 4). Whereas the high-affinity ZnAF-2 (K_d = 2.7 nM) can report increases in Zn^{2+} concentrations throughout the hippocampal slice upon depolarization, the weaker-binding ZnAF-3 (K_d = 0.79 μm) only detects increased levels of Zn^{2+} in the dentate gyrus. The weakest-affinity probe, ZnAF-4 (K_d = 25 μM), detects no changes in Zn^{2+} concentration. These results, as well as the QZ2/ZP3 comparison, highlight the importance of developing metal ion probes with a range of available binding affinities for imaging studies.

2.3.3.4. Intensity-Based Zinc Sensors with Near-Infrared Excitation. Fluorescent sensors that absorb and emit light in the near-infrared (NIR) region of the electromagnetic spectrum are of great interest for potential *in vivo* imaging applications. In particular, the optical window between 650 and 900 nm is capable of penetrating skin and tissue with minimal cellular autofluorescence. These features, combined with the low scattering ability of emitted NIR photons, presages a rich future for molecular sensors that operate in this optical region.[182] To the best of our knowledge at this time, only one intensity-based fluorescent zinc sensor with NIR excitation and emission has been reported (Chart 4).[183] The sensor DPA-Cy (**44**) combines the familiar DPA Zn^{2+}

Chart 4. An Intensity-Based Zn^{2+} Sensor with Near-Infrared Excitation

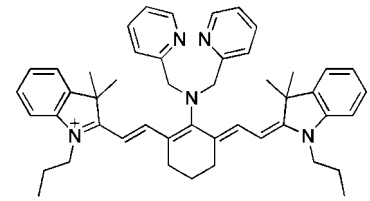

DPA-Cy, **44**

receptor with a propyl-substituted tricarbocyanine fluorophore. Apo- and holo-DPA-Cy both have a 730 nm excitation wavelength and a 780 nm emission wavelength in 9:1 water−acetonitrile solution. Binding of Zn^{2+} to the probe furnishes a 20-fold increase in quantum efficiency (Φ_{apo} = 0.02, Φ_{bound} = 0.41, measured in methanol) with high affinity for Zn^{2+} (K_d = 63 nM). DPA-Cy responds to exogenously applied Zn^{2+} in live macrophages.

2.3.3.5. Ratiometric Fluorescent Zinc Sensors. Intensity-based fluorescent zinc sensors are of practical utility for tracking labile pools of Zn^{2+} in biological systems. However, using these reagents to quantify changes in dynamic Zn^{2+} concentrations in these complex environments is challenging owing to variations that can arise from excitation input and collected emission output intensities, as well as heterogeneities in biological sample dissections and preparations. Ratiometric sensors offer the ability to simultaneously monitor both the free and bound states of the probe using

Chart 5. Ratiometric Fluorescent Zn^{2+} Sensors

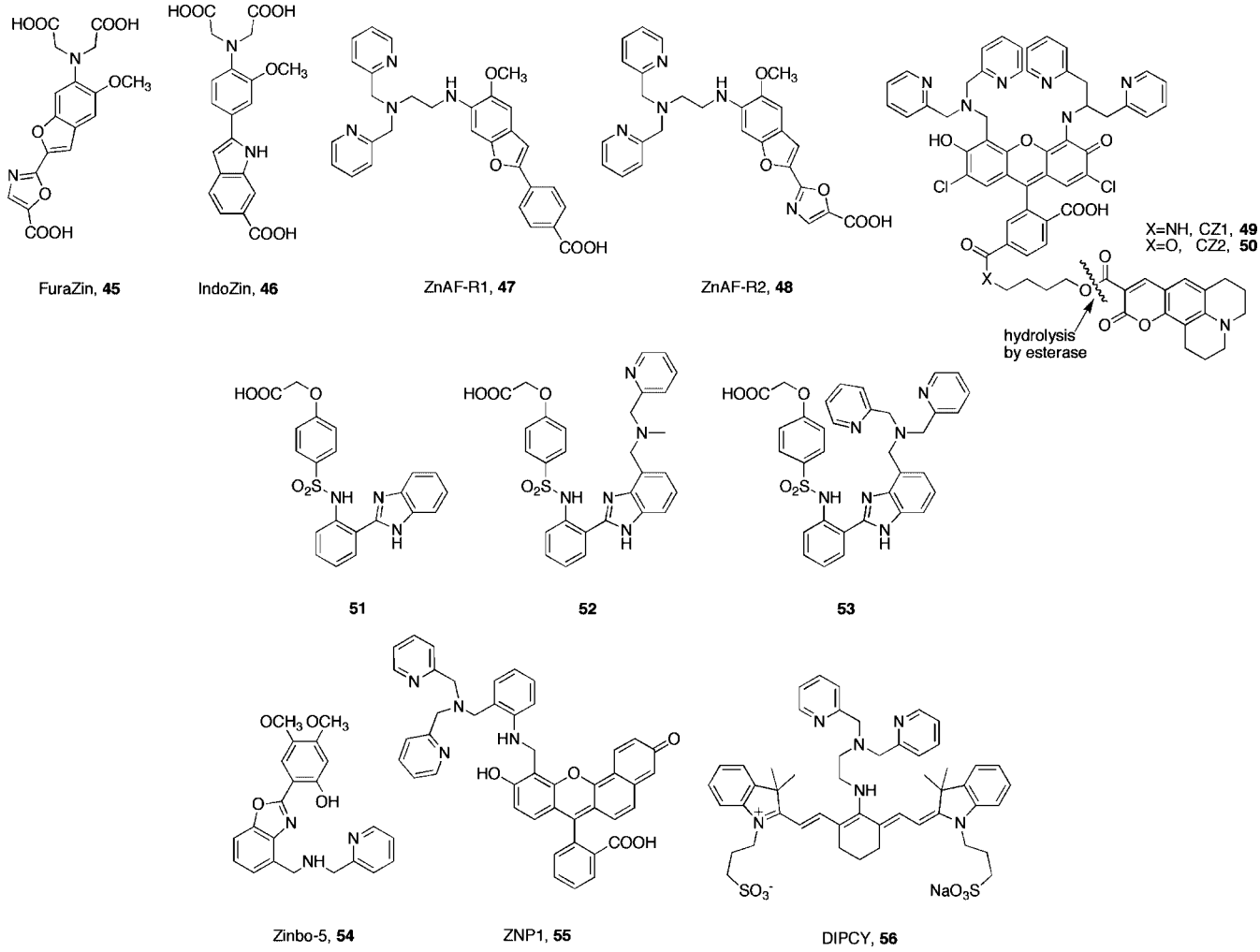

dual excitation or dual emission measurements. The internal standard afforded by ratiometric imaging has prompted interest in devising sensors that shift their excitation or emission profiles upon Zn^{2+} recognition. Chart 5 shows some ratiometric fluorescent Zn^{2+} probes that have appeared in the literature.

FuraZin (**45**) and IndoZin (**46**) are PIDA-modified ratiometric Zn^{2+} sensors derived from classic Fura and Indo Ca^{2+} sensors.[174] These probes utilize an internal charge transfer (ICT) mechanism for sensing, where metal ion binding tunes the electron-donating properties of the receptor. Upon binding Zn^{2+}, FuraZin undergoes an excitation wavelength shift from 378 to 330 nm with a constant emission wavelength (510 nm). In contrast, IndoZin exhibits a blue shift of its emission wavelength from 480 to 395 nm upon Zn^{2+} recognition with a constant excitation maximum (350 nm), giving a >100-fold fluorescence ratio change. FuraZin and IndoZin both show moderate Zn^{2+} affinities ($K_d = 3.4$ μM for FuraZin, $K_d = 3.0$ μM for IndoZin) with good selectivity over cellular concentrations of Ca^{2+} and Mg^{2+}. ZnAF-R1 (**47**) and ZnAF-R2 (**48**) are a related pair of ratiometric Zn^{2+} sensors based on the Fura platform.[184] Both reagents utilize a DPA receptor for specific Zn^{2+} detection. ZnAF-R2 displays a blue shift in excitation wavelength from 365 to 335 nm when Zn^{2+} is added with an emission maximum at 495 nm, giving a ca. 4-fold fluorescence ratio change in the presence of 1 equiv of Zn^{2+}. ZnAF-R2 has a K_d of 2.8 nM for Zn^{2+}. The ethyl ester of ZnAF-R2 is cell-permeable and was used to image labile Zn^{2+} in live macrophages.

A different approach to ratiometric Zn^{2+} sensing involves a two-fluorophore system that is cleaved into two independent molecules by esterases upon entry into the cell. One part of the prosensor cassette is zinc-responsive and the other moiety serves as a constant standard. Coumazin-1 (CZ1, **49**) is a first-generation probe based on this concept and is comprised of a ZP-derived Zn^{2+} sensing portion and an ester-linked coumarin appendage that is insensitive to Zn^{2+}.[185] The two-fluorophore sensor exhibits low background fluorescence due to intramolecular quenching ($\Phi = 0.04$). Upon esterase cleavage, the coumarin ($\lambda_{ex} = 445$ nm, $\lambda_{em} = 488$ nm) and ZP ($\lambda_{ex} = 505$ nm, $\lambda_{em} = 534$ nm) fragments are separated. The I_{534}/I_{488} emission ratio is 0.5 in the absence of $Zn^{2+}$and increases by over 8-fold upon addition of Zn^{2+}. As with its ZP1 analog, CZ1 has low nanomolar affinity for Zn^{2+} ($K_d = 0.25$ nM) with good metal ion selectivity. Experiments with HeLa cells show that CZ1 is membrane-permeable and can be used for ratiometric Zn^{2+} detection in living systems. CZ2 (**50**) is a more rapidly cleaved second-generation analog that also can operate within cells.[186]

Another strategy for ratiometric Zn^{2+} detection exploits an excited-state intramolecular proton transfer (ESIPT) mechanism using benzimidazole and benzoxazole scaffolds.[187,188] In these types of probes, disruption of hydrogen bonding between the heterocyclic nitrogen atom lone pairs and

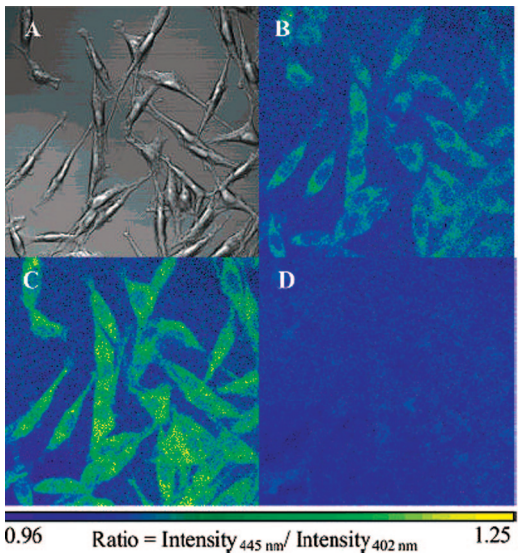

Figure 5. Emission ratio images of fibroblast [L(TK)−] cells stained with Zinbo-5 (**51**).: (A) brightfield transmission image; (B) ratio of images collected at 445 and 402 nm emission wavelengths; (C) ratio image following a 30 min treatment with 10 μM zinc sulfate and 20 μM pyrithione at pH 7.4, 25 °C, followed by incubation with Zinbo-5; (D) ratio image of the same field after a 15 min treatment with 1 mM TPEN. Reprinted with permission from ref 188. Copyright 2004 American Chemical Society.

pendant hydrogen-bond donors by Zn^{2+} chelation modulates ESIPT with concomitant shifts in excitation or emission profiles. For example, benzimidazole dyes containing zinc-chelating sulfonamides exhibit a wide range of substituent-dependent Zn^{2+} binding affinities and optical responses (e.g., **51**−**53**).[187] By changing the benzimidazole substituent from hydrogen (**51**) to monopicolylamine (**52**) to DPA (**53**), a range of binding affinities is obtained (K_d = 32 μM, 0.6 nM, and 0.8 pM respectively). In addition, these probes are selective for Zn^{2+} over other biologically relevant cations, with some response seen toward Cd^{2+}. The ratio of emission intensities at 400 and 500 nm for these probes can change by up to 82-fold upon Zn^{2+} coordination. Zinbo-5 (**54**) is a ratiometric Zn^{2+} sensor that combines a benzoxazole reporter with an appended phenolic group and a picolyl amine group for tighter Zn^{2+} binding (K_d = 2.2 nM) and higher Zn^{2+} selectivity.[188] Zn^{2+} binding produces changes in excitation (λ_{apo} = 337 nm to λ_{bound} = 376 nm) and emission (λ_{apo} = 407 nm to λ_{bound} = 443 nm) wavelengths with a slight increase in quantum yield (Φ_{apo} = 0.02; Φ_{bound} = 0.10); the fluorescence intensity ratio (I_{443}/I_{395}) changes by over 30-fold upon coordination of Zn^{2+}. Moreover, Zinbo-5 is capable of detecting changes in intracellular Zn^{2+} concentrations in fibroblast cells using two-photon microscopy in a ratiometric imaging mode (Figure 5).

Zin-naphthopyr-1 (ZNP1, **55**) is a ratiometric zinc sensor based on a hybrid seminaphthofluorescein scaffold.[189] This tautomeric sensor has two mesomers with fluorescein-like (naphthoxyquinone mesomer) and naphthofluorescein-like (phenoxynaphthoquinone mesomer) optical properties. Apo-ZNP1 exhibits properties of both mesomers with two absorption (λ = 503 and 539 nm) and emission (λ = 528 and 604 nm) bands in the visible region. In contrast, the Zn^{2+}-bound form of ZNP1 displays only one absorption band at 547 nm and one dominant emission band at 624 nm with a minor band at 545 nm. Addition of Zn^{2+} causes the I_{624}/I_{528} fluorescence intensities to rise from 0.4 to 7.1, a ca. 18-fold ratio increase. ZNP1 binds Zn^{2+} with nanomolar affinity (K_d = 0.55 nM) with good selectivity over other biologically relevant cations. The ZNP1 diacetate derivative is membrane-permeable and capable of imaging NO-induced release of endogenous Zn^{2+} stores in live COS-7 cells.

A final ratiometric Zn^{2+} sensor with NIR excitation and emission profiles is DIPCY (**56**), which combines a tricarbocyanine reporter dye with a DPA zinc receptor.[190] Zn^{2+} binding causes a large red shift in absorption maximum for the sensor from 627 to 671 nm. The ratio of emission intensities collected at 760 nm upon excitation at 671 and 627 nm increases by ca. 5-fold upon Zn^{2+} binding with high affinity (K_d = 98 nM). No biological applications of this probe have been reported as of yet.

2.3.3.6. MR-Based Zinc Sensors. A relatively small number of MR-based zinc sensors exist compared with their fluorescent counterparts (Chart 6). The few examples reported so far rely largely on modulating the local environment around a metal contrast agent center by peripheral Zn^{2+} binding, an approach inspired by the smart MRI contrast agents pioneered by Meade for reporting enzyme activity.[191] The first MRI contrast agents designed for Zn^{2+} sensing feature Gd^{3+}-DTPA (diethylenetriaminepentaacetic acid) derivatives modified with two to four picolyl groups for external Zn^{2+} chelation.[136,137] The tetrapicolyl sensor Gd-**57** exhibits a 33% decrease in relaxivity from 6.06 to 3.98 mM^{-1} s^{-1} upon binding 1 equiv of Zn^{2+}.[136] Surprisingly, the addition of excess Zn^{2+} increases the observed relaxivity back to original values by formation of 2:1 Zn^{2+}/sensor adducts. To avoid this type of Zn^{2+} concentration dependence, two new Gd^{3+} chelates were prepared containing two pyridine and two acetate groups for Zn^{2+} recognition.[137] One of these sensors, Gd-**58** displays a similar decrease in relaxivity that plateaus at 1 equiv of Zn^{2+}.

A Eu^{3+}-based PARACEST MR contrast agent for sensing Zn^{2+} has also been reported (Eu-**59**).[192] PARACEST (paramagnetic chemical exchange saturation transfer) contrast agents induce hyperfine shifts in the signals of proximal NMR-active nuclei; such shifts can be modulated by changes in the lanthanide coordination environment.[193] Eu-**59** is a DOTA (1,4,7,10-tetraazacyclododecane-1,4,7,10-tetraacetic acid) analog bearing two additional Zn^{2+}-responsive DPA groups. Binding of Zn^{2+} to Eu-**59** triggers a linear decrease in its CEST effect, with up to 50% quenching at 1 equiv of Zn^{2+}. Phantom MR images (i.e., MR images of contrast agent solutions) show that the response of Eu-**59** is selective for Zn^{2+} over Ca^{2+} and Mg^{2+}.

Recently, two new additional smart agents for MR detection of Zn^{2+} have been reported. The first agent is a dual-function porphyrin-based Zn^{2+}-responsive sensor for MR and fluorescence imaging (Mn-**60**). Such multimodal imaging agents are gaining popularity because they afford an efficient and versatile approach to target validation by multiple imaging techniques. The water -soluble porphyrin $(DPA\text{-}C_2)_2TPPS_3$ can be used as a fluorescent Zn^{2+} sensor within cells, whereas its Mn^{3+} complex can detect Zn^{2+} using MRI.[138] Mn-**60** exhibits an unexpected decrease in R_1 relaxivity from 8.70 to 6.65 mM^{-1} s^{-1} upon addition of Zn^{2+} with a concomitant increase in R_2 relaxivity. However, in cell pellet experiments, increases in both R_1 and R_2 were observed in Zn^{2+}-treated cells versus untreated cells. Finally, a Gd^{3+}-based contrast agent (Gd-**61**) utilizing a DO3A (1,4,7,10-tetraazacyclododecane-1,4,7-triacetic acid) platform for lanthanide chelation and a PIDA moiety has been described as a Zn^{2+}-responsive MR agent.[139] This sensor

Chart 6. MR-Based Zn^{2+} Sensors

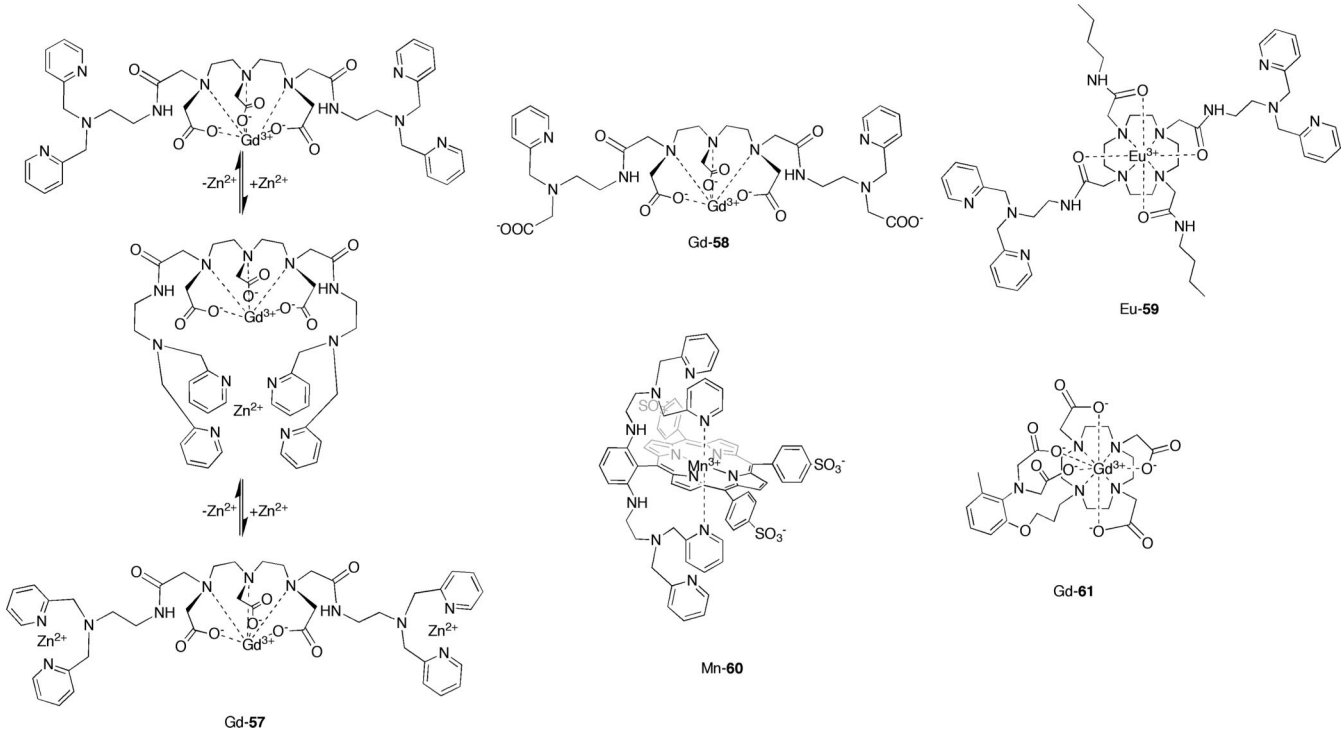

displays good selectivity for Zn^{2+} over alkali and alkaline earth cations.

3. Iron in Neurobiology

3.1. Basic Aspects of Iron in the Brain

3.1.1. Tissue Concentrations and Distributions

The average human adult requires approximately 5 g of iron, making this nutrient the most abundant transition metal in the body. Iron is also the most abundant transition metal in the brain because this organ has the highest rate of oxidative metabolism in the body, and brain tissue utilizes iron as a key component of enzymes involved in oxygen transport and metabolism.[194] The levels of iron in the brain vary from region to region and can reach >1 mM concentrations in localized neurons. The highest concentrations of neuronal Fe are found in the basal ganglia,[195–198] a region of the brain associated with motor function, cognition, emotions, and learning. Globally, brain cell types that typically stain for iron in healthy systems are oligodendrocytes, microglia, some astrocytes, and neurons, with oligodendrocytes being the most rich in iron.[199,200] These iron concentrations typically correspond to the ferritin concentrations in these cells with exception in dopaminergic neurons within the substantia nigra and noradrenergic neurons of the locus ceruleus, where instead, much of the iron is localized in neuromelanin granules.[201] Biological iron is most commonly found in the +2 (ferrous) and +3 (ferric) oxidation states, though higher oxidation states can be generated in enzymatic catalytic cycles. $Fe^{2+/3+}$ concentrations in the extracellular environment are in the low micromolar range in the cerebrospinal fluid (CSF)[202] and are typically between 20 and 30 μM in the blood serum of a normal human adult. Intracellular iron concentrations in neurons can range from 0.5 to 1.0 mM.[203] A majority of this brain iron is tightly held by the storage protein ferritin (Ft). Other protein-bound iron stores are housed in the iron transport protein transferrin (Tf), iron−sulfur proteins (e.g., aconitase), heme enzymes (e.g., cytochrome *c* oxidase, catalase, cytochrome P-450), and nonheme iron enzymes (e.g., tyrosine hydroxylase, ribonucleotide reductase). Despite the widespread need for iron in brain tissue, only about 5−10% of brain iron is estimated to be essential for iron-dependent processes.[204] A large portion of this unutilized Fe, estimated to be between 33%[202] and 90%,[205] is chelated as Fe^{3+} in Ft. The presence of exchangeable iron in the brain has been proposed to exist in the intracellular environment, in a store termed the labile iron pool (LIP).[206–208] This putative buffered reservoir contains labile Fe^{2+} and Fe^{3+} ions bound by small anions (PO_4^{3-}, CO_3^{2-}, citrate), polypeptides, and surface components of membranes (i.e., phospholipid head groups).[209] The existence of this pool is still under active debate as methods for probing the LIP have not yet been optimized and standardized. Despite only being vaguely defined, estimated concentrations of Fe in the LIP range from 50 to 100 μM under normal conditions and can vary during times of iron overload or deprivation.[210] We note that this potential labile iron pool in the brain is redox-active whereas the labile zinc pool is not, which offers a new dimension of reactivity for the former. The large amount of iron in the brain, questions regarding its function, and the observation that iron accumulates in the brain with age have made its neurobiology a subject of great interest to chemists and biologists alike.

3.1.2. Brain Iron Homeostasis

The abundance of iron in the brain and throughout the body and its potent redox activity requires tight regulation to avoid oxidative damage to the cell by unbridled iron-based Fenton chemistry, as illustrated in Figure 6.[211–214] To circumvent the insolubility of Fe^{3+} at neutral pH, the body extensively utilizes two proteins, ferritin (Ft) and transferrin (Tf), for the storage and trafficking of iron. Ft is a globular iron storage protein[215] consisting of 24 subunits[216] that can bind up to 4500 iron atoms in its 80 Å cavity in a nontoxic,

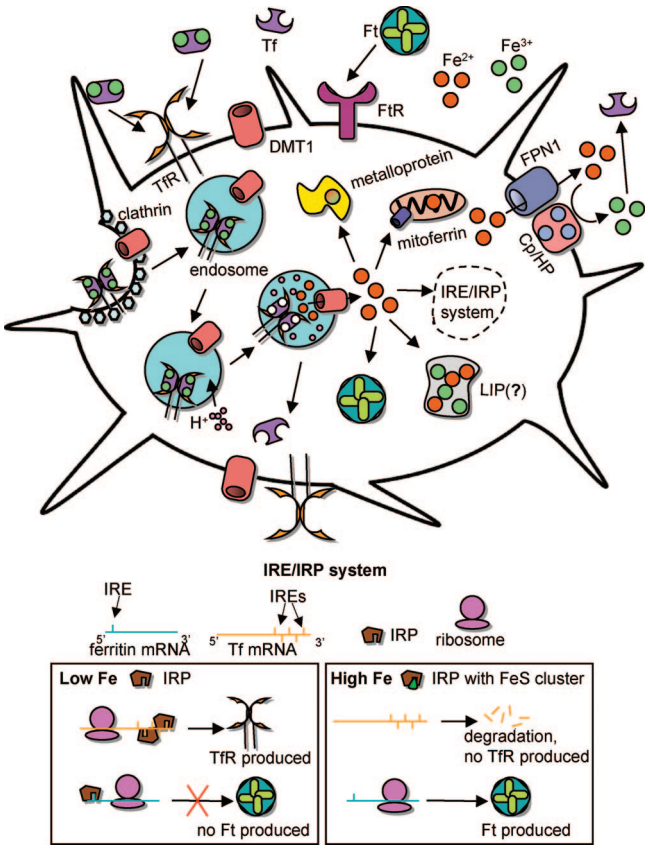

Figure 6. A schematic model for brain iron homeostasis. List of abbreviations: Cp, ceruloplasmin; DMT1, divalent metal transporter-1; FPN1, ferroportin-1; Ft, ferritin; FtR, ferritin receptor; HP, hephaestin; IRE, iron responsive element; IRP, iron regulatory protein; LIP, labile iron pool; Tf, transferrin; TfR, transferrin receptor.

water-soluble, and bioavailable form. In humans and other mammals, Ft consists of two types of polypeptide chains, termed heavy (H) and light (L), that are present in variable amounts in the protein. H chains possess ferroxidase centers that rapidly oxidize Fe^{2+} to Fe^{3+}, which then binds to L chains present in the core of the protein for storage. The relative ratios of H- and L-ferritin depend on cell type, with neurons expressing predominantly H-ferritin, microglia expressing mostly L-ferritin, and oligodendrocytes containing equal amounts of both chains.[217] Tf is an abundant bilobal protein found most commonly in plasma[218] and contains two high-affinity ferric binding sites ($K_d \approx 10^{-22}$ M)[219] for transporting iron throughout the body. Tf in the brain is produced almost exclusively by oligodendrocytes (~95%)[220,221] and, in conjunction with the storage protein ferritin, plays a critical role in brain iron homeostasis.

Iron is initially absorbed through the gastrointestinal tract and eventually incorporated into proteins such as Ft and plasma Tf, and uptake of iron into the brain through the blood−brain barrier (BBB) requires Tf and the transferrin receptor (TfR).[213] In the diferric state, Tf is recognized by TfR and the resulting $TfFe_2$−TfR complex is endocytosed. Evidence that these proteins are essential for transport of iron across the BBB comes from antibody studies of brain endothelial cells,[222] which showed that the tightly packed endothelial cells that compose blood capillaries of the BBB contain TfRs in mice and humans. In contrast, endothelial cells of other organs do not express TfRs, suggesting that this receptor may be a key mediator of iron transfer into the brain. After the $TfFe_2$−TfR complex is internalized by the brain endothelial cells, the precise mechanism(s) by which Fe is subsequently released into the brain remain(s) unresolved; plausible possibilities include transcytosis of the complex, a process in which the complex is endocytosed on one side of the cell and exocytosed on the other, or proton-induced release of the metal ions within the endosome.[213]

Once in the brain, iron can enter cells through a few major pathways, depending on the cell type and brain region. The most common pathway occurs mainly in neurons in the gray matter and employs Tf and TfR in the transferrin-to-cell cycle. The initial step, similar to the proposed mechanism for Fe uptake through the BBB, involves the internalization of the $TfFe_2$−TfR complex into the cell via clathrin-coated endosomes. Acidification of the endosome releases Fe^{3+} from Tf, and the Fe^{3+} is subsequently reduced to Fe^{2+} through a mechanism that has yet to be elucidated. The divalent metal transporter-1 (DMT1) transports Fe^{2+} out of the endosome to mitochondria via mitoferrin, a mitochondrial iron importer that is a member of the SLC25 solute carrier family,[223] and other unidentified Fe transporters for the biosynthesis of heme and iron−sulfur clusters. Any spillover iron is subsequently stored in Ft. The apoTf−TfR complex is shuttled back to the cell membrane and released to position Tf for another Fe binding cycle. An alternative pathway for iron uptake into cells employs Ft and Ft receptors (FtR), chiefly expressed in the white matter (that is, the brain region containing myelinated fibers that connect different regions of gray matter) in oligodendrocytes.[224,225] Similar to the Tf/TfR pathway, the Ft/FtR complex is endocytosed into cells in an ATP- and clathrin-dependent fashion, and ultimately, Ft-derived Fe ions are delivered to the cell.[226] A third potential distinct pathway for brain cell iron uptake utilizes another iron-binding protein, lactoferrin, for importing iron into neuromelanin cells.[212]

Iron homeostasis within the cell is regulated on a translational level with iron responsive elements (IREs) and iron regulatory proteins (IRPs).[227−231] IREs are nucleotide sequences found on mRNA, while IRPs recognize and bind IREs to control the translation of a mRNA sequence. Two main IRPs have been identified: IRP1, which is ubiquitously expressed throughout the body, and IRP2, which is localized mainly to the intestine and the brain. Expression of TfR, Ft, and other proteins involved in iron metabolism is tightly orchestrated by IRP/IRE interactions. Five IREs are present on the 3′ end of TfR mRNA and one IRE appears on the 5′ end of Ft mRNA. During times of iron depletion, the cell compensates through an elegant balance of translational regulation: IRPs bind to IREs of TfR mRNA to prevent the message degradation and ensure that iron uptake is maximized, whereas translation of Ft mRNA is halted when an IRP binds to the Ft mRNA IRE to minimize the population of iron bound in storage proteins. An overabundance of intracellular iron induces a conformational change in the IRPs to prevent IRE binding. This conformational change is due to the formation of an iron−sulfur cluster within the protein.[232] The consequences of this change are 2-fold: Ft synthesis is up-regulated in order to sequester the excess iron, and TfR mRNA degradation is increased to minimize further uptake. In addition to Ft and TfR, other proteins whose expression is controlled by the IRP/IRE system include DMT1, ferroportin-1 (FPN1), and cytochrome *b* reductase-1 (DCYTB).

Export of iron from the cell is controlled by ferroportin-1 (FPN1), also known as iron-regulated transporter-1 (IREG1)

or metal transport protein-1 (MTP1).[233–236] FPN1 is expressed in the basolateral surfaces of duodenal enterocytes, placental syncytiotrophoblasts, liver and spleen macrophages, and the brain.[233,234,237,238] Genetic evidence for the role of FPN1 in iron transport was obtained from studies of zebrafish with the *weissherbst* mutation that affects the FPN1 gene; these organisms suffer from hyperchromic anemia due to low iron levels in the blood.[234] A separate study showed that overexpression of FPN1 leads to intracellular iron deficiency,[233] indicating a role for this protein in cellular iron efflux. FPN1 transports Fe out of cells in the form of Fe^{2+}, and while the exact source of Fe^{2+} is unknown, the LIP or an Fe-chaperone protein have been proposed. Fe^{2+} efflux requires the presence of a ferroxidase, such as ceruloplasmin (Cp) or hephaestin (HP), which presumably oxidizes the Fe^{2+} to Fe^{3+} in the extracellular space.[234,235,239,240] For example, experiments in *Xenopus* oocytes establish that FPN1 mediates iron efflux out of the cell only in the presence of HP[235] and that mutations in the HP gene result in altered cellular Fe homeostasis.[240] Glycosylphosphatidylinositol-anchored Cp (GPI-Cp) is highly expressed in brain astrocytes and plays a similar role in mediating iron efflux from these cells.[241] Recently, colocalization of FPN1 and HP has also been reported in astrocytes, microglia, oligodendrocytes, and neurons,[242] providing further evidence for the need for a ferroxidase. The IRP/IRE system regulates FPN1 expression, but in addition, FPN1 is post-translationally regulated by the peptide hormone hepcidin[243] found in regions including the liver and the central nervous system.[244] Binding of hepcidin to FPN1 induces endocytosis of the protein, preventing iron export.[243]

3.2. Physiological and Pathological Functions of Brain Iron

3.2.1. Iron Neurophysiology

Iron is an indispensable metal in the body as a component of numerous metalloproteins.[194] In addition to Fe storage and transport proteins, many enzymes exploit the ability of Fe to attain several oxidation states, including the heme-containing oxygen transport proteins hemoglobin and myoglobin, oxygenase enzymes such as cytochrome P450 and tyrosine hydroxylase, and electron transfer proteins that require Fe−S clusters or heme-containing cytochromes *a*, *b*, and *c*.

The brain has specialized requirements for Fe redox chemistry above normal oxidative metabolism. In particular, enzymes involved in neurotransmitter synthesis have a more specific significance with respect to neurophysiology. Fe is a required cofactor for three tetrahydrobiopterin-dependent metalloenzymes that are key players in neurotransmitter synthesis: phenylalanine hydroxylase, tyrosine hydroxylase, and tryptophan hydroxylase. Phenylalanine hydroxylase converts phenylalanine to tyrosine, which is then shuttled to tyrosine hydroxylase to convert tyrosine to dihydroxyphenylalanine (L-DOPA). L-DOPA is an essential precursor to dopamine, a neurotransmitter important in motor function, behavior and cognition, motivation and reward, etc. Changes in Fe concentration in the brain greatly affect this dopaminergic system, with noticeable behavioral changes in subjects when brain iron content drops more than 15% below normal levels.[245] Dopamine is in turn a precursor to norepinephrine and epinephrine, neurotransmitters responsible for the body's "fight or flight" response. As a component of tryptophan hydroxylase, Fe facilitates the conversion of tryptophan to 5-hydroxytryptophan; the latter is an essential precursor to serotonin, a neurotransmitter connected to appetite, sleep, anger, aggression, etc.

Iron also plays direct and indirect roles in myelin synthesis in the brain.[246] Myelin is the insulating phospholipid layer found on oligodendrocytes and other cells in the white matter, which serves to increase the speed of impulses that run along myelinated fibers in the brain. Two key components of myelin are cholesterol and lipids, and iron is required for proteins that synthesize and metabolize organic myelin building blocks. For example, the heme-dependent cytochrome P450 family is important in cholesterol synthesis, whereas nonheme iron is required for enzymatic lipid synthesis and degradation through fatty acid desaturases and lipid dehydrogenases, respectively. Iron deficiency results in hypomyelinization[247,248] and is associated with multiple sclerosis and several other neurodegenerative diseases.[249,250]

3.2.2. Iron Neuropathology

An intriguing and unexplained fact is that iron levels rise in the brain as a function of age. Fe accumulation occurs in specific areas of the brain and is associated with a variety of neurodegenerative diseases, including Alzheimer's disease (AD) and Parkinson's disease (PD).[212,251] The propensity of Fe ions to participate in redox chemistry poses risks for oxidative damage if unregulated, as Fe accumulation can promote aggregation and formation of plaques by Fenton-type oxidation of biomolecules and coordination-mediated cross-linking.

PD is the second most common neurodegenerative disease after AD, affecting 2% of people over the age of 65.[252] One main characteristic of this disease is the loss of neuromelanin-containing (pigmented) dopaminergic neurons in the substantia nigra, leading to decreased levels of dopamine and subsequent motor symptoms including tremors, rigidity, and motor slowing.[212,253] The precise cause(s) of PD remains largely unknown, but a hallmark of this disease is a perturbation of brain iron homeostasis. In particular, elevated levels of iron in PD in the basal ganglia, the region of the brain that controls motor function, may trigger neurite degeneration via oxidative stress.[253–255] Moreover, imbalances in the ratio of iron between the lateral globus pallidus and the medial globus pallidus within the basal ganglia occur in this neurodegenerative disease, resulting in more iron in the lateral versus medial region.[256,257] Abnormal iron deposits are present in oligodendrocytes, astrocytes, microglia, and pigmented neurons and in the rim of Lewy bodies in PD patients (*vide infra*).[258]

The source(s) of excess iron in PD remain(s) insufficiently defined, but one hypothesis is that localized disruptions in the BBB result in increased brain iron content.[259] This proposal is supported by a study using radiolabeled verapamil hydrochloride, a substrate for the P-glycoprotein multidrug resistance system in the cell membrane that does not typically cross the BBB. Uptake of verapamil into the midbrain is observed in PD patients but not in healthy subjects. An alternative pathway for disruption of Fe homeostasis occurs via misregulation of normal brain iron regulatory systems as serum iron levels are largely unaltered in PD patients.[260,261] Though increases in TfR are observed in the caudate nucleus and putamen, TfR levels in dopaminergic melanized neurons are within normal ranges, suggesting that the Tf/TfR system is not a likely source of excess Fe accumulation in these

neurons.[262] Increased loading of ferritin is observed in PD[257] but has not been verified as causal. Lactotransferrin and lactotransferrin receptors are elevated in the substantia nigra of PD brains and are a potential source of Fe accumulation within this region of the brain.[263,264] Internal iron redistribution in PD is plausible, but no data to support this notion have been obtained.[253]

Interactions between excess Fe ions and various molecules in the brain are implicated in the pathology of PD. For example, Fe^{3+} complexes of the pigment neuromelanin (NM) have been identified in neurons within the substantia nigra.[265,266] In these dopaminergic neurons, NM−Fe^{3+} complexes are sequestered in neuromelanin granules,[201] which can then be released into the extracellular environment. Because these species can then in turn induce the release of neurotoxins from microglia,[267] formation and translocation of NM−Fe^{3+} complexes from degenerating neurons can trigger a cascade of events leading to neurodegeneration via microglial toxins. PD patients that exhibit the largest increases in NM−Fe^{3+} in their substantia nigra neurons also suffer the most severe neuronal loss.[268] Also present in PD brains are Lewy bodies, which are aggregates of the protein α-synuclein.[269,270] Interactions between the ferric ion and α-synuclein have been studied, and the presence of Fe^{2+}/Fe^{3+} with H_2O_2 causes *in vitro* aggregation of α-synuclein into fibrils that resemble those found in Lewy bodies in PD patients.[271]

Iron accumulation in the brain is also connected to AD. Abnormally high levels of Fe (in addition to Zn and Cu) occur in Aβ plaques in postmortem AD brains[110] and can potentially impact the formation of Aβ plaques via several different pathways, including oxidative stress caused by buildup of redox-active metals Fe and Cu, which results in the oxidation and subsequent cross-linking of Aβ species.[272] On a translational level, intracellular iron levels and distributions may also affect the expression of APP, the precursor to Aβ.[273] In this regard, an IRE has been identified on the 5′ end of APP mRNA, indicating that APP production is up-regulated in situations of iron overload. Cellular Fe also affects the post-translational processing of APP, slowing the activity of the α-secretase protein that generates nonamyloidogenic fragments from APP.[274] Elevations in the amyloidogenic processing of APP generate more Aβ and increase the likelihood of plaque formation. In addition to being present in Aβ plaques, Fe is also found in the neurofibrillary tangles (NFT) observed in AD.[275] These protein aggregates are comprised of oxidatively damaged Tau protein that likely result from metal-induced oxidative stress.

Aside from PD and AD, several other neurodegenerative diseases can be linked to alterations in brain iron homeostasis. In the genetic disorder Huntington's disease (HD),[276] increased iron content in the striatum is observed both in early stage HD[277] and in postmortem HD brains,[278–280] accompanied by an increased density of oligodendrocytes, the most iron-rich cells in the brain, and the iron-containing myelin they produce.[281,282] Other diseases whose pathologies comprise iron trafficking and distribution in the brain include Friedreich's ataxia, [283] aceruloplasminemia,[284] Hallervorden−Spatz syndrome,[285] neuroferritinopathy,[286] and multiple sclerosis.[287]

3.3. Molecular Imaging of Brain Iron

3.3.1. Overview of Traditional Iron Detection Methods

The ability to specifically detect ferrous (Fe^{2+}) and ferric (Fe^{3+}) ions in biological environments is critical for fully elucidating the complex physiological and pathological roles of Fe in living systems. Both Fe^{2+} ($4s^23d^6$) and Fe^{3+} ($4s^23d^5$) are well suited for interrogation by several spectroscopic techniques due to their unfilled d-shells, their paramagnetic nature (labile Fe^{2+} is predominantly high spin in aqueous biological environments), and their various isotopes. In addition to AA[288] and inductively coupled plasma (ICP) spectroscopy,[256,289] histochemical staining is another traditional method to study iron in the brain. One of the earliest assays for detecting Fe^{3+} is Perls' method,[290] a histochemical stain that exploits the ability of labile Fe^{3+} to react with ferrocyanide ($[Fe(CN)_6]^{4-}$ to yield the intensely colored Prussian blue compound ($Fe_7(CN)_{18}\cdot xH_2O$). Administration of the colorless ferrocyanide and HCl (to release nonheme iron) to postmortem brains of PD patients elicits bright blue-colored staining in oligodendrocytes, microglia, and macrophages but not in neurons, demonstrating the relative insensitivity of this technique.[258] The addition of diaminobenzidine[197,291] or Ag^{+}[292] provides some improvement for iron detection. The Turnbull method is a modified Perls' method that uses ferricyanide ($[Fe(CN)_6]^{3-}$) instead of ferrocyanide to detect Fe^{2+},[293] following pretreatment with ammonium sulfide as a reducing agent to prevent air oxidation.[294] Although these methods are of utility for qualitative Fe^{3+} and Fe^{2+} detection, they suffer from several disadvantages including insensitivity, toxicity, and the need to use fixed samples.

Various isotopes of Fe have also been utilized to track iron in the brain. Radioactive ^{59}Fe, with a half-life of almost 45 days, can probe the transport of Fe across the BBB and throughout the brain.[202] ^{59}Fe detection can provide useful information regarding the gross distribution of iron but lacks subcellular resolution and cannot distinguish between different oxidation states of the metal. Moreover, this isotope exposes subjects to ionizing radiation. Another iron isotope, ^{57}Fe, can be monitored using Mössbauer spectroscopy and has been applied to characterize Fe content in the substantia nigra of postmortem PD brains.[295] Mössbauer spectroscopy is a potentially powerful technique for probing brain iron owing to its ability to aid in determining oxidation state, spin state, and sometimes speciation. Unfortunately, ^{57}Fe is only 2% naturally abundant, so signal-to-noise is an issue unless samples are enriched with this expensive isotope. In addition, the lower temperatures typically used in Mössbauer experiments most likely limits measurements to fixed biological samples.

Finally, more sophisticated methods, including extended X-ray absorption fine structure (EXAFS),[257] X-ray fluorescence,[296] and laser microprobe mass analysis (LAMMA), have been used to characterize iron in biological samples. For example, in LAMMA, a small portion of a sample is vaporized, ionized by a high-energy laser pulse, and analyzed by mass spectrometry. The detection limit for LAMMA is ca. 3 ppm, allowing this technique to identify increased iron and aluminum concentrations in neurons bearing NFT in AD patients[275] and in NM granules.[297] However, LAMMA and the other aforementioned techniques are sample destructive and cannot be used in live biological settings.

Chart 7. Turn-off Fluorescent Sensors for Fe^{2+}

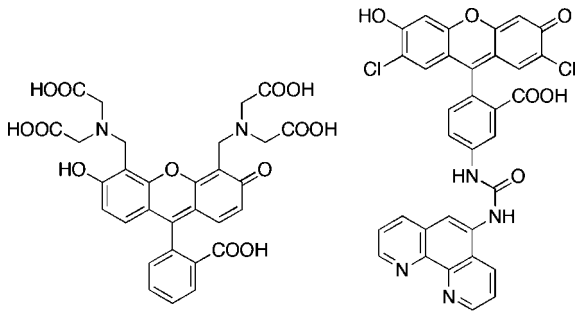

Calcein, **62** Phen Green SK, **63**

3.3.2. Criteria for Molecular Imaging of Iron in Living Systems

Effective fluorescence- and MR-based probes for studying iron in living systems must meet the same general criteria as for other metal sensors, including selectivity, optical qualities, and biological compatibility. In addition, methods that would allow for selective Fe^{3+} or Fe^{2+} detection would be desirable. One major challenge for systems involving iron chelators is the propensity for oxidation of Fe^{2+} to Fe^{3+} under ambient conditions, preventing differentiation between these two oxidation states. Another challenge is the issue of spin, because the spin-state plasticity of d^5 and d^6 iron ions in different electronic and structural environments can greatly complicate sensor design. With specific regard to fluorescent sensing, probes that exhibit a turn-on increase response to Fe ions are preferred but are difficult to obtain owing to the paramagnetic quenching nature of Fe^{2+} and Fe^{3+} in aqueous, biological environments. Table 2 provides a summary of properties for Fe^{2+}/Fe^{3+} detectors.

3.3.3. Survey of Fluorescent and MRI Iron Sensors

3.3.3.1. Turn-off Fluorescent Sensors for Iron. Two commercially available fluorophores for general metal ion detection have been applied as turn-off sensors for Fe^{2+} ions (Chart 7), calcein (**62**) and Phen Green SK (**63**). Calcein is a fluorescein-based probe with an EDTA-like chelating moiety for metal ion binding. A 46% decrease in calcein fluorescence is observed upon addition of excess Fe^{2+}, whereas Fe^{3+} elicits only a 6% emission turn-off.[298] Calcein binds Fe^{2+} tightly ($K_d = 10^{-14}$ M), but this probe is not iron-selective because it also exhibits high turn-off responses to Cu^{2+}, Ni^{2+}, and Co^{2+}. Phen Green SK is another commercially available probe that displays a nonspecific fluorescence turn-off with Fe^{2+} (93% quenching), Fe^{3+} (51%), and other metal ions (Cu^{2+}, Cu^{+}, Hg^{2+}, Pb^{2+}, Cd^{2+}, and Ni^{2+}).[299] Cells loaded with Phen Green SK show weak fluorescence that increases upon addition of 2,2′-bipyridine. Though these experiments suggest that Phen Greek SK is capable of responding to iron levels in the cell, given the low selectivity of both the probe and bipyridine for Fe^{2+}, a portion of the response may be due to binding of other metal ions.

Several turn-off probes for Fe^{3+} have been developed using receptors derived from siderophores, which are chelating natural products excreted by microorganisms for Fe^{3+} sequestration (Chart 8). Intrinsically fluorescent siderophores such as azotobactin ∂ (**64**) ($\lambda_{ex} = 380$ nm; $\lambda_{em} = 490$ nm) have been employed for ferric ion detection.[300] Azotobactin ∂ is a highly sensitive probe for Fe^{3+} ($K_d = 8 \times 10^{-29}$ M) with relatively good selectivity, showing some interference only with Cu^{2+} and Al^{3+}. Siderophores tethered to fluorescent dyes have also been reported for iron sensing, including desferrioxamine with appended fluorescein (FL-DFO, **65**)[301] or nitrobenzoxadiazole (FL-NBD, **66**)[302] moieties, as well as a ferrichrome-type siderophore linked to NBD (**67**).[303] These probes maintain the high sensitivity and selectivity of unmodified siderophores but still respond by quenching. Finally, fluorophores bearing siderophore-inspired hydroxypyridinone groups for Fe^{3+} chelation have been reported.[155,304,305] A library of compounds using a coumarin scaffold modified with a bidentate chelator were synthesized including coumarins **68**[155] and **69**.[305] These cell-permeable fluorophores are efficiently quenched (>90%) by Fe^{3+} and bind the metal ion in a 3:1 ligand to metal stoichiometry. A smaller analog (**70**), in which the fluorescent moiety and the hydroxypyridinone chelator are incorporated into a more compact unit has been explored to study the distribution of therapeutic iron chelators in biological settings.[304]

3.3.3.2. Turn-on Fluorescent Probes for Iron. A few probes have been described that exhibit a turn-on fluorescence response to iron ions but none have been utilized successfully for biological assays (Chart 9). A coumarin platform (**71**) modified with two aza-18-crown-6 moieties displays increased fluorescence ($\lambda_{ex} = 336$ nm; $\lambda_{em} = 412$ nm) in the presence of aqueous Fe^{3+} with a moderate affinity for Fe^{3+} ($K_d = 6.7$ μM).[306] BODIPY-based **72** contains a pendant dithia-aza-oxa macrocycle and exhibits a turn-on response in acidic aqueous solution (pH 5−6).[307] This dye exhibits dual emission profiles in aqueous solution from locally excited (LE, $\lambda_{em} = 508$ nm) and charge transfer (CT, $\lambda_{em} = 634$ nm) states. The ratio of fluorescence intensities between these bands (I_{CT}/I_{LE}) in the apo state is ∼5.5, a value that changes to ∼0.5 with Fe^{3+} binding as LE emission increases and CT emission decreases.

Another approach to Fe^{3+} detection exploits the reversible equilibrium between the spirolactam and ring-opened forms of rhodamine, an approach that has also been used for detection of Cu^{2+} (*vide infra*).[308] Two rhodamine B scaffolds were linked with diethylenetriamine to make sensor **73**.[309] Fe^{3+} binding to the diethylenetriamine linker converts the nonfluorescent spirolactam into its fluorescent ring-opened form ($\lambda_{ex} = 510$ nm; $\lambda_{em} = 575$ nm). In aqueous solution, **73** responds selectively to Fe^{3+}, though its affinity for Fe^{3+} is weak ($K_d = 316$ μM). A similar design has been reported on a single rhodamine scaffold (FDI, **74**).[310]

Finally, a turn-on probe for Fe^{2+} has been developed based on the ability of this ion to reduce the organic radical TEMPO in aqueous solution (Chart 10).[311] Attachment of TEMPO to pyrene produces weakly fluorescent spin fluorescent probe **75** ($\lambda_{ex} = 358$ nm, $\lambda_{em} = 430$ nm). Addition of Fe^{2+} under acidic aqueous conditions triggers an increase in fluorescence, presumably due to loss of the TEMPO radical according to EPR measurements. This reaction is selective for Fe^{2+} over other metal ions including Fe^{3+} but can proceed with other radicals, which will limit its utility in biological settings.

3.3.3.3. MR Methods for Detecting Iron. No smart MRI probes for specific detection of biological iron have been reported in the literature, though one trimeric contrast agent has been described in which three Gd^{3+}-DO3A complexes are linked via the supramolecular assembly of a tris-phenanthroline−Fe^{2+} complex.[312] This assembly is not selective for iron but does provide evidence that iron binding

Chart 8. Turn-off Fluorescent Sensors for Fe^{3+}

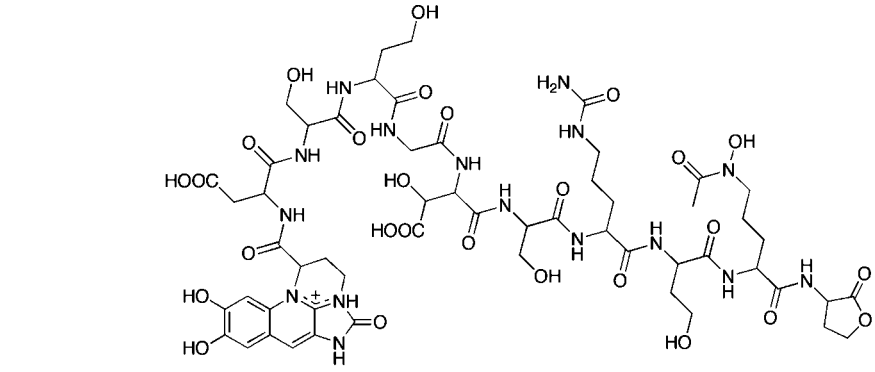

azotobactin ∂, **64**

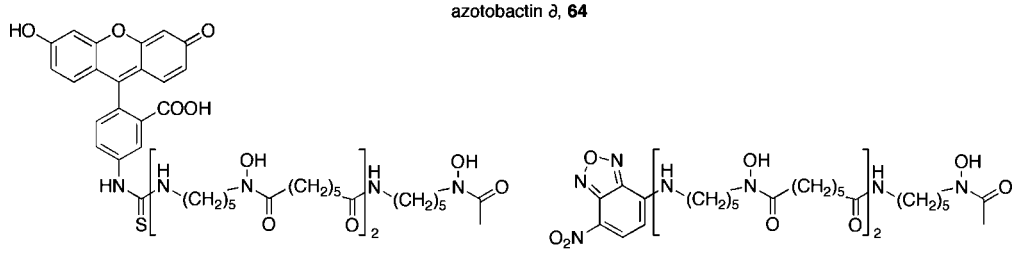

FL-DFO, **65** NBD-DFO, **66**

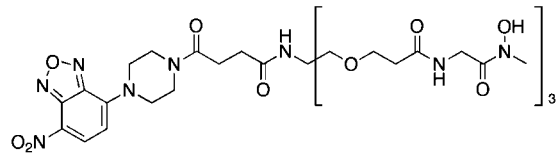

Ferrichrome-NBD, **67**

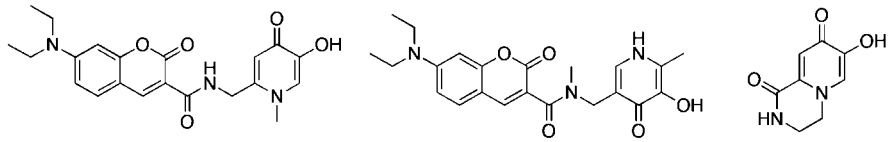

68 **69** **70**

Chart 9. Turn-on Fluorescent Sensors for Fe^{3+}

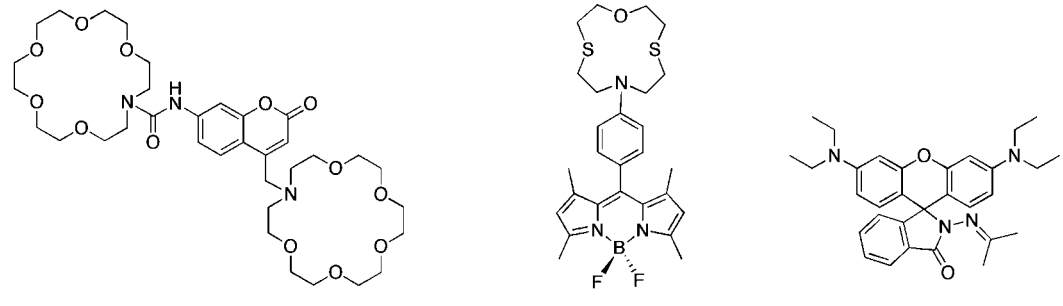

71 **72** **74**

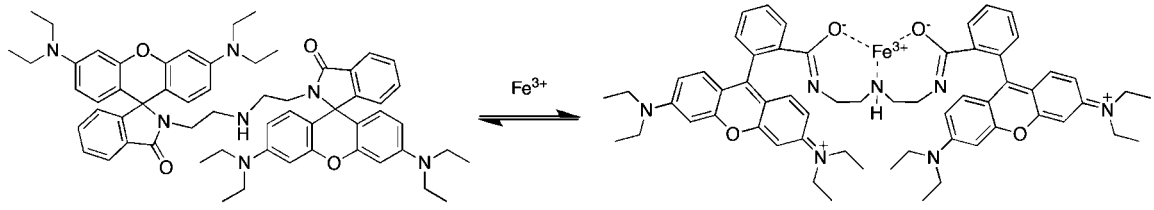

73

can change relaxivity values for Gd-based MRI contrast agents. As such, current MRI of iron in living systems is confined to probing naturally occurring iron stores in the body, including the brain.[313] Owing to their largely para-

Chart 10. A Turn-on Fluorescent Probe for Fe^{2+}

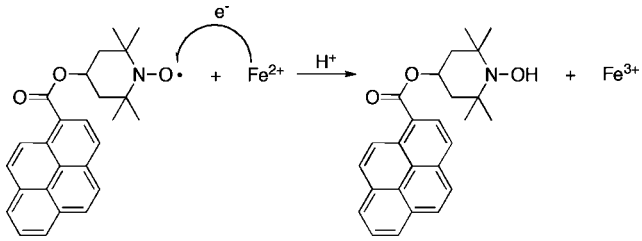

75

magnetic nature in biological settings, Fe ions themselves can affect the relaxation rate of interacting water molecules to an extent observable by MRI. In the brain, approximately $^1/_3$ of nonheme iron is stored in Ft and can be visualized by MRI by either T_1 or T_2 water relaxation, though the latter is more effective. Some results on intrinsic iron-based MRI have been reported and compared with histochemical staining; regions of high iron content visualized by MRI (globus pallidum, reticular substantia nigra, red nucleus, and dentate nucleus) corresponded well to the areas of highest staining using Perls' method.[314] In addition, MRI studies of diseased states, such as Parkinson's disease and Alzheimer's disease, have revealed notable differences in iron homeostasis.[315–317] For example, MRI studies of AD patients revealed increased iron content in the basal ganglia,[318,319] and increased iron content in the substantia nigra was observed using MRI measurements in PD patients.[320–326] The substantia nigra data are particularly informative due to the robust signal from ferritin in this brain region; not only can increased iron deposition be detected in PD patients, but changes in the width of the pars compacta of the substantia nigra can be detected as well.

4. Copper in Neurobiology

4.1. Basic Aspects of Copper in the Brain

4.1.1. Tissue Concentrations and Distributions

Copper is the third-most abundant transition metal in the body[327] and in the brain, with average neural copper concentrations on the order of 0.1 mM.[328] This redox-active nutrient is distributed unevenly within brain tissue, as copper levels in the gray matter are 2- to 3-fold higher than those in the white matter.[329] Copper is particularly abundant in the locus ceruleus (1.3 mM), the neural region responsible for physiological responses to stress and panic, as well as the substantia nigra (0.4 mM), the center for dopamine production in the brain.[328] The major oxidation states for copper ions in biological systems are cuprous Cu^+ and cupric Cu^{2+}; the former is more common in the reducing intracellular environment, and the latter is dominant in the more oxidizing extracellular environment. Levels of extracellular Cu^{2+} vary, with Cu^{2+} concentrations of 10−25 μM in blood serum,[330] 0.5−2.5 μM in cerebrospinal fluid (CSF),[331] and 30 μM in the synaptic cleft.[1] Intracellular copper levels within neurons can reach 2 to 3 orders of magnitude higher concentrations.[332]

Like zinc and iron, brain copper is partitioned into tightly bound and labile pools.[333] Owing to its redox activity, copper is an essential cofactor in numerous enzymes, including cytochrome *c* oxidase (CcO), Cu/Zn superoxide dismutase (SOD1), ceruloplasmin (Cp), and dopamine β monooxygenase (DβM), that handle the chemistry of oxygen or its metabolites. Labile brain copper stores have been identified in the soma of cortical pyramidal and cerebellar granular neurons, as well as in neuropil within the cerebral cortex, hippocampus, red nucleus, cerebellum, and spinal cord.[334] Additional pools of exchangeable copper are located in synaptic terminal membranes of afferent neurons throughout the brain, including the locus ceruleus.[335] Pools of labile copper in low micromolar concentrations may also exist in the extracellular environment as demonstrated by depolarization experiments (*vide infra*).[336,337] The widespread distribution and mobility of copper required for normal brain function, along with the numerous connections between copper misregulation and a variety of neurodegenerative diseases, have prompted interest in studying its roles in neurophysiology and neuropathology.

4.1.2. Brain Copper Homeostasis

Because of its central importance to neurological health and its propensity to trigger aberrant redox chemistry and oxidative stress when unregulated, the brain maintains strict control over its copper levels and distributions.[333,338–340] An overview of homeostatic copper pathways in the brain is summarized in Figure 7. Many of the fundamental concepts for neuronal copper homeostasis are derived from rigorous studies of simple model bacterial or yeast microbes, but the brain provides a more complex system with its own unique and largely unexplored inorganic physiology. For example, work by O'Halloran and co-workers indicates that there is little "free" copper in the cytoplasm of bacteria and yeast, which is due to the tight regulation of metallochaperones.[341] However, many open questions remain concerning the homeostasis of organelle copper stores, particularly in higher organisms with specialized tissues. In this context, Winge and co-workers have presented data that suggests that even yeast possess stores of labile copper in their mitochondria.[342]

Uptake of copper by the blood−brain barrier (BBB) is not well understood but is proposed to occur through the P-type ATPase ATP7A, which can pump copper into the brain. Mutations in this specific gene lead to Menkes disease, an inherited neurodegenerative disorder that is characterized by global brain copper deficiency. This phenotype is mirrored by Wilson disease, which involves mutations in the related ATP7B gene responsible for excretion of excess copper from the liver into the bile.[343] Loss of ATP7B function leads to abnormal buildup of copper in the liver. The extracellular trafficking of brain copper is also different from that in the rest of the body. Cerebrospinal fluid (CSF), the extracellular medium of the brain and central nervous system, possesses a distinct copper homeostasis from blood plasma, which carries copper to organs throughout the rest of the body. Ceruloplasmin (Cp), a multicopper oxidase that is essential in iron metabolism,[344] is the major carrier of Cu^{2+} in plasma, but houses less than 1% of copper in extracellular CSF.[332] The primary protein or small-molecule ligands for copper in CSF remain unidentified.

Uptake of copper into brain cells requires reduction of Cu^{2+} to Cu^+. Ferric reductases Fre1p and Fre2p fulfill this role in yeast,[345,346] but brain analogs have yet to be identified in humans and other higher eukaryotic organisms. Following reduction, Cu^+ ions can be transported into cells through a variety of protein-based pathways. For example, a major class of proteins involved in cellular copper uptake is the copper transport protein (Ctr) family. Human copper transporter-1 (hCtr1) is a representative member that is expressed ubiq-

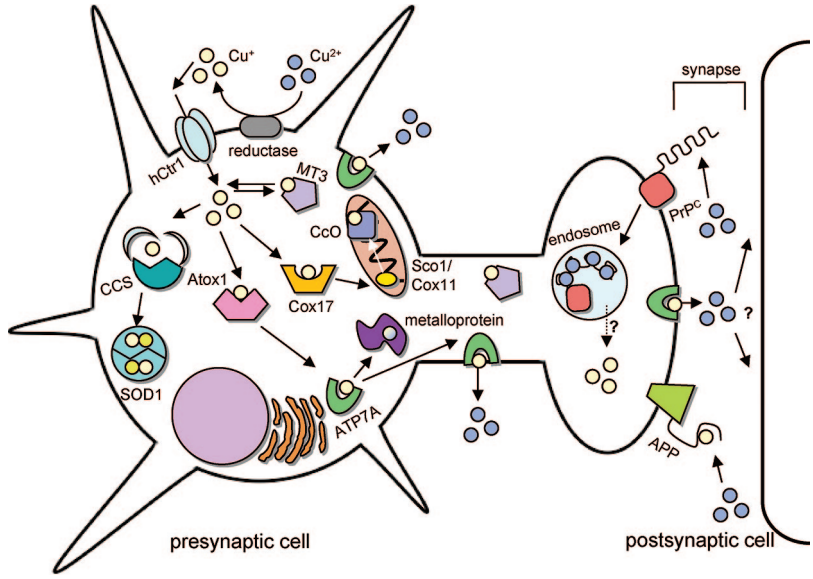

Figure 7. A schematic model of neuronal copper homeostasis. List of abbreviations: APP, amyloid precursor protein; Atox1, copper chaperone for ATP7A/B; ATP7A, Menkes P-type ATPase; CcO cytochrome *c* oxidase; CCS, copper chaperone for superoxide dismutase; Cox11, cytochrome *c* oxidase assembly protein; Cox17, copper chaperone for cytochrome *c* oxidase; hCtr1, human copper transporter-1; MT3, metallothionein-3; PrP^c, prion protein cellular form; Sco1, cytochrome oxidase deficient homologue 1; SOD1, Cu/Zn superoxide dismutase.

uitously in all tissues.[347–349] The energy-independent uptake of Cu^+ uptake by hCtr1 is induced by high concentrations of H^+ or K^+ or both in the extracellular milieu and is time-dependent and saturable.[327] This transport protein resides in the intracellular space until copper deficiency induces its movement to the plasma membrane. In situations of high cellular copper content, hCtr1 is endocytosed and subsequently degraded.[327,350,351] Two methionine-rich recognition motifs (Mets motifs) are implicated in this endocytotic response: (i) an extracellular domain (^{40}MMMMPM^{45}) that responds to low concentrations of copper for copper-stimulated endocytosis and (ii) a transmembrane domain (^{150}MXXXM^{154}) that is required for all hCtr1 endocytosis.[348] In addition to hCtr1 and its congeners, prion protein (PrP) and amyloid precursor protein (APP) are two other abundant copper-binding proteins found specifically at brain cell surfaces implicated in copper uptake/efflux.[352–359] The existence of these additional copper-handling proteins on brain cell surfaces implies a distinct homeostasis for copper at the plasma membrane of neurons compared with other cell types.

Upon its entry into brain cells, Cu^+ can be funneled to its ultimate intracellular destinations through the use of copper chaperone proteins or buffering by metallothioneins (MTs). Metallothioneins, in addition to aiding in cellular zinc homeostasis, can also bind Cu^+ and participate in the homeostasis of this metal ion. Although the molecular interactions between Cu^+ ions and brain-abundant metallothioneins such as MT1 (ubiquitously expressed) and MT3 (expressed in the brain) remain insufficiently understood, a recent structure of yeast MT shows eight bound Cu^+ ions in two thiolate clusters with an additional two cysteine residues not involved in copper binding that may mediate the exchange of Cu^+ between MT and copper chaperones.[360] In addition to MT, glutathione provides another abundant source of thiols within the cytosol for potential copper and/or redox buffering purposes.

The three most well-understood copper-specific metallochaperones in humans are Atox1 (or HAH1), CCS, and Cox17. These metallochaperones function not only as intracellular copper delivery agents but also as additional protective agents against toxicity resulting from unbound and unregulated copper ions. Atox1/HAH1 is the first reported human copper chaperone and loads Cu^+ into the Menkes and Wilson P-type ATPases, ATP7A and ATP7B, which are essential for the secretory pathway from the trans-Golgi network (TGN) to the plasma membrane. Its yeast analog, Atx1, was first identified as an antioxidant protein[361] but was later shown to be a copper chaperone for *Ccc*2, the yeast equivalent of ATP7A/B.[362] The human homologue Atox1 is a key component in the proper functioning of ATP7A[363] and ATP7B,[364] and both Atox1 and ATP7A/B contain MT/HCXXC sequence motifs that are proposed to be crucial for the interchange of copper between the two proteins. The X-ray crystal structure of the Cu^+ complex of Atox1 reveals a three-coordinate Cu^+ center bound by two Atox1 proteins via cysteine residues within these MT/HCXXC cassettes,[365] with an extended hydrogen-bonding network stabilizing the metal binding site.[366] The combination of available structural and biochemical data suggests a docking model that involves Cu^+ transfer through two- and three-coordinate Cu^+ intermediates.

The copper chaperone for superoxide dismutase, CCS, inserts Cu^+ into SOD1.[367] SOD1 exists as a homodimer, and examination of the amino acid sequences of SOD1 and CCS reveals a high degree of sequence homology. CCS domain II is 47% identical to SOD1 and includes the amino acids found along the SOD1 dimer interface, as well as the majority of the amino acids used for metal binding in SOD1.[368] The crystal structure of the yeast SOD1−yeast CCS heterodimer complex shows a heterodimer interface that is strikingly similar to the interface between the homodimers of its individual components. However, other data suggests that this interface alone is not sufficient for efficient transfer of Cu^+ between CCS and SOD1. For example, domain I contains the MXCXXC copper binding domain also found in the chaperone Atox1; however, deletion of this domain only slightly diminishes SOD1 activity, indicating that

domain I may only be essential in situations of copper starvation. On the other hand, domain III is highly conserved in many CCS homologues and may play a more direct role in copper transfer to SOD1. This domain possesses a CXC motif that can insert Cu^+ into SOD1 via potential interactions with domain I prior to metal ion relocation.[369]

A third copper chaperone found in humans is Cox17, which is one of the major proteins involved in delivering Cu^+ to cytochrome *c* oxidase (CcO) in mitochondria.[370] Because CcO is a complex, membrane-bound protein machine containing 13 subunits and numerous metal-dependent cofactors including copper, zinc, magnesium, and heme iron, a myriad of protein partners are required for its proper assembly, folding, and metal loading.[371–373] Cox17 shuttles between the cytoplasm and mitochondrial membrane space, where it can deliver Cu^+ to various CcO assembly proteins. This metallochaperone works in concert with Sco1 and Sco2 to load Cu^+ into the Cu_A electron transfer site of CcO,[371,374] and additional data suggests that Cox17 works with Cox11 to insert Cu^+ into the Cu_B site where catalytic O_2 reduction occurs.[372] Recent work establishes that Cox17 is capable of transferring Cu^+ to both Sco1 and Cox11, making this protein the first copper chaperone that can deliver Cu^+ into two different partners.[375] Cox17 contains three essential cysteine residues and can bind up to four Cu^+ ions in a polycuprous−thiolate cluster,[376] but the precise molecular interactions between Cox17 and these other assembly proteins have not been structurally characterized.

The secretion of copper from brain cells is governed by ATP7A and ATP7B, which shuttle from the trans-Golgi network (TGN) to the plasma membrane. These two proteins have 67% sequence homology and differ mainly in their tissue distribution and expression; ATP7A is expressed ubiquitously in all tissues whereas ATP7B is expressed predominantly in the liver with some expression in isolated regions of the brain.[327] These proteins can play multiple roles in neurons from the delivery of copper to cuproenzymes involved in neurotransmitter synthesis and metabolism to the removal of excess copper via secretion or intracellular sequestration.[377] Both ATP7A and ATP7B contain N-terminal metal binding MXCXXC motifs that can coordinate up to six Cu^+ ions with micromolar affinity[378,379] with an additional phosphatase domain and motifs for ATP binding, phosphorylation, and internalization. The growing list of functions of these ATPases in the brain and central nervous system and throughout the body remains an exciting and open frontier.[380] For example, studies of the cerebellum reveal that expression of ATP7A and ATP7B is cell specific in this region of the brain, with ATP7A expressed exclusively in Bergmann glia and ATP7B confined solely to Purkinje neurons, where the latter delivers Cu^+ to ceruloplasmin. In addition to ATP7A/B, APP and PrP are two other abundant neuronal proteins that may play a role in copper regulation at the plasma membrane in copper efflux capacities.

4.2. Physiological and Pathological Functions of Brain Copper

4.2.1. Copper Neurophysiology

Copper is a redox-active nutrient that is needed at unusually high bodily levels for normal brain function. Owing to the large oxygen capacity and oxidative metabolism of brain tissue, neurons and glia alike require copper for the basic respiratory and antioxidant enzymes cytochrome *c* oxidase (CcO) and Cu/Zn superoxide dismutase (SOD1), respectively. In addition, copper is a necessary cofactor for many brain-specific enzymes that control the homeostasis of neurotransmitters, neuropeptides, and dietary amines. Included are dopamine β monooxygenase (DβM), peptidylglycine α-hydroxylating monooxygenase (PHM), tyrosinase, and various copper amine oxidases.

Not only is brain copper required as a tightly bound cofactor for various enzymes and proteins, but labile and mobile stores of this redox-active element are also connected to basic brain function, particularly during neural activity. Early studies using isolated hypothalamus tissue[336] or synaptosomes[337] and radioactive copper isotopes provided evidence for release of copper ions at micromolar levels into the extracellular medium upon depolarization. A fluorescence assay in synaptosomes corroborated these findings,[381] and recent work by Dunn and Gitlin has linked the intracellular source of this released copper to the Menkes ATPase ATP7A via activation of NMDA receptors.[382,383] Another protein implicated in copper trafficking during neurotransmission is the prion protein (PrP^c), which is localized to synaptic membranes of presynaptic neurons.[357,358] Within the brains of higher mammals, PrP^c contains at least four octapeptide repeat domains in its N-terminal region that can bind Cu^{2+}.[331,384–388] Exposure of cells to millimolar concentrations of Cu^{2+} induces endocytosis of PrP^c,[359,389] an event that does not occur upon mutation of the copper binding region.[390] Because PrP^c knockout mice do not display major differences in total copper content or cuproenzyme activity compared with wild-type mice, PrP^c is probably not the primary source of copper in neurons.[391,392] However, this neuron-abundant protein may act as a buffer for copper in the synaptic cleft, maintaining presynaptic copper concentrations while preventing Cu^{2+}-related toxicity in the extracellular space.[356] Once released from neurons, copper is proposed to affect a variety of functions. Experiments regarding the purpose of this excreted copper pool have not yet employed endogenous copper stores, but several studies have focused on the effects of exogenously applied copper. For example, applications of micromolar concentrations of Cu^{2+} to neurons trigger antagonistic effects on NMDA, GABA, and sometimes glycine receptors[393] and suppress long-term potentiation.[394,395] Exogenous copper ions have also been shown to influence the function of rectifier-type K^+ channels and voltage-gated Ca^{2+} channels[396] as well as TREK-1 K^+ channels.[397] The foregoing results connecting copper trafficking to neurotransmission are engaging, but much work remains to be done to fully elucidate the molecular roles of labile copper and its contributions to basic aspects of signaling within and between brain cells. In particular, new ways to study endogenous copper pools and their effects on neurons in resting or excited states will have an impact on this field.

4.2.2. Copper Neuropathology

Disruption of copper homeostasis is implicated in a number of neurodegenerative diseases, including Alzheimer's disease (AD), Prion diseases, Parkinson's disease (PD), familial amyotrophic lateral sclerosis (fALS), Menkes disease, and Wilson disease.[1,251,327,398–402] In all these disorders, the deleterious effects of copper stem from its dual abilities to bind ligands and trigger uncontrolled oxidation−reduction chemistry. An excellent comprehensive review has been published recently that details the roles of copper in

neurodegenerative diseases with a focus on the nature of the copper−protein interactions.[327]

The connection between copper and AD pathology is due mainly to its molecular reactions with APP and its β-amyloid cleavage product (Aβ) that result in imbalance of extracellular and intracellular brain copper pools. The function of APP in the brain has not been fully elucidated but is plausibly linked to copper homeostasis.[352–355] However, aberrant binding of Cu^{2+} to APP triggers its reduction to Cu^{+} with concomitant disulfide bond formation;[403–405] this misregulated metalloprotein intermediate can then participate in harmful Fenton-type chemistry.[406] For example, the reaction between the APP−Cu^{+} complex and H_2O_2 causes oxidation to Cu^{2+} and APP fragmentation,[407] leading to a cycle of oxidative stress and aggregation of Aβ peptides that results in the ultimate formation of amyloid plaques in the extracellular cerebrospinal fluid.[408,409] Extracellular amyloid deposits from the brains of AD patients are rich in Cu in addition to Zn and Fe,[110] and Raman studies of senile plaques reveal Cu^{2+} centers bound by histidine donors[410] that can result from direct cascade reactions between Cu^{2+} and Aβ peptides.[411] Moreover, administration of Zn/Cu chelators such as clioquinol can redistribute brain metal pools and reverse amyloid aggregation.[412] Finally, addition of Cu^{2+} to cell cultures alters APP processing, resulting in increased levels of intracellular and secreted forms of APP and decreased levels of Aβ.[413]

Prion diseases also have links to brain copper misregulation,[327,400,402] where opposing Cu^{2+} and Mn^{2+} levels and availabilities may influence the conversion of the protease-sensitive PrP^{C} into the toxic, protease-resistant form, PrP^{Sc}.[414] PrP^{C} can bind between four and seven Cu^{2+} ions[415] at various binding sites, including the octapeptide repeat regions that have micromolar affinity for Cu^{2+}.[328,386,416–420] In one proposal for prion toxicity, PrP^{C} is involved in copper homeostasis and binding of Mn^{2+} to the protein facilitates its conversion to toxic PrP^{Sc}; the resulting excess free copper further exacerbates the disease by promoting oxidative stress. In the presence of copper, PrP^{C} also possesses SOD-like activity,[331,421–423] though the consequences of this redox chemistry *in vivo* remain under debate.[391,424,425] Finally, Cu^{2+} can retard degradation of the toxic PrP^{Sc} in low ionic strength buffers as well as control the conformation of the protease-resistant fragment of PrP^{Sc}, namely, PrP27−30.[426] Thus, abnormalities in the PrP^{C} protein are linked to disruption of copper homeostasis, and copper can also affect the degradation pathways of prion proteins.

Onset of Parkinson's disease is accompanied by death of dopaminergic neurons and intracellular accumulation of Lewy bodies, which are protein aggregates of the brain protein α-synuclein.[269,270] In its unmodified form, α-synuclein exists as an unfolded protein,[427] but factors including oxidative stress[270,428–430] and presence of various metal cations[431–433] promote its fibrillation. In particular, Cu^{2+} effectively promotes the self-oligomerization of α-synuclein through the acidic C-terminal region of the protein[432,434] and its oxidation and aggregation in the presence of H_2O_2.[431] Structural details of the Cu^{2+}−α-synuclein interaction have been reported recently and identify two main copper binding sites in the protein.[435,436] One site is comprised of the carboxylate-rich C-terminus of the protein and has a micromolar affinity for copper. The other site binds copper with nanomolar affinity; initial reports suggested that both the N-terminus and His50 were necessary in Cu^{2+} binding,[435] but more recent work refutes the involvement of His50 as a ligand.[436]

Familial amyotrophic lateral sclerosis (fALS) is an inherited neurodegenerative disorder stemming from mutations in the copper-dependent metalloprotein Cu/Zn SOD1.[437] Three main hypotheses exist regarding the molecular mechanism(s) of deterioration in this disease: (i) the loss-of-function mechanism, which results in toxic accumulation of superoxide by lack of SOD1 protection, (ii) the gain-of-function mechanism, in which SOD1 exhibits enhanced peroxidase activity by aberrant redox chemistry, and (iii) the aggregation mechanism, where SOD1 aggregates are formed by increased or decreased availability of copper for binding. The roles of copper homeostasis in this disease remain ambiguous because modifications of the metal-binding domains in the enzyme active site can lead to activity associated with the loss- or gain-of-function mechanisms[438,439] and mice expressing SOD1 mutants unable to bind copper ions still exhibit symptoms of ALS.[440]

Finally, Menkes and Wilson diseases are diseases in which the failure of p-type ATPases ATP7A (Menkes) and ATP7B (Wilson) results in disrupted copper homeostasis. Menkes patients with various ATP7A mutations are unable to transport copper across the gastrointestinal tract, placenta, and blood−brain barrier,[398,399] resulting in systemic brain copper deficiency and reduced activity of copper-containing enzymes such as DβM, SOD1, and CcO.[441–443] In Wilson disease, malfunctions of ATP7B activity result in the hyperaccumulation of copper in the liver and the brain.[398] In both Menkes and Wilson disease patients, the abnormal levels and distributions of brain copper are thought to contribute to detrimental neurological effects.

4.3. Molecular Imaging of Brain Copper

4.3.1. Overview of Traditional Copper Detection Methods

The broad participation of copper in both neurophysiological and neuropathological events has prompted demand for ways to trace this metal in biological systems. In this regard, both major oxidation states of copper, the $4s^23d^{10}$ cuprous oxidation state (Cu^{+}) and the $4s^23d^9$ cupric oxidation state (Cu^{2+}), are important for rigorous considerations of its chemistry in natural settings. Radioactive copper isotopes such as ^{67}Cu[336] and atomic absorption spectroscopy[337] have proven to be useful for studying many aspects of copper biology but lack spatial resolution and cannot differentiate between Cu^{+} and Cu^{2+}. The existence of two high abundance naturally occurring isotopes of copper, ^{63}Cu (69.17%) and ^{65}Cu (30.83%), has also been exploited to study copper in specific organs by analyzing the $^{63}Cu/^{65}Cu$ ratio using inductively coupled plasma mass spectrometry (ICP/MS) or thermal-ionization mass spectrometry (TIMS).[444–447] These methods are quite useful for studying complex organisms but again lack subcellular resolution and cannot distinguish between different oxidation states of copper. Finally, a myriad of histochemical indicators have been developed to stain for copper, including hemotoxylin,[448–450] rubeanic acid (dithiooxamide),[451,452] rhodanine and diphenylcarbazide,[448,453] diethyldithiocarbamate,[453] dithizone,[454] Timm's staining,[455,456] orcein,[457,458] and bathocuproine disulfonate (BCS).[459] A modified Timm's method using trichloroacetic acid can isolate Cu^{2+} pools with some fidelity,[460] whereas BCS is a dual colorimetric and fluorescence quenching indicator for

Chart 11. Turn-on Fluorescent Sensors for Cu^+

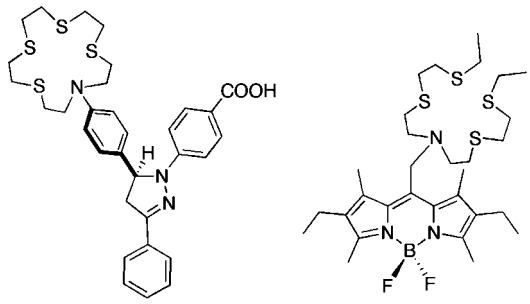

CTAP-1, **76** CS1, **77**

Cu^+ and Cu^{2+}.[459,461] The main disadvantages of these histochemical stains are that they cannot image copper in living samples and are limited in terms of metal and redox specificity.

4.3.2. Criteria for Molecular Imaging of Copper in Living Systems

Similar criteria exist for fluorescence and MR-based probes for detecting copper in living systems as for other metals. First and foremost is selectivity in terms of both the metal itself (Cu) and relevant oxidation states (Cu^+ or Cu^{2+}). Fluorescence detection of Cu^{2+} by a turn-on response is particularly difficult due to its paramagnetic nature, as unpaired electrons in close proximity to fluorescent dyes tend to quench emission. Thus, as is the case for iron, the selection of optical fluorescence and MR probes that have been utilized successfully for tracking copper in biological samples remains limited. Features of Cu^+/Cu^{2+} probes are presented in Table 3.

4.3.3. Survey of Fluorescent and MRI Copper Sensors

4.3.3.1. Turn-on Fluorescent Cu^+ Sensors with Reversible Binding. Because of the ability for Cu^+ to serve as an efficient fluorescence quencher by electron or energy transfer and its propensity to disproportionate in water to Cu^{2+} and Cu metal, Cu^+ fluorescent sensors with the capacity to sense this ion in aqueous solution with a turn-on response remain rare (Chart 11). CTAP-1 (**76**) was the first such probe and combines a triarylpyrazoline fluorophore with a tetrathiaaza crown for Cu^+ binding.[462] Upon UV excitation at 365 nm, the probe shows a 4.6-fold fluorescence increase in emission at 480 nm with 1 equiv of added Cu^+ ($\Phi_{apo} = 0.03$; $\Phi_{bound} = 0.14$). CTAP-1 binds Cu^+ tightly ($K_d = 40$ pM) with high selectivity over other metal ions and has been used to detect exogenous labile Cu^+ pools in NIH 3T3 fibroblasts. A study using CTAP-1 along with microXRF (micro X-ray fluorescence) indicates the presence of labile Cu^+ pools localized to the Golgi and mitochondrial organelles within this cell type (Figure 8).

Our laboratory has developed Coppersensor-1 (CS1, **77**), a BODIPY-based indicator for Cu^+.[463,464] The compound possesses excitation and emission wavelengths in the visible region ($\lambda_{ex} = 540$ nm; $\lambda_{em} = 566$ nm) and exhibits a 10-fold response to Cu^+ in aqueous media ($\Phi_{apo} = 0.016$; $\Phi_{bound} = 0.13$) with high selectivity over competing metal ions at cellular concentrations, including Cu^{2+}. This probe is membrane-permeable and can be used to sense both increases and decreases in the levels and distributions of labile cellular Cu^+; for example, live HEK 293 cells or neurons from primary culture incubated with CS1 showed a marked fluorescence increase upon introduction of exogenous Cu^+ (Figure 9); the observed fluorescence enhancements are readily reversed by addition of a cell-permeable copper ion chelator.

4.3.3.2. Fluorescent Chemodosimeters for Detecting Cu^+ by an Irreversible Response. The Cu^+-catalyzed 1,3-dipolar cycloaddition of a terminal alkyne to an azide to form a triazole is the archetypical example of a "click" reaction as popularized by Sharpless[465–467] and has been utilized to develop two types of fluorescent chemodosimeters for Cu^+ (Chart 12). Fahrni and co-workers first reported a virtually nonfluorescent alkynyl coumarin derivative ($\lambda_{ex} = 325$ nm; $\lambda_{em} = 388$ nm; $\Phi = 0.014$) that is converted to its fluorescent triazole congener ($\lambda_{ex} = 328$ nm; $\lambda_{em} = 415$ nm; $\Phi = 0.25$) upon reaction with 4-azidomethylbenzoic acid in the presence of Cu^+ in aqueous buffer (**78**).[468] A Eu^{3+} complex (Eu-**79**) has also been reported for the luminescent detection of Cu^+ using click chemistry.[469] This detection system consists of a Eu^{3+} DO3A propynylamide complex and a dansyl azide that can be coupled using the glutathione complex of Cu^+ in water. The resulting dansyl−triazole Eu^{3+} chelate possesses a 10-fold higher luminescence than its starting alkyne complex due to the antenna effect ($\lambda_{ex} = 350$ nm; $\lambda_{em} = 615$ nm). Neither of these probes has been utilized to detect Cu^+ in biological systems. A potential barrier for their use in complex biological environments is that detection requires the interaction of three different entities at appropriate concentrations for the reaction to proceed.

4.3.3.3. Turn-on and Ratiometric Fluorescent Sensors for Detecting Cu^{2+} with Reversible Binding. The development of fluorescent Cu^{2+} sensors that operate by a turn-on or ratiometric response is challenging because coordination of Cu^{2+} to an ionophore−fluorophore pair often results in fluorescence quenching by interference from intervening charge transfer states. Accordingly, the vast majority of fluorogenic reagents that have sensitivity and selectivity for Cu^{2+} report this ion by a turn-off response,[470–475] which is of limited utility for visualization of biological copper pools with spatial resolution.

Turn-on and ratiometric sensors for Cu^{2+} have been developed, but most only work well in organic solution or mixed aqueous−organic solution, and none have been applied to biological imaging (Chart 13). One example is the BODIPY derivative **80** that contains an azathiacrown metal binding group that turns on with Cu^{2+}, Hg^{2+}, and Ag^+.[476] This molecule displays a sizable (2500-fold) fluorescence increase in response to Cu^{2+} in acetonitrile solution ($\Phi_{apo} = 0.0001$; $\Phi_{bound} = 0.25$) with visible excitation and emission ($\lambda_{ex} = 501$ nm; $\lambda_{em} = 513$ nm), but loses its response to Cu^{2+} in 3:1 CH_3CN/H_2O solution compared with Hg^{2+} and Ag^+. The rhodamine-based probe **81** reports Cu^{2+} chelation by influencing the equilibrium between the closed, nonfluorescent spirolactam form and open, fluorescent acid form of rhodamine.[308] Upon Cu^{2+} binding, the ring-opened form of rhodamine is preferred, and fluorescence is turned on by 9.4-fold ($\lambda_{ex} = 520$ nm; $\lambda_{em} = 585$ nm). This sensor has a moderate affinity for Cu^{2+} ($K_d = 14$ μM) with good selectivity over other biologically relevant metal ions. Finally, naphthalimide derivatives have been utilized for ratiometric sensing of Cu^{2+} in mixed alcohol−water solution. Their ratiometric responses to Cu^{2+} are attributed to an ICT mechanism in which metal binding tunes the electronic properties of the fluorophore. The platform containing two

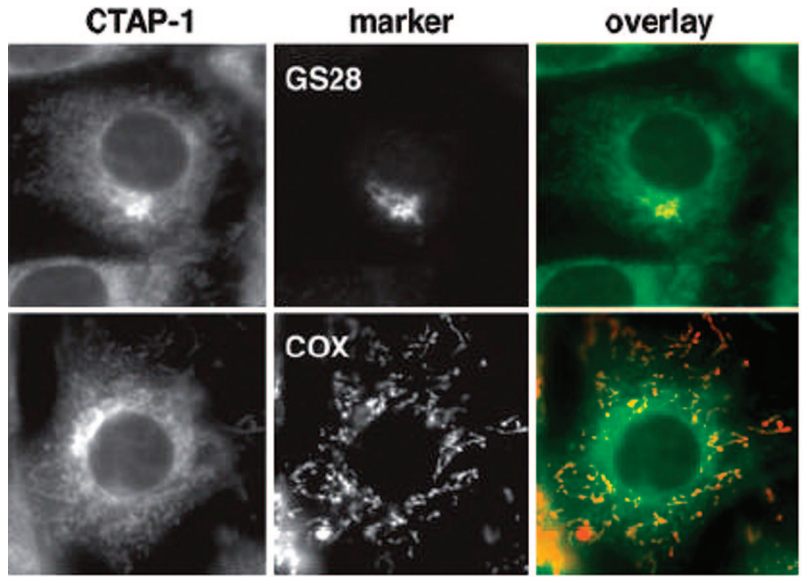

Figure 8. Fluorescence images showing the intracellular staining pattern of NIH 3T3 cells incubated with 10 μM CTAP-1 (**76**) for 50 min. Immunofluorescence colocalization of the CTAP-1 staining pattern (left) with two cellular marker antibodies (center) [(top) anti-GS28 to visualize the Golgi apparatus; (bottom) anti-OxPhos complex V to visualize mitochondria] and (right) false color overlay (CTAP-1, green; antibody, red; areas of colocalization appear in orange/yellow). Reprinted with permission from ref 462. Copyright 2005 National Academy of Sciences, U.S.A.

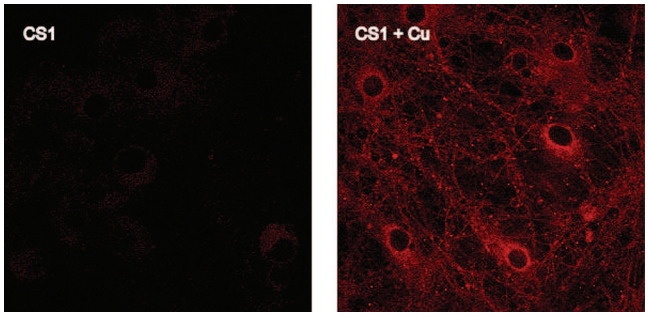

Figure 9. Fluorescence images of live rat hippocampal neurons incubated with 10 μM CS1 (**77**) for 15 min at 37 °C (left) and live rat hippocampal neurons incubated with 150 μM $CuCl_2$ for 18 h at 37 °C and then stained with 10 μM CS1 at 37 °C for 15 min to visualize exogenous copper uptake (right).

amide and two pyridyl donors (**82**) exhibits a blue shift upon Cu^{2+} binding,[477] whereas a second naphthalimide sensor containing two amide and two aniline donors (**83**) displays a red shift in fluorescence with Cu^{2+} coordination.[478]

4.3.3.4. Fluorescent Chemodosimeters for Detecting Cu^{2+} by an Irreversible Response. As a means of avoiding fluorophore quenching by direct binding of paramagnetic Cu^{2+}, researchers have explored an alternative approach to turn-on Cu^{2+} detection in which Cu^{2+} is used as a catalyst to promote the hydrolysis of specific bonds to yield a fluorescent product (Chart 14). Some of these probes can operate in water but have not been utilized successfully for imaging biological copper. The resulting chemodosimeters respond irreversibly to the targeted analyte, and thus their response is representative of a cumulative exposure to analyte. In an early example of this strategy, Czarnik elegantly exploited the known Cu^{2+}-catalyzed hydrolysis of α-amino acid esters[479–481] to develop the new Cu^{2+} chemodosimeter, Rhodamine B hydrazide (**84**). Appending this hydrazide mask favors the nonfluorescent spirolactam form of rhodamine, which can be converted to its fluorescent acid form by Cu^{2+} catalysis.[482] Reaction of **84** with Cu^{2+} in 20% acetonitrile/water solution proceeds rapidly (<1 min) at even low concentrations of Cu^{2+} (10 nM). This chemodosimeter is highly selective for Cu^{2+} over a range of competing metal ions. A fluorescein analog of this molecule (**85**) has also been reported and can respond to Cu^{2+} in 100% aqueous solution.[483] Finally, a bis(picolinate) ester of fluorescein (**86**) can furnish the parent dye upon Cu^{2+}-induced ester cleavage.[484]

4.3.3.5. Copper Sensing by MRI. Currently, only one MR-based sensor for specific detection of copper has been reported in the literature.[485] Copper Gad-1 (CG1, Gd-**87**) is a Gd-based smart MRI contrast agent that combines a DO3A core for Gd^{3+} binding and a PIDA moiety for Cu^{2+} chelation (Chart 15). In the absence of Cu^{2+}, water access to CG1 is limited by the PIDA cap, leading to a reduced proton relaxivity. Binding of Cu^{2+} to the PIDA receptor relieves steric congestion at the Gd^{3+} center, resulting in increased water access and higher proton relaxivity. CG1 exhibits an increase in relaxivity in response to Cu^{2+} ($R_1 = 3.76\ mM^{-1}\ s^{-1}$ to $R_1 = 5.29\ mM^{-1}\ s^{-1}$) with high selectivity over other biologically relevant metal ions, including Ca^{2+} and Zn^{2+}, in either *N*-2-hydroxyethylpiperazine-*N*′-2-ethanesulfonic acid (HEPES) or phosphate-buffered saline (PBS) aqueous solution within physiological ranges (pH 6.8−7.4). Luminescence lifetime measurements on the Tb^{3+} analog of CG1 indicate an increase in the number of bound water molecules (q) at the lanthanide center after addition of Cu^{2+}. CG1 responds reversibly to Cu^{2+} with moderate affinity (K_d = 167 μM). This compound provides a starting point for the development of functional probes for visualizing biological copper pools by MRI.

5. Conclusions and Future Prospects

Transition metals such as zinc, iron, and copper are emerging as major contributors to the complex chemistry and biology of the brain in stages of health, aging, and disease. Because of the unique physiology, specialization, and complexity of brain tissue, these metal nutrients are required at unusually high levels compared with the rest of the body. Redox-active iron and copper are particularly

Chart 12. Irreversible Turn-on Fluorescent Chemodosimeters for Cu^{+}

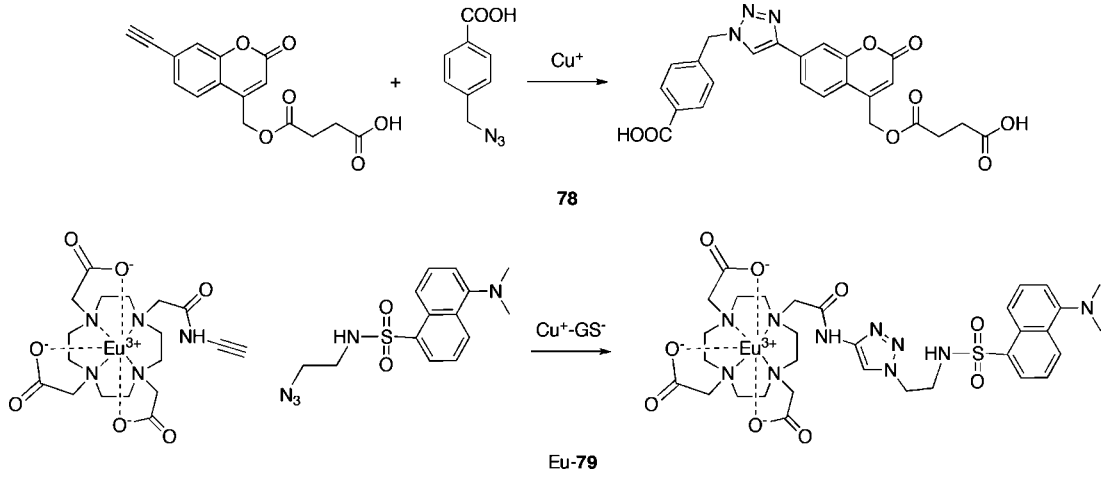

78

Eu-79

Chart 13. Turn-on and Ratiometric Fluorescent Sensors for Cu^{2+}

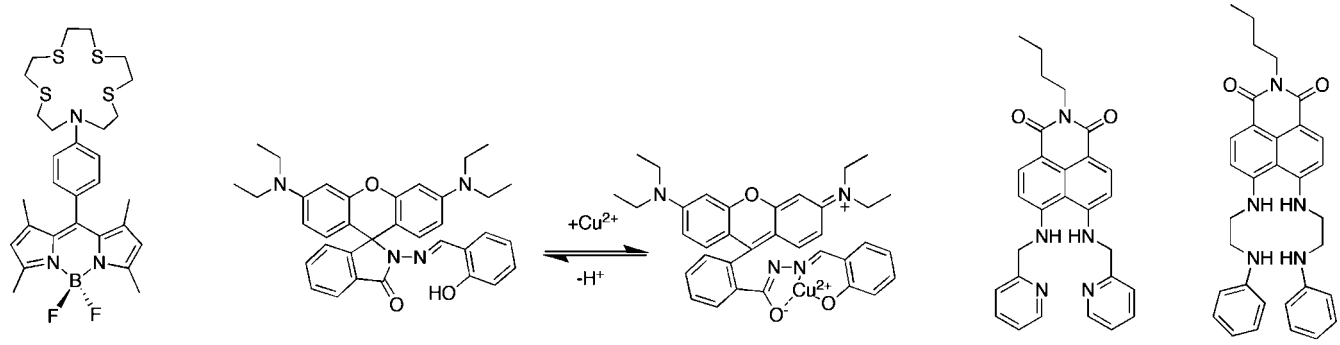

80 81 82 83

Chart 14. Irreversible Turn-on Fluorescent Chemodosimeters for Cu^{2+}

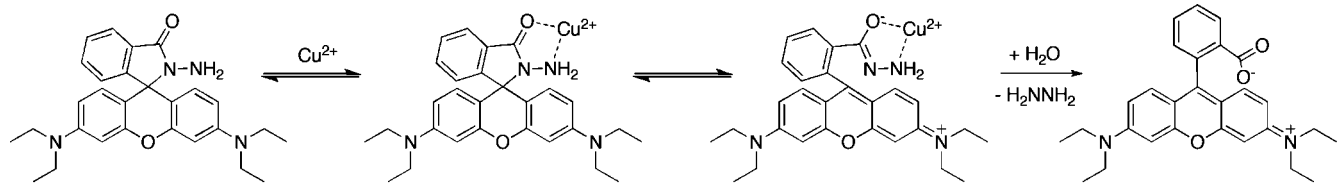

Rhodamine B hydrazide, 84

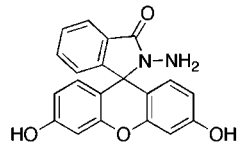

85

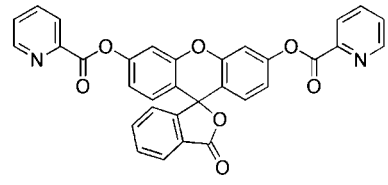

86

important owing to the large oxygen consumption and oxidative capacity of brain cell neurons and glia. Tightly bound forms of these metals are found as cofactors in essential metalloenzymes throughout the brain and central nervous system, and labile metal ion pools are present in all brain cells; in the cases of zinc and copper, these labile stores may play critical roles in signaling within and between cells during neurotransmission and general membrane depolarization. On the other hand, metals accumulate in the brain as a function of aging, and misregulation of brain metal ion pools is linked with several neurodegenerative diseases, including Alzheimer's and Parkinson's diseases, where

Chart 15. An MR-Based Sensor for Cu^{2+}

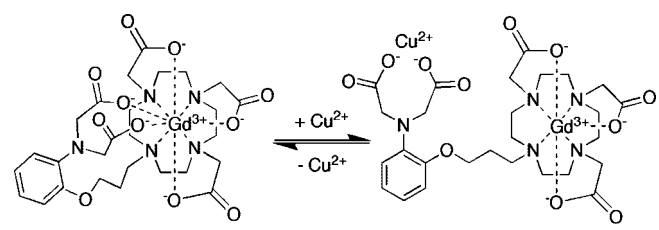

CG1, Gd-87

oxidative stress and damage as well as protein misfolding and aggregation are a hallmark of their pathology.

Questions regarding the far-ranging neurophysiological and neuropathological functions of these metal ions have and will continue to motivate the development of new chemical tools, including optical fluorescence and magnetic resonance imaging (MRI) probes, for the purpose of studying metal ions such as Zn^{2+}, $Fe^{2+/3+}$, and $Cu^{+/2+}$ in the brain and other dynamic biological systems. The most well-elaborated types of such reagents are fluorescent sensors for Zn^{2+}, which have found utility in a variety of biological settings and are worthy of further pursuit and optimization. By comparison, the development of fluorescent sensors for redox-active $Fe^{2+/3+}$ and $Cu^{+/2+}$ ions is in its nascent stages; for example, turn-on probes for Cu^{+} have been applied successfully in cells and show promise for further physiological and pathological studies, but Cu^{2+} fluorescence detection in live biological settings has not been achieved as of yet. Smart MRI contrast agents that are responsive to specific metal ions of interest also occupy an open field for further investigation, as well as other imaging modalities such as PET, single photon emission computerized tomography (SPECT), and ultrasound. In addition, there are numerous other transition and heavy metals for which studies of their complex neurophysiologies and neuropathologies could benefit from the development of new molecular imaging probes for their detection, including both essential metals (e.g., Cr, Mn, Co, Ni, Mo) and toxic metals (e.g., Cd, Hg, Pb). In this regard, some progress in the detection of heavy metal ions such as Cd^{2+}, Hg^{2+}, and Pb^{2+} in live cells and tissues has appeared in the recent literature.[486–489] The rich and open field of metals in neurobiology, which has largely been confined to studies of the s-block alkali and alkaline earth metals, is now rapidly expanding to include many of the d- and p-block metals in the periodic table. This emerging frontier at the interface of inorganic chemistry and biology will continue to prosper from the combined talents of scientists that can tackle Nature's most complex and beautiful biological system from a molecular perspective.

6. Acknowledgments

We thank the University of California, Berkeley, the Dreyfus Foundation, the Beckman Foundation, the American Federation for Aging Research, the Packard Foundation, the Sloan Foundation, the US National Science Foundation (Grant CAREER CHE-0548245), and the US National Institute of General Medical Sciences (Grant NIH GM 79465) for funding our laboratory's work on metal sensors. D.W.D. thanks the Chemical Biology Graduate Program sponsored by the US National Institutes of Health (Grant T32 GM066698) for support, and E.L.Q. acknowledges a Branch graduate fellowship from the University of California, Berkeley.

7. References

(1) Bush, A. I. *Curr. Opin. Chem. Biol.* **2000**, *4*, 184.
(2) Kandel, E. R.; Schwartz, J. H.; Jessell, T. J. *Principles of Neural Science*, 4th ed.; McGraw-Hill: New York, 2000.
(3) Götz, M. E.; Kunig, G.; Riederer, P.; Youdim, M. B. H. *Pharmacol. Ther.* **1994**, *63*, 37.
(4) Burdette, S. C.; Lippard, S. J. *Proc. Natl. Acad. Sci. U.S.A.* **2003**, *100*, 3605.
(5) Alberts, B.; Johnson, A.; Lewis, J.; Raff, M.; Roberts, K.; Walter, P. *Molecular Biology of the Cell*, 4th ed.; Taylor & Francis Group: New York, 2002.
(6) Debanne, D. *Nat. Rev. Neurosci.* **2004**, *5*, 304.
(7) Roeper, J.; Pongs, O. *Curr. Opin. Neurobiol.* **1996**, *6*, 338.
(8) Berridge, M. J. *Neuron* **1998**, *21*, 13.
(9) Berridge, M. J.; Bootman, M. D.; Lipp, P. *Nature* **1998**, *395*, 645.
(10) Bito, H.; Deisseroth, K.; Tsien, R. W. *Curr. Opin. Neurobiol.* **1997**, *7*, 419.
(11) Clapham, D. E. *Cell* **2007**, *131*, 1047.
(12) Wolf, F. I.; Torsello, A.; Fasanella, S.; Cittadini, A. *Mol. Aspects Med.* **2003**, *24*, 11.
(13) Tsien, R. Y. *Biochemistry* **1980**, *19*, 2396.
(14) Louie, A. Y.; Huber, M. M.; Ahrens, E. T.; Rothbacher, U.; Moats, R.; Jacobs, R. E.; Fraser, S. E.; Meade, T. J. *Nat. Biotechnol.* **2000**, *18*, 321.
(15) Frederickson, C. J. *Int. Rev. Neurobiol.* **1989**, *31*, 145.
(16) Lippard, S. J.; Berg, J. M. *Principles of Bioinorganic Chemistry*; 1 ed.; University Science Books: Mill Valley, CA, 1994.
(17) Vallee, B. L.; Falchuk, K. H. *Physiol. Rev.* **1993**, *73*, 79.
(18) Berg, J. M.; Shi, Y. *Science* **1996**, *271*, 1081.
(19) Sensi, S. L.; Canzoniero, L. M.; Yu, S. P.; Ying, H. S.; Koh, J. Y.; Kershner, G. A.; Choi, D. W. *J. Neurosci.* **1997**, *17*, 9554.
(20) Coleman, J. E. *Curr. Opin. Chem. Biol.* **1998**, *2*, 222.
(21) Kambe, T.; Iwai-Yamaguchi, Y.; Sasaki, R.; Nagao, M. *Cell. Mol. Life Sci.* **2004**, *61*, 49.
(22) McMahon, R. J.; Cousins, R. J. *Proc. Natl. Acad. Sci. U.S.A.* **1998**, *95*, 4841.
(23) Langmade, S. J.; Ravindra, R.; Daniels, P. J.; Andrews, G. K. *J. Biol. Chem.* **2000**, *275*, 34803.
(24) Palmiter, R. D.; Cole, T. B.; Findley, S. D. *EMBO J.* **1996**, *15*, 1784.
(25) Kobayashi, T.; Beuchat, M. H.; Lindsay, M.; Frias, S.; Palmiter, R. D.; Sakuraba, H.; Parton, R. G.; Gruenberg, J. *Nat. Cell Biol.* **1999**, *1*, 113.
(26) Kambe, T.; Narita, H.; Yamaguchi-Iwai, Y.; Hirose, J.; Amano, T.; Sugiura, N.; Sasaki, R.; Mori, K.; Iwanaga, T.; Nagao, M. *J. Biol. Chem.* **2002**, *277*, 19049.
(27) Huang, L.; Kirschke, C. P.; Gitschier, J. *J. Biol. Chem.* **2002**, *277*, 26389.
(28) Kirschke, C. P.; Huang, L. *J. Biol. Chem.* **2003**, *278*, 4096.
(29) Liuzzi, J. P.; Blanchard, R. K.; Cousins, R. J. *J. Nutr.* **2001**, *131*, 46.
(30) Chimienti, F.; Devergnas, S.; Favier, A.; Seve, M. *Diabetes* **2004**, *53*, 2330.
(31) Sim, D. L. C.; Yeo, W. M.; Chow, V. T. K. *Int. J. Biochem. Cell Biol.* **2002**, *34*, 487.
(32) Seve, M.; Chimienti, F.; Devergnas, S.; Favier, A. *BMC Genomics* **2004**, *5*, 32.
(33) Palmiter, R. D.; Cole, T. B.; Quaife, C. J.; Findley, S. D. *Proc. Natl. Acad. Sci. U.S.A.* **1996**, *93*, 14934.
(34) Wenzel, H. J.; Cole, T. B.; Born, D. E.; Schwartzkroin, P. A.; Palmiter, R. D. *Proc. Natl. Acad. Sci. U.S.A.* **1997**, *94*, 12676.
(35) Salazar, G.; Craige, B.; Love, R.; Kalman, D.; Faundez, V *J. Cell Sci* **2005**, *118*, 1911.
(36) Vasak, M.; Hasler, D. W. *Curr. Opin. Chem. Biol.* **2000**, *4*, 177.
(37) Maret, W. *Biochemistry* **2004**, *43*, 3301.
(38) Hidalgo, J.; Aschner, M.; Zatta, P.; Vasak, M. *Brain Res. Bull.* **2001**, *55*, 133.
(39) Palmiter, R. D. *Proc. Natl. Acad. Sci. U.S.A.* **1998**, *95*, 8428.
(40) Maret, W.; Vallee, B. L. *Proc. Natl. Acad. Sci. U.S.A.* **1998**, *95*, 3478.
(41) Maret, W. *J. Nutr.* **2000**, *130*, 1455S.
(42) Maret, W. *Proc. Natl. Acad. Sci. U.S.A.* **1994**, *91*, 237.
(43) Meloni, G.; Zovo, K.; Kazantseva, J.; Palumaa, P.; Vasak, M. *J. Biol. Chem.* **2006**, *281*, 14588.
(44) Masters, B. A.; Quaife, C. J.; Erickson, J. C.; Kelly, E. J.; Froelick, G. J.; Zambrowicz, B. P.; Brinster, R. L.; Palmiter, R. D. *J. Neurosci.* **1994**, *14*, 5844.
(45) Palumaa, P.; Tammiste, I.; Kruusel, K.; Kangur, L.; Jörnvall, H.; Sillard, R. *Biochim. Biophys. Acta-Proteins Proteomics* **2005**, *1747*, 205.
(46) Maret, W.; Jacob, C.; Vallee, B. L.; Fischer, E. H. *Proc. Natl. Acad. Sci. U.S.A.* **1999**, *96*, 1936.
(47) Jacob, C.; Maret, W.; Vallee, B. L. *Proc. Natl. Acad. Sci. U.S.A.* **1998**, *95*, 3489.
(48) Chung, R. S.; West, A. W. *Neuroscience* **2004**, *123*, 595.
(49) Maret, W. *Neurochem. Int.* **1995**, *27*, 111.
(50) Quesada, A. R.; Byrnes, R. W.; Krezoski, S. O.; Petering, D. H. *Arch. Biochem. Biophys.* **1996**, *334*, 241.
(51) Pearce, L. L.; Gandley, R. E.; Han, W. P.; Wasserloos, K.; Stitt, M.; Kanai, A. J.; McLaughlin, M. K.; Pitt, B. R.; Levitan, E. S. *Proc. Natl. Acad. Sci. U.S.A.* **2000**, *97*, 477.
(52) Kroncke, K. D.; Fehsel, K.; Schmidt, T.; Zenke, F. T.; Dasting, I.; Wesener, J. R.; Bettermann, H.; Breunig, K. D.; Kolb-Bachofen, V. *Biochem. Biophys. Res. Commun.* **1994**, *200*, 1105.
(53) Chen, Y.; Irie, Y.; Keung, W. M.; Maret, W. *Biochemistry* **2002**, *41*, 8360.
(54) Berendji, D.; Kolb-Bachofen, V.; Meyer, K. L.; Grapenthin, O.; Weber, H.; Wahn, V.; Kroncke, K. D. *FEBS Lett.* **1997**, *405*, 37.

(55) St.Croix, C. M.; Wasserloos, K. J.; Dineley, K. E.; Reynolds, I. J.; Levitan, E. S.; Pitt, B. R *Am. J. Physiol. Lung C* **2002**, *282*, 185.
(56) Spahl, D. U.; Berendji-Grun, D.; Suschek, C. V.; Kolb-Bachofen, V.; Kroncke, K. D. *Proc. Natl. Acad. Sci. U.S.A.* **2003**, *100*, 13952.
(57) Andrews, G. K. *BioMetals* **2001**, *14*, 223.
(58) Maske, H. *Klin. Wochenschr.* **1955**, *33*, 1058.
(59) Frederickson, C. J.; Koh, J. Y.; Bush, A. I. *Nat. Rev. Neurosci.* **2005**, *6*, 449.
(60) Frederickson, C. J.; Bush, A. I. *BioMetals* **2001**, *14*, 353.
(61) Kay, A. R. *J. Neurosci.* **2003**, *23*, 6847.
(62) Kay, A. R. *Trends Neurosci.* **2006**, *29*, 200.
(63) Frederickson, C. J. *Sci. STKE* **2003**, *2003*, pe18.
(64) Li, Y. V.; Hough, C. J.; Sarvey, J. M. *Sci. STKE* **2003**, *2003*, pe19.
(65) Assaf, S. Y.; Chung, S.-H. *Nature* **1984**, *308*, 734.
(66) Howell, G. A.; Welch, M. G.; Frederickson, C. J. *Nature* **1984**, *308*, 736.
(67) Budde, T.; Minta, A.; White, J. A.; Kay, A. R. *Neuroscience* **1997**, *79*, 347.
(68) Thompson, R. B., Jr.; Maliwal, B. P.; Fierke, C. A.; Frederickson, C. J. *J. Neurosci. Methods* **2000**, *96*, 35.
(69) Varea, E.; Ponsoda, X.; Molowny, A.; Danscher, G.; Lopez-Garcia, C. *J. Neurosci. Methods* **2001**, *110*, 57.
(70) Li, Y.; Hough, C. J.; Frederickson, C. J.; Sarvey, J. M. *J. Neurosci.* **2001**, *21*, 8015.
(71) Li, Y.; Hough, C. J.; Suh, S. W.; Sarvey, J. M.; Frederickson, C. J. *J. Neurophysiol.* **2001**, *86*, 2597.
(72) Ueno, S.; Tsukamoto, M.; Hirano, T.; Kikuchi, K.; Yamada, M. K.; Nishiyama, N.; Nagano, T.; Matsuki, N.; Ikegaya, Y. *J. Cell Biol.* **2002**, *158*, 215.
(73) Vogt, K.; Mellor, J.; Tong, G.; Nicoll, R. *Neuron* **2000**, *26*, 187.
(74) Chen, N.; Moshaver, A.; Raymond, L. A. *Mol. Pharmacol.* **1997**, *51*, 1015.
(75) Choi, Y. B.; Lipton, S. A. *Neuron* **1999**, *23*, 171.
(76) Paoletti, P.; Ascher, P.; Neyton, J. *J. Neurosci.* **1997**, *17*, 5711.
(77) Peters, S.; Koh, J.; Choi, D. W. *Science* **1987**, *236*, 589.
(78) Traynelis, S. F.; Burgess, M. F.; Zheng, F.; Lyuboslavsky, P.; Powers, J. L. *J. Neurosci.* **1998**, *18*, 6163.
(79) Westbrook, G. L.; Mayer, M. *Nature* **1987**, *328*, 640.
(80) Williams, K. *Neurosci. Lett.* **1996**, *215*, 9.
(81) Rachline, J.; Perin-Dureau, F.; Le Goff, A.; Neyton, J.; Paoletti, P. *J. Neurosci.* **2005**, *25*, 308.
(82) Koh, J. Y.; Choi, D. W. *Neuroscience* **1994**, *60*, 1049.
(83) Ruiz, A.; Walker, M. C.; Fabian-Fine, R.; Kullmann, D. M. *J. Neurophysiol.* **2004**, *91*, 1091.
(84) Weiss, J. H.; Sensi, S. L. *Trends Neurosci.* **2000**, *23*, 365.
(85) Keizer, J.; Levine, L. *Biophys. J.* **1996**, *71*, 3477.
(86) Murakami, K.; Whiteley, M. K.; Routtenberg, A. *J. Biol. Chem.* **1987**, *262*, 13902.
(87) Lengyel, I.; Fieuw-Makaroff, S.; Hall, A. L.; Sim, A. T. R.; Rostas, J. A. P.; Dunkley, P. R. *J. Neurochem.* **2000**, *75*, 594.
(88) Manzerra, P.; Behrens, M. M.; Canzoniero, L. M. T.; Wang, X. Q.; Heidinger, V.; Ichinose, T.; Yu, S. P.; Choi, D. W. *Proc. Natl. Acad. Sci. U.S.A.* **2001**, *98*, 11055.
(89) Bossy-Wetzel, E.; Talantova, M. V.; Lee, W. D.; Schölzke, M. N.; Harrop, A.; Mathews, E.; Götz, T.; Han, J.; Ellisman, M. H.; Perkins, G. A.; Lipton, S. A. *Neuron* **2004**, *41*, 351.
(90) Sensi, S. L.; Ton-That, D.; Sullivan, P. G.; Jonas, E. A.; Gee, K. R.; Kaczmarek, L. K.; Weiss, J. H. *Proc. Natl. Acad. Sci. U.S.A.* **2003**, *100*, 6157.
(91) Hirzel, K.; Muller, U.; Latal, A. T.; Hulsmann, S.; Grudzinska, J.; Seeliger, M. W.; Betz, H.; Laube, B. *Neuron* **2006**, *52*, 679.
(92) Kay, A. R. *J. Neurosci.* **2003**, *23*, 6847.
(93) Sloviter, R. S. *Brain Res.* **1985**, *330*, 150.
(94) Choi, D. W.; Koh, J. Y. *Annu. Rev. Neurosci.* **1998**, *21*, 347.
(95) Frederickson, C. J.; Maret, W.; Cuajungco, M. P. *Neuroscientist* **2004**, *10*, 18.
(96) Weiss, J. H.; Sensi, S. L.; Koh, J. Y. *Trends Neurosci.* **2000**, *21*, 395.
(97) Canzoniero, L. M. T.; Turetsky, D. M.; Choi, D. W. *J. Neurosci.* **1999**, *19*, RC31.
(98) Kim, E. Y.; Koh, J. Y.; Kim, Y. H.; Sohn, S.; Joe, E.; Gwag, B. J. *Eur. J. Neurosci.* **1999**, *11*, 327.
(99) Koh, J.-Y.; Suh, S. W.; Gwag, B. J.; He, Y. Y.; Hsu, C. Y.; Choi, D. W. *Science* **1996**, *272*, 1013.
(100) Canzoniero, L. M. T.; Manzerra, P.; Sheline, C. T.; Choi, D. W. *Neuropharmacology* **2003**, *45*, 420.
(101) Hellmich, H. L.; Frederickson, C. J.; DeWitt, D. S.; Saban, R.; Parsley, M. O.; Stephenson, R.; Velasco, M.; Uchida, T.; Shimamura, M.; Prough, D. S. *Neurosci. Lett.* **2004**, *355*, 221.
(102) Lee, J.-M.; Zipfel, G. J.; Park, K. H.; He, Y. Y.; Hsu, C. Y.; Choi, D. W. *Neuroscience* **2002**, *115*, 871.
(103) Jiang, D.; Sullivan, P. G.; Sensi, S. L.; Steward, O.; Weiss, J. H. *J. Biol. Chem.* **2001**, *276*, 47524.
(104) Sensi, S. L.; Yin, H. Z.; Weiss, J. H. *Eur. J. Neurosci.* **2000**, *12*, 3813.
(105) Kim, Y.-H.; Kim, E. Y.; Gwag, B. J.; Sohn, S.; Koh, J.-Y. *Neuroscience* **1999**, *89*, 175.
(106) Noh, K.-M.; Koh, J.-Y. *J. Neurosci.* **2000**, *20*, RC111.
(107) Frederickson, C. J.; Cuajungco, M. P.; Labuda, C. J.; Suh, S. W. *Neuroscience* **2002**, *115*, 471.
(108) Wei, G.; Hough, C. J.; Li, Y.; Sarvey, J. M. *Neuroscience* **2004**, *125*, 867.
(109) Bush, A. I.; Tanzi, R. E. *Proc. Natl. Acad. Sci. U.S.A.* **2002**, *99*, 7317.
(110) Lovell, M. A.; Robertson, J. D.; Teesdale, W. J.; Campbell, J. L.; Markesbery, W. R. *J. Neurol. Sci.* **1998**, *158*, 47.
(111) Bush, A. I.; Pettingell, W. H., Jr.; de Paradis, M.; Tanzi, R. E.; Wasco, W *J. Biol. Chem.* **1994**, *269*, 26618.
(112) Bush, A. I.; Multhaup, G.; Moir, R. D.; Williamson, T. G.; Small, D. H.; Rumble, B.; Pollwein, P.; Beyreuther, K.; Masters, C. L. *J. Biol. Chem.* **1993**, *268*, 16109.
(113) Bush, A. I.; Pettingell, W. H., Jr.; Paradis, M. D.; Tanzi, R. E *J. Biol. Chem.* **1994**, *269*, 12152.
(114) Bush, A. I.; Pettingell, W. H., Jr.; Multhaup, G.; d Paradis, M.; Vonsattel, J. P.; Gusella, J. F.; Beyreuther, K.; Masters, C. L.; Tanzi, R. E. *Science* **1994**, *265*, 1464.
(115) Suh, S. W.; Jensen, K. B.; Jensen, M. S.; Silva, D. S.; Kesslak, P. J.; Danscher, G.; Frederickson, C. J. *Brain Res.* **2000**, *852*, 274.
(116) Lee, J.-Y.; Mook-Jung, I.; Koh, J.-Y. *J. Neurosci.* **1999**, *19*, RC10.
(117) Cole, T. B.; Wenzel, H. J.; Kafer, K. E.; Schwartzkroin, P. A.; Palmiter, R. D. *Proc. Natl. Acad. Sci. U.S.A.* **1999**, *96*, 1716.
(118) Regland, B.; Lehmann, W.; Abedini, I.; Blennow, K.; Jonsson, M.; Karlsson, I.; Sjogren, M.; Wallin, A.; Xilinas, M.; Gottfries, C. G. *Dementia Geriatr. Cognit. Disord.* **2001**, *12*, 408.
(119) Ritchie, C. W.; Bush, A. I.; Mackinnon, A.; Macfarlane, S.; Mastwyk, M.; MacGregor, L.; Kiers, L.; Cherny, R.; Li, Q. X.; Tammer, A.; Carrington, D.; Mavros, C.; Volitakis, I.; Xilinas, M.; Ames, D.; Davis, S.; Volitakis, I.; Xilinas, M.; Ames, D.; Davis, S.; Beyreuther, K.; Tanzi, R. E.; Masters, C. L. *Arch. Neurol.* **2003**, *60*, 1685.
(120) Takeda, A.; Tamano, H.; Enomoto, S.; Oku, N. *Cancer Res.* **2001**, *61*, 5065.
(121) Danscher, G.; Howell, G.; Perezclausell, J.; Hertel, N. *Histochemistry* **1985**, *83*, 419.
(122) Frederickson, C. J.; Howell, G. A.; Frederickson, M. H. *Exp. Neurol.* **1981**, *73*, 812.
(123) Danscher, G. In *The Neurobiology of Zinc*; Frederickson, C. J., Howell, G. A., Kasarskis, E. J., Eds.; Alan R. Liss: New York, 1984; Vol *A*, p 273.
(124) Danscher, G. In *The Neurobiology of Zinc*; Frederickson, C. J., Howell, G. A., Kasarskis, E. J., Eds.; Alan R. Liss: New York, 1984; Vol. B, p 177.
(125) Danscher, G. In *The Neurobiology of Zinc*; Frederickson, C. J., Howell, G. A., Kasarskis, E. J., Eds.; Alan R. Liss: New York, 1984; Vol *A*, p 229.
(126) Danscher, G. *Histochemistry* **1984**, *81*, 331.
(127) Danscher, G. *Histochemistry* **1982**, *76*, 281.
(128) Danscher, G. *Histochemistry* **1981**, *71*, 1.
(129) Chang, C. J.; Lippard, S. J. In *Metal Ions in Life Sciences*; Sigel, A., Sigel, H., Sigel, R. K. O., Eds.; John Wiley & Sons, Ltd.: West Sussex, England, 2006; Vol. 1, p 321.
(130) Frederickson, P. D.; Fierke, C. A.; Westerberg, N. M.; Bozym, R. A.; Bs, M. L. C.; Hershfinkel, M. In *Fluorescence Sensors and Biosensors*; Thompson, R. B., Ed.; CRC Press LLC: Boca Raton, FL, 2006, p 351.
(131) Jiang, P.; Guo, Z. *Coord. Chem. Rev.* **2004**, *248*, 205.
(132) Kimura, E.; Koike, T. *Chem. Soc. Rev.* **1998**, *27*, 179.
(133) Lim, N. C.; Freake, H. C.; Brueckner, C. *Chem.—Eur. J.* **2005**, *11*, 38.
(134) Carol, P.; Sreejith, S.; Ajayaghosh, A. *Chem.—Asian J.* **2007**, *2*, 338.
(135) Kikuchi, K.; Komatsu, K.; Nagano, T. *Curr. Opin. Chem. Biol.* **2004**, *8*, 182.
(136) Hanaoka, K.; Kikuchi, K.; Urano, Y.; Nagano, T. *J. Chem. Soc., Perkin Trans.* **2001**, *2*, 1840.
(137) Hanaoka, K.; Kikuchi, K.; Urano, Y.; Narazaki, M.; Yokawa, T.; Sakamoto, S.; Yamaguchi, K.; Nagano, T. *Chem. Biol.* **2002**, *9*, 1027.
(138) Zhang, X.; Lovejoy, K. S.; Jasanoff, A.; Lippard, S. J. *Proc. Natl. Acad. Sci. U.S.A.* **2007**, *104*, 10780.
(139) Major, J. L.; Parigi, G.; Luchinat, C.; Meade, T. J. *Proc. Natl. Acad. Sci. U.S.A.* **2007**, *104*, 13881.
(140) Frederickson, C. J.; Kasarskis, E. J.; Ringo, D.; Frederickson, R. E. *J. Neurosci. Methods* **1987**, *20*, 91.
(141) Meervelt, L. V.; Goethals, M.; Leroux, N.; Zeegers-Huyskens, T. *J. Phys. Org. Chem.* **1997**, *10*, 680.
(142) Leroux, N.; Goethals, M.; Zeegers-Huyskens, T. *Vib. Spectrosc.* **1995**, *9*, 235.

(143) Zalewski, P. D.; Millard, S. H.; Forbes, I. J.; Kapaniris, O.; Slavotinek, A.; Betts, W. H.; Ward, A. D.; Lincoln, S. F.; Mahadevan, I. *J. Histochem. Cytochem.* **1994**, *42*, 877.
(144) Fahrni, C. J.; O'Halloran, T. V. *J. Am. Chem. Soc.* **1999**, *121*, 11448.
(145) Soroka, K.; Vithanage, R. S.; Philips, D. A.; Walker, B.; Dasgupta, P. K. *Anal. Chem.* **1987**, *59*, 629.
(146) Snitsarev, V.; Budde, T.; Stricker, T. P.; Cox, J. M.; Krupa, D. J.; Geng, L.; Kay, A. R. *Biophys. J.* **2001**, *80*, 1538.
(147) Kimura, E.; Aoki, S.; Kikuta, E.; Koike, T. *Proc. Natl. Acad. Sci. U.S.A.* **2003**, *100*, 3731.
(148) Koike, T.; Watanabe, T.; Aoki, S.; Kimura, E.; Shiro, M. *J. Am. Chem. Soc.* **1996**, *118*, 12696.
(149) Lim, N. C.; Brückner, C. *Chem. Commun.* **2004**, 1094.
(150) Lim, N. C.; Yao, L.; Freake, H. C.; Brückner, C. *Bioorg. Med. Chem. Lett.* **2003**, *13*, 2251.
(151) Hanaoka, K.; Kikuchi, K.; Kojima, H.; Urano, Y.; Nagano, T. *Angew. Chem., Int. Ed.* **2003**, *42*, 2996.
(152) Pope, S. J. A.; Laye, R. H. *Dalton Trans.* **2006**, 3108.
(153) Reany, O.; Gunnlaugsson, T.; Parker, D. *J. Chem. Soc., Perkin Trans.* **2000**, *2*, 1819.
(154) Reany, O.; Gunnlaugsson, T.; Parker, D. *Chem. Commun.* **2000**, 473.
(155) Hanaoka, K.; Kikuchi, K.; Kojima, H.; Urano, Y.; Nagano, T. *J. Am. Chem. Soc.* **2004**, *126*, 12470.
(156) Walkup, G. K.; Burdette, S. C.; Lippard, S. J.; Tsien, R. Y. *J. Am. Chem. Soc.* **2000**, *122*, 5644.
(157) Burdette, S. C.; Walkup, G. K.; Spingler, B.; Tsien, R. Y.; Lippard, S. J. *J. Am. Chem. Soc.* **2001**, *123*, 7831.
(158) Chang, C. J.; Nolan, E. M.; Jaworski, J.; Burdette, S. C.; Sheng, M.; Lippard, S. J. *Chem. Biol.* **2004**, *11*, 203.
(159) Burdette, S. C.; Frederickson, C. J.; Bu, W.; Lippard, S. J. *J. Am. Chem. Soc.* **2003**, *125*, 1778.
(160) Frederickson, C. J.; Burdette, S. C.; Frederickson, C. J.; Sensi, S. L.; Weiss, J. H.; Yin, H. Z.; Balaji, R. V.; Truong-Tran, A. Q.; Bedell, E.; Prough, P. S.; Lippard, S. J. *J. Neurosci. Methods* **2004**, *139*, 79.
(161) Nolan, E. M.; Burdette, S. C.; Harvey, J. H.; Hilderbrand, S. A.; Lippard, S. J. *Inorg. Chem.* **2004**, *43*, 2624.
(162) Chang, C. J.; Nolan, E. M.; Jaworski, J.; Okamoto, K.; Hayashi, Y.; Sheng, M.; Lippard, S. J. *Inorg. Chem.* **2004**, *43*, 6774.
(163) Woodroofe, C. C.; Masalha, R.; Barnes, K. R.; Frederickson, C. J.; Lippard, S. J. *Chem. Biol.* **2004**, *11*, 1659.
(164) Hirano, T.; Kikuchi, K.; Urano, Y.; Higuchi, T.; Nagano, T. *J. Am. Chem. Soc.* **2000**, *122*, 12399.
(165) Hirano, T.; Kikuchi, K.; Urano, Y.; Nagano, T. *J. Am. Chem. Soc.* **2002**, *124*, 6555.
(166) Takeda, A.; Yamada, K.; Minami, A.; Nagano, T.; Oku, N. *Epilepsy Res.* **2005**, *63*, 77.
(167) Gee, K. R.; Brown, K. A.; Chen, W. N. U.; Bishop-Stewart, J.; Gray, D.; Johnson, I. *Cell Calcium* **2000**, *27*, 97.
(168) Minta, A.; Kao, J. P.; Tsien, R. Y. *J. Biol. Chem.* **1989**, *264*, 8171.
(169) Gee, K. R.; Zhou, Z.-L.; Qian, W.-J.; Kennedy, R. *J. Am. Chem. Soc.* **2002**, *124*, 776.
(170) Sensi, S. L.; Ton-That, D.; Weiss, J. H.; Rothe, A.; Gee, K. R. *Cell Calcium* **2003**, *34*, 281.
(171) Wu, Y.; Peng, X.; Guo, B.; Fan, J.; Zhang, Z.; Wang, J.; Cui, A.; Gao, Y. *Org. Biomol. Chem.* **2005**, *3*, 1387.
(172) Wang, J.; Xiao, Y.; Zhang, Z.; Qian, X.; Yang, Y.; Xu, Q. *J. Mater. Chem.* **2005**, *15*, 2836.
(173) Haugland, R. P. *Handbook of Fluorescent Probes and Research Products*, 9th ed.; Molecular Probes, Inc.: Eugene, OR, 2002.
(174) Gee, K. R.; Zhou, Z. L.; Ton-That, D.; Sensi, S. L.; Weiss, J. H. *Cell Calcium* **2002**, *31*, 245.
(175) Sensi, S. L.; Yin, H. Z.; Carriedo, S. G.; Rao, S. S.; Weiss, J. H. *Proc. Natl. Acad. Sci. U.S.A.* **1999**, *96*, 2414.
(176) Yin, H. Z.; Sensi, S. L.; Ogoshi, F.; Weiss, J. H. *J. Neurosci.* **2002**, *22*, 1273.
(177) Nolan, E. M.; Ryu, J. W.; Jaworski, J.; Feazell, R. P.; Sheng, M.; Lippard, S. J. *J. Am. Chem. Soc.* **2006**, *128*, 15517.
(178) Nolan, E. M.; Lippard, S. J. *Inorg. Chem.* **2004**, *43*, 8310.
(179) Nolan, E. M.; Jaworski, J.; Racine, M. E.; Sheng, M.; Lippard, S. J. *Inorg. Chem.* **2006**, *45*, 9748.
(180) Nolan, E. M.; Jaworski, J.; Okamoto, K. I.; Hayashi, Y.; Sheng, M.; Lippard, S. J. *J. Am. Chem. Soc.* **2005**, *127*, 16812.
(181) Komatsu, K.; Kikuchi, K.; Kojima, H.; Urano, Y.; Nagano, T. *J. Am. Chem. Soc.* **2005**, *127*, 10197.
(182) Frangioni, J. V. *Curr. Opin. Chem. Biol.* **2003**, *7*, 626.
(183) Tang, B.; Huang, H.; Xu, K. H.; Tong, L. L.; Yang, G. W.; Liu, X.; An, L. G. *Chem. Commun.* **2006**, 3609.
(184) Maruyama, S.; Kikuchi, K.; Hirano, T.; Urano, Y.; Nagano, T. *J. Am. Chem. Soc.* **2002**, *124*, 10650.
(185) Woodroofe, C. C.; Lippard, S. J. *J. Am. Chem. Soc.* **2003**, *125*, 11458.
(186) Woodroofe, C. C.; Won, A. C.; Lippard, S. J. *Inorg. Chem.* **2005**, *44*, 3112.
(187) Henary, M. M.; Wu, Y.; Fahrni, C. J. *Chem.—Eur. J.* **2004**, *10*, 3015.
(188) Taki, M.; Wolford, J. L.; O'Halloran, T. V. *J. Am. Chem. Soc.* **2004**, *126*, 712.
(189) Chang, C. J.; Jaworski, J.; Nolan, E. M.; Sheng, M.; Lippard, S. J. *Proc. Natl. Acad. Sci. U.S.A.* **2004**, *101*, 1129.
(190) Kiyose, K.; Kojima, H.; Urano, Y.; Nagano, T. *J. Am. Chem. Soc.* **2006**, *128*, 6548.
(191) Moats, R. A.; Fraser, S. E.; Meade, T. J. *Angew. Chem., Int. Ed. Engl.* **1997**, *36*, 726.
(192) Trokowski, R.; Ren, J.; Kálmán, F. K.; Sherry, A. D. *Angew. Chem., Int. Ed.* **2005**, *44*, 6920.
(193) Zhang, S.; Merritt, M.; Woessner, D. E.; Lenkinski, R. E.; Sherry, A. D. *Acc. Chem. Res.* **2003**, *36*, 783.
(194) Wrigglesworth, J. M.; Baum, H. *Iron-dependent Enzymes in the Brain*; Taylor and Francis: New York, 1988.
(195) Dwork, A. J.; Lawler, G.; Zybert, P. A.; Durkin, M.; Osman, M.; Willson, N.; Barkai, A. I. *Brain Res.* **1990**, *518*, 31.
(196) Hallgren, B.; Sourander, P. *J. Neurochem.* **1958**, *3*, 41.
(197) Hill, J. M.; Switzer, R. C. *Neuroscience* **1984**, *11*, 595.
(198) Hill, J. M. *The Distribution of Iron in the Brain*; Taylor and Francis: New York, 1988.
(199) Connor, J. R.; Menzies, S. L. *J. Neurol. Sci.* **1995**, *134*, S33.
(200) Koeppen, A. H. *J. Neurol. Sci.* **1995**, *134*, 1.
(201) Zecca, L.; Stroppolo, A.; Gatti, A.; Tampellini, D.; Toscani, M.; Gallorini, M.; Giaveri, G.; Arosio, P.; Santambrogio, P.; Fariello, R. G.; Karatekin, E.; Kleinman, M. H.; Turro, N.; Hornykiewicz, O.; Zucca, F. A. *Proc. Natl. Acad. Sci. U.S.A.* **2004**, *101*, 9843.
(202) Bradbury, M. W. B. *J. Neurochem.* **1997**, *69*, 443.
(203) Fiedler, A.; Reinert, T.; Morawski, M.; Bruckner, G.; Arendt, T.; Butz, T. *Nucl. Instrum. Methods Phys. Res., Sect. B* **2007**, *260*, 153.
(204) Ward, R. J.; Crichton, R. R. In *Metal Ions in Life Sciences*; Sigel, A., Sigel, H., Sigel, R. K. O., Eds.; John Wiley & Sons, Ltd.: West Sussex, England, 2006; Vol. 1, p 227.
(205) Double, K. L.; Maywald, M.; Schmittel, M.; Riederer, P.; Gerlach, M. *J. Neurochem.* **1998**, *70*, 2492.
(206) Greenberg, G. R.; Wintrobe, M. M. *J. Biol. Chem.* **1946**, *165*, 397.
(207) Jacobs, A. *Ciba Found. Symp.* **1977**, *51*, 91.
(208) Kruszewski, M. *Mutat. Res.* **2003**, *531*, 81.
(209) Kakhlon, O.; Cabantchik, Z. I. *Free Radical Biol. Med.* **2002**, *33*, 1037.
(210) Epsztejn, S.; Glickstein, H.; Picard, V.; Slotki, I. N.; Breuer, W.; Beaumont, C.; Cabantchik, Z. I. *Blood* **1999**, *94*, 3593.
(211) Andrews, N. C.; Schmidt, P. J. *Annu. Rev. Physiol.* **2007**, *69*, 69.
(212) Zecca, L.; Youdim, M. B. H.; Riederer, P.; Connor, J. R.; Crichton, R. R. *Nat. Rev. Neurosci.* **2004**, *5*, 863.
(213) Burdo, J. R.; Connor, J. R. *Biometals* **2003**, *16*, 63.
(214) Aisen, P.; Wessling-Resnick, M.; Leibold, E. A. *Curr. Opin. Chem. Biol.* **1999**, *3*, 200.
(215) Theil, E. C. *Annu. Rev. Nutr.* **2004**, *24*, 327.
(216) Harrison, P. M.; Arosio, P. *Biochim. Biophys. Acta-Bioenerg.* **1996**, *1275*, 161.
(217) Connor, J. R.; Boeshore, K. L.; Benkovic, S. A.; Menzies, S. L. *J. Neurosci. Res.* **1994**, *37*, 461.
(218) Schade, A. L.; Caroline, L. *Science* **1946**, *104*, 340.
(219) Aisen, P.; Listowsky, I. *Annu. Rev. Biochem.* **1980**, *49*, 357.
(220) Bartlett, W. P.; Li, X. S.; Connor, J. R. *J. Neurochem.* **1991**, *57*, 318.
(221) Connor, J. R.; Phillips, T. M.; Lakshman, M. R.; Barron, K. D.; Fine, R. E.; Csiza, C. K. *J. Neurochem.* **1987**, *49*, 1523.
(222) Jefferies, W. A.; Brandon, M. R.; Hunt, S. V.; Williams, A. F.; Gatter, K. C.; Mason, D. Y. *Nature* **1984**, *312*, 162.
(223) Shaw, G. C.; Cope, J. J.; Li, L.; Corson, K.; Hersey, C.; Ackermann, G. E.; Gwynn, B.; Lambert, A. J.; Wingert, R. A.; Traver, D.; Trede, N. S.; Barut, B. A.; Zhou, Y.; Minet, E.; Donovan, A.; Brownlie, A.; Balzan, R.; Weiss, M. J.; Peters, L. L.; Kaplan, J.; Zon, L. I.; Paw, B. H. *Nature* **2006**, *440*, 96.
(224) Hulet, S. W.; Hess, E. J.; Debinski, W.; Arosio, P.; Bruce, K.; Powers, S.; Connor, J. R. *J. Neurochem.* **1999**, *72*, 868.
(225) Hulet, S. W.; Powers, S.; Connor, J. R. *J. Neurol. Sci.* **1999**, *165*, 48.
(226) Hulet, S. W.; Heyliger, S. O.; Powers, S.; Conner, J. R. *J. Neurosci. Res.* **2000**, *61*, 52.
(227) Eisenstein, R. S. *Annu. Rev. Nutr.* **2000**, *20*, 627.
(228) Hentze, M. W.; Kuhn, L. C. *Proc. Natl. Acad. Sci. U.S.A.* **1996**, *93*, 8175.
(229) Klausner, R. D.; Rouault, T. A.; Harford, J. B. *Cell* **1993**, *72*, 19.
(230) Rouault, T. A.; Hentze, M. W.; Caughman, S. W.; Harford, J. B.; Klausner, R. D. *Science* **1988**, *241*, 1207.
(231) Aziz, N.; Munro, H. N. *Proc. Natl. Acad. Sci. U.S.A.* **1987**, *84*, 8478.
(232) Rouault, T. A.; Haile, D. J.; Downey, W. E.; Philpott, C. C.; Tang, C.; Samaniego, F.; Chin, J.; Paul, I.; Orloff, D.; Harford, J. B.; Klausner, R. D. *BioMetals* **1992**, *5*, 131.
(233) Abboud, S.; Haile, D. J. *J. Biol. Chem.* **2000**, *275*, 19906.

(234) Donovan, A.; Brownlie, A.; Zhou, Y.; Shepard, J.; Pratt, S. J.; Moynihan, J.; Paw, B. H.; Drejer, A.; Barut, B.; Zapata, A.; Law, T. C.; Brugnara, C.; Kingsley, P. D.; Palis, J.; Fleming, M. D.; Andrews, N. C.; Zon, L. I. *Nature* **2000**, *403*, 776.
(235) McKie, A. T.; Marciani, P.; Rolfs, A.; Brennan, K.; Wehr, K.; Barrow, D.; Miret, S.; Bomford, A.; Peters, T. J.; Farzaneh, F.; Hediger, M. A.; Hentze, M. W.; Simpson, R. J. *Mol. Cell* **2000**, *5*, 299.
(236) Dunn, L. L.; Rahmanto, Y. S.; Richardson, D. R. *Trends Cell Biol.* **2007**, *17*, 93.
(237) Burdo, J. R.; Menzies, S. L.; Simpson, I. A.; Garrick, L. M.; Garrick, M. D.; Dolan, K. G.; Haile, D. J.; Beard, J. L.; Connor, J. R. *J. Neurosci. Res.* **2001**, *66*, 1198.
(238) Jiang, D. H.; Ke, Y.; Cheng, Y. Z.; Ho, K. P.; Qian, Z. M. *Dev. Neurosci.* **2002**, *24*, 94.
(239) Chen, H. J.; Attieh, Z. K.; Su, T.; Syed, B. A.; Gao, H.; Alaeddine, R. M.; Fox, T. C.; Usta, J.; Naylor, C. E.; Evans, R. W.; McKie, A. T.; Anderson, G. J.; Vulpe, C. D. *Blood* **2004**, *103*, 3933.
(240) Vulpe, C. D.; Kuo, Y. M.; Murphy, T. L.; Cowley, L.; Askwith, C.; Libina, N.; Gitschier, J.; Anderson, G. J. *Nat. Genet.* **1999**, *21*, 195.
(241) Jeong, S. Y.; David, S. *J. Biol. Chem.* **2003**, *278*, 27144.
(242) Wang, J.; Jiang, H.; Xie, J.-X. *Eur. J. Neurosci.* **2007**, *25*, 2766.
(243) Nemeth, E.; Tuttle, M. S.; Powelson, J.; Vaughn, M. B.; Donovan, A.; Ward, D. M.; Ganz, T.; Kaplan, J. *Science* **2004**, *306*, 2090.
(244) Zechel, S.; Huber-Wittmer, K.; von Bohlen und Halbach, O. *J. Neurosci. Res.* **2006**, *84*, 790.
(245) Beard, J. L. *J. Nutr.* **2001**, *131*, 568.
(246) Connor, J. R.; Menzies, S. L. *Glia* **1996**, *17*, 83.
(247) Larkin, E. C.; Rao, G. A. In Brain, behavior and iron in the infant diet; Dobbing, J., Ed.; Springer-Verlag: London, 1990; p 43.
(248) Oloyede, O. B.; Folayan, A. T.; Odutuga, A. A. *Biochem. Int.* **1992**, *27*, 913.
(249) Craelius, W.; Migdal, M. W.; Luessenhop, C. P.; Sugar, A.; Mihalakis, I. *Arch. Pathol. Lab. Med.* **1982**, *106*, 397.
(250) Drayer, B.; Burger, P.; Hurwitz, B.; Dawson, D.; Cain, J. *Am. J. Neuroradiol.* **1987**, *8*, 413.
(251) Madsen, E.; Gitlin, J. D. *Annu. Rev. Neurosci.* **2007**, *30*, 317.
(252) de Rijk, M. C.; Tzourio, C.; Breteler, M. M.; Dartigues, J. F.; Amaducci, L.; Lopez-Pousa, S.; Manubens-Bertran, J. M.; Alperovitch, A.; Rocca, W. A. *J. Neurol. Neurosurg. Psychiatry* **1997**, *62*, 10.
(253) Gerlach, M.; Double, K.; Götz, M. E.; Youdim, M. B. H.; Riederer, P. In *Metal Ions in Life Sciences*; Sigel, A., Sigel, H., Sigel, R. K. O., Eds.; John Wiley & Sons, Ltd.: West Sussex, England, 2006; Vol. 1, p 125.
(254) Gerlach, M.; Benshachar, D.; Riederer, P.; Youdim, M. B. H. *J. Neurochem.* **1994**, *63*, 793.
(255) Götz, M. E.; Double, K.; Gerlach, M.; Youdim, M. B. H.; Riederer, P. *Ann. N.Y. Acad. Sci.* **2004**, *1012*, 193.
(256) Dexter, D. T.; Carayon, A.; Javoy-; Agid, F.; Agid, Y.; Wells, F. R.; Daniel, S. E.; Lees, A. J.; Jenner, P.; Marsden, C. D *Brain* **1991**, *114*, 1953.
(257) Griffiths, P. D.; Dobson, B. R.; Jones, G. R.; Clarke, D. T. *Brain* **1999**, *122*, 667.
(258) Jellinger, K.; Paulus, W.; Grundkeiqbal, I.; Riederer, P.; Youdim, M. B. H. *J. Neural Transm.: Parkinson's Dis. Dementia Sect.* **1990**, *2*, 327.
(259) Kortekaas, R.; Leenders, K. L.; van Oostrom, J. C. H.; Vaalburg, W.; Bart, J.; Willemsen, A. T. M.; Hendrikse, N. H. *Ann. Neurol.* **2005**, *57*, 176.
(260) Logroscino, G.; Marder, K.; Graziano, J.; Freyer, G.; Slavkovich, V.; LoIacono, N.; Cote, L.; Mayeux, R. *Neurology* **1997**, *49*, 714.
(261) Torsdottir, G.; Kristinsson, J.; Sveinbjornsdottir, S.; Snaedal, J.; Johannesson, T. *Pharmacol. Toxicol.* **1999**, *85*, 239.
(262) Faucheux, B. A.; Hauw, J. J.; Agid, Y.; Hirsch, E. C. *Brain Res.* **1997**, *749*, 170.
(263) Faucheux, B. A.; Nillesse, N.; Damier, P.; Spik, G.; Mouattprigent, A.; Pierce, A.; Leveugle, B.; Kubis, N.; Hauw, J. J.; Agid, Y.; Hirsch, E. C. *Proc. Natl. Acad. Sci. U.S.A.* **1995**, *92*, 9603.
(264) Leveugle, B.; Faucheux, B. A.; Bouras, C.; Nillesse, N.; Spik, G.; Hirsch, E. C.; Agid, Y.; Hof, P. R. *Acta Neuropathol.* **1996**, *91*, 566.
(265) Jellinger, K.; Kienzl, E.; Rumpelmair, G.; Riederer, P.; Stachelberger, H.; Benshachar, D.; Youdim, M. B. H. *J. Neurochem.* **1992**, *59*, 1168.
(266) Zecca, L.; Shima, T.; Stroppolo, A.; Goj, C.; Battiston, G. A.; Gerbasi, R.; Sarna, T.; Swartz, H. M. *Neuroscience* **1996**, *73*, 407.
(267) Wilms, H.; Rosenstiel, P.; Sievers, J.; Deuschl, G.; Zecca, L.; Lucius, R. *FASEB J.* **2003**, *17*, 500.
(268) Faucheux, B. A.; Martin, M. E.; Beaumont, C.; Hauw, J. J.; Agid, Y.; Hirsch, E. C. *J. Neurochem.* **2003**, *86*, 1142.
(269) Lcking, C. B.; Brice, A *Cell. Mol. Life Sci.* **2000**, *57*, 1894.
(270) Dawson, T. M.; Dawson, V. L. *Science* **2003**, *302*, 819.
(271) Hashimoto, M.; Hsu, L. J.; Xia, Y.; Takeda, A.; Sisk, A.; Sundsmo, M.; Masliah, E. *Neuroreport* **1999**, *10*, 717.
(272) Bush, A. I. *Trends Neurosci.* **2003**, *26*, 207.
(273) Rogers, J. T.; Randall, J. D.; Cahill, C. M.; Eder, P. S.; Huang, X. D.; Gunshin, H.; Leiter, L.; McPhee, J.; Sarang, S. S.; Utsuki, T.; Greig, N. H.; Lahiri, D. K.; Tanzi, R. E.; Bush, A. I.; Giordano, T.; Gullans, S. R. *J. Biol. Chem.* **2002**, *277*, 45518.
(274) Bodovitz, S.; Falduto, M. T.; Frail, D. E.; Klein, W. L. *J. Neurochem.* **1995**, *64*, 307.
(275) Good, P. F.; Perl, D. P.; Bierer, L. M.; Schmeidler, J. *Ann. Neurol.* **1992**, *31*, 286.
(276) Bartzokis, G.; Lu, P. H.; Tishler, T. A.; Perlman, S. In *Metal Ions in Life Sciences*; Sigel, A., Sigel, H., Sigel, R. K. O., Eds.; John Wiley & Sons, Ltd.: West Sussex, England, 2006; Vol. 1, p 151.
(277) Bartzokis, G.; Cummings, J.; Perlman, S.; Hance, D. B.; Mintz, J. *Arch. Neurol.* **1999**, *56*, 569.
(278) Klintworth, G. K. In *Advances in Neurology: Huntington's Chorea*; Barbeau, A., Paulson, G. W., Chase, T. N., Eds.; Raven Press: New York, 1973; Vol. 1, p 353.
(279) Chen, J. C.; Hardy, P. A.; Kucharczyk, W.; Clauberg, M.; Joshi, J. G.; Vourlas, A.; Dhar, M.; Henkelman, R. M. *Am. J. Neuroradiol.* **1993**, *14*, 275.
(280) Dexter, D. T.; Jenner, P.; Schapira, A. H. V.; Marsden, C. D. *Ann. Neurol.* **1992**, *32*, S94.
(281) Gomez-Tortosa, E.; MacDonald, M. E.; Friend, J. C.; Taylor, S. A. M.; Weiler, L. J.; Cupples, L. A.; Srinidhi, J.; Gusella, J. F.; Bird, E. D.; Vonsattel, J. P.; Myers, R. H. *Ann. Neurol.* **2001**, *49*, 29.
(282) Myers, R. H.; Vonsattel, J. P.; Paskevich, P. A.; Kiely, D. K.; Stevens, T. J.; Cupples, L. A.; Richardson, E. P.; Bird, E. D. *J. Neuropathol. Exp. Neurol.* **1991**, *50*, 729.
(283) Bradley, J. L.; Blake, J. C.; Chamberlain, S.; Thomas, P. K.; Cooper, J. M.; Schapira, A. H. V. *Hum. Mol. Genet.* **2000**, *9*, 275.
(284) Harris, Z. L.; Takahashi, Y.; Miyajima, H.; Serizawa, M.; Macgillivray, R. T. A.; Gitlin, J. D. *Proc. Natl. Acad. Sci. U.S.A.* **1995**, *92*, 2539.
(285) Swaiman, K. F. *Arch. Neurol.* **1991**, *48*, 1285.
(286) Crompton, D. E.; Chinnery, P. F.; Fey, C.; Curtis, A. R. J.; Morris, C. M.; Kierstan, J.; Burt, A.; Young, F.; Coulthard, A.; Curtis, A.; Ince, P. G.; Bates, D.; Jackson, M. J.; Burn, J. *Blood Cell Mol. Dis.* **2002**, *29*, 522.
(287) LeVine, S. M. *Brain Res.* **1997**, *760*, 298.
(288) Uitti, R. J.; Rajput, A. H.; Rozdilsky, B.; Bickis, M.; Wollin, T.; Yuen, W. K. *Can. J. Neurol. Sci.* **1989**, *16*, 310.
(289) Dexter, D. T.; Wells, F. R.; Agid, F.; Agid, Y.; Lees, A. J.; Jenner, P.; Marsden, C. D. *Lancet* **1987**, *2*, 1219.
(290) Perls, M. *Virchows Arch. Pathol. Anat. Physiol. Klin. Med.* **1867**, *39*, 42.
(291) Nguyen-Legros, J.; Bizot, J.; Bolesse, M.; Pulicani, J. P. *Histochemistry* **1980**, *66*, 239.
(292) Parmley, R. T.; Gilbert, C. S.; White, D. A.; Barton, J. C. *J. Histochem. Cytochem.* **1988**, *36*, 433.
(293) Spatz, H. *Z. Ges. Neurol. Psychiat.* **1922**, *77*, 261.
(294) Gomori, G. *Am. J. Pathol.* **1936**, *12*, 655.
(295) Galazka-Friedman, J.; Bauminger, E. R.; Friedman, A.; Barcikowska, M.; Hechel, D.; Nowik, I. *Mov. Disord.* **1996**, *11*, 8.
(296) Schochet, S. S.; Lampert, P. W.; Earle, K. M. *J. Neuropathol. Exp. Neurol.* **1968**, *27*, 645.
(297) Good, P. F.; Olanow, C. W.; Perl, D. P. *Brain Res.* **1992**, *593*, 343.
(298) Breuer, W.; Epsztejn, S.; Millgram, P.; Cabantchik, I. Z. *Am. J. Physiol.* **1995**, *268*, C1354.
(299) Petrat, F.; Rauen, U.; de Groot, H. *Hepatology* **1999**, *29*, 1171.
(300) Palanché, T.; Marmolle, F.; Abdallah, M. A.; Shanzer, A.; Albrecht-Gary, A. M. *J. Biol. Inorg. Chem.* **1999**, *4*, 188.
(301) Breuer, W.; Ermers, M. J. J.; Pootrakul, P.; Abramov, A.; Hershko, C.; Cabantchik, Z. I. *Blood* **2001**, *97*, 792.
(302) Lytton, S. D.; Mester, B.; Libman, J.; Shanzer, A.; Cabantchik, Z. I. *Anal. Biochem.* **1992**, *205*, 326.
(303) Ouchetto, H.; Dias, M.; Mornet, R.; Lesuisse, E.; Camadro, J. M. *Bioorg. Med. Chem.* **2005**, *13*, 1799.
(304) Ma, Y.; Luo, W.; Camplo, M.; Liu, Z.; Hider, R. C. *Bioorg. Med. Chem. Lett.* **2005**, *15*, 3450.
(305) Ma, Y.; de Groot, H.; Liu, Z.; Hider, R. C.; Petrat, F. *Biochem. J.* **2006**, *395*, 49.
(306) Hua, J.; Wang, Y. G. *Chem. Lett.* **2005**, *34*, 98.
(307) Bricks, J. L.; Kovalchuk, A.; Trieflinger, C.; Nofz, M.; Buschel, M.; Tolmachev, A. I.; Daub, J.; Rurack, K. *J. Am. Chem. Soc.* **2005**, *127*, 13522.
(308) Xiang, Y.; Tong, A. J.; Jin, P. Y.; Ju, Y. *Org. Lett.* **2006**, *8*, 2863.
(309) Xiang, Y.; Tong, A. J. *Org. Lett.* **2006**, *8*, 1549.
(310) Zhang, M.; Gao, Y. H.; Li, M. Y.; Yu, M. X.; Li, F. Y.; Li, L.; Zhu, M. W.; Zhang, J. P.; Yi, T.; Huang, C. H. *Tetrahedron Lett.* **2007**, *48*, 3709.
(311) Chen, J. L.; Zhuo, S. J.; Wu, Y. Q.; Fang, F.; Li, L.; Zhu, C. Q. *Spectrochim. Acta A* **2006**, *63*, 438.
(312) Paris, J.; Gameiro, C.; Humblet, V.; Mohapatra, P. K.; Jacques, V.; Desreux, J. F. *Inorg. Chem.* **2006**, *45*, 5092.

(313) Vymazal, J.; Brooks, R. A.; Patronas, N.; Hajek, M.; Bulte, J. W.; Di Chiro, G. *J. Neurol. Sci.* **1995**, *134*, 19.
(314) Drayer, B.; Burger, P.; Darwin, R.; Riederer, S.; Herfkens, R.; Johnson, G. A. *Am. J. Roentgenol.* **1986**, *147*, 103.
(315) Brass, S. D.; Chen, N. P. D.; Mulkern, R. V.; Bakshi, R. *Top. Magn. Reson. Imag.* **2006**, *17*, 31.
(316) Bartzokis, G.; Tishler, T. A.; Shin, I. L. S.; Lu, P. O. H.; Cummings, J. L. *Ann. N.Y. Acad. Sci.* **2004**, *1012*, 224.
(317) Schenck, J. F.; Zimmerman, E. A. *NMR Biomed.* **2004**, *17*, 433.
(318) Bartzokis, G.; Sultzer, D.; Cummings, J.; Holt, L. E.; Hance, D. B.; Henderson, V. W.; Mintz, J. *Arch. Gen. Psychiatry* **2000**, *57*, 47.
(319) Bartzokis, G.; Tishler, T. A. *Cell. Mol. Biol.* **2000**, *46*, 821.
(320) Gorell, J. M.; Ordidge, R. J.; Brown, G. G.; Deniau, J.-C.; Buderer, N. M.; Helpern, J. A. *Neurology* **1995**, *45*, 1138.
(321) Antonini, A.; Leenders, K. L.; Meier, D.; Oertel, W. H.; Boesiger, P.; Anliker, M. *Neurology* **1993**, *43*, 697.
(322) Duguid, J. R.; De La Paz, R.; DeGroot, J. *Ann. Neurol.* **1986**, *20*, 744.
(323) Hutchinson, M.; Raff, U. *Brit. Med. J.* **1999**, *67*, 815.
(324) Hutchinson, M.; Raff, U. *Am. J. Neuroradiol.* **2000**, *21*, 697.
(325) Ordidge, R. J.; Gorell, J. M.; Deniau, J. C.; Knight, R. A.; Helpern, J. A. *Magn. Reson. Med.* **1994**, *32*, 335.
(326) Mauricio, J. C.; Coelho, H.; Sa, J.; Martins, A. *Acta Med. Port.* **1990**, *3*, 85.
(327) Gaggelli, E.; Kozlowski, H.; Valensin, D.; Valensin, G *Chem. Rev* **2006**, *106*, 1995.
(328) Stöckel, J.; Safar, J.; Wallace, A. C.; Cohen, F. E.; Prusiner, S. B. *Biochemistry* **1998**, *37*, 7185.
(329) Prohaska, J. R. *Physiol. Rev.* **1987**, *67*, 858.
(330) Danks, D. M. *The Metabolic Basis of Inherited Disease*, 6th ed.; McGraw-Hill Inc.: New York, 1989.
(331) Brown, D. R.; Qin, K. F.; Herms, J. W.; Madlung, A.; Manson, J.; Strome, R.; Fraser, P. E.; Kruck, T.; vonBohlen, A.; SchulzSchaeffer, W.; Giese, A.; Westaway, D.; Kretzschmar, H. *Nature* **1997**, *390*, 684.
(332) Atwood, C. S.; Huang, X. D.; Moir, R. D.; Tanzi, R. E.; Bush, A. I. In *Metal Ions in Biological Systems*; Sigel, A., Sigel, H., Eds.; Marcel Dekker, Inc.: New York, 1999; Vol. 36, p 309.
(333) Schlief, M.; Gitlin, J. *Mol. Neurobiol.* **2006**, *33*, 81.
(334) Kozma, M.; Szerdahelyi, P.; Kasa, P. *Acta Histochem.* **1981**, *69*, 12.
(335) Sato, M.; Ohtomo, K.; Daimon, T.; Sugiyama, T.; Iijima, K. *J. Histochem. Cytochem.* **1994**, *42*, 1585.
(336) Hartter, D. E.; Barnea, A. *Synapse* **1988**, *2*, 412.
(337) Kardos, J.; Kovacs, I.; Hajos, F.; Kalman, M.; Simonyi, M. *Neurosci. Lett.* **1989**, *103*, 139.
(338) Puig, S.; Thiele, D. J. *Curr. Opin. Chem. Biol.* **2002**, *6*, 171.
(339) Prohaska, J. R.; Gybina, A. A. *J. Nutr.* **2004**, *134*, 1003.
(340) Kim, B.-E.; Nevitt, T.; Thiele, D. J. *Nat. Chem. Biol.* **2008**, *4*, 176.
(341) Rae, T. D.; Schmidt, P. J.; Pufahl, R. A.; Culotta, V. C.; O'Halloran, T. V. *Science* **1999**, *284*, 805.
(342) Cobine, P. A.; Ojeda, L. D.; Rigby, K. M.; Winge, D. R. *J. Biol. Chem.* **2004**, *279*, 14447.
(343) Mercer, J. F. B.; Llanos, R. M. *J. Nutr.* **2003**, *133*, 1481.
(344) Hellman, N. E.; Gitlin, J. D. *Annu. Rev. Nutr.* **2002**, *22*, 439.
(345) Georgatsou, E.; Mavrogiannis, L. A.; Fragiadakis, G. S.; Alexandraki, D. *J. Biol. Chem.* **1997**, *272*, 13786.
(346) Hassett, R.; Kosman, D. J. *J. Biol. Chem.* **1995**, *270*, 128.
(347) Eisses, J. F.; Kaplan, J. H. *J. Biol. Chem.* **2002**, *277*, 29162.
(348) Guo, Y.; Smith, K.; Lee, J.; Thiele, D. J.; Petris, M. J. *J. Biol. Chem.* **2004**, *279*, 17428.
(349) Zhou, B.; Gitschier, J. *Proc. Natl. Acad. Sci. U.S.A.* **1997**, *94*, 7481.
(350) Klomp, A. E. M.; Tops, B. B. J.; van den Berg, I. E. T.; Berger, R.; Klomp, L. W. J. *Biochem. J.* **2002**, *364*, 497.
(351) Petris, M. J.; Smith, K.; Lee, J.; Thiele, D. J. *J. Biol. Chem.* **2003**, *278*, 9639.
(352) Maynard, C. J.; Cappai, R.; Volitakis, I.; Cherny, R. A.; White, A. R.; Beyreuther, K.; Masters, C. L.; Bush, A. I.; Li, Q. X. *J. Biol. Chem.* **2002**, *277*, 44670.
(353) White, A. R.; Reyes, R.; Mercer, J. F. B.; Camakaris, J.; Zheng, H.; Bush, A. I.; Multhaup, G.; Beyreuther, K.; Masters, C. L.; Cappai, R. *Brain Res.* **1999**, *842*, 439.
(354) Okamoto, T.; Takeda, S.; Murayama, Y.; Ogata, E.; Nishimoto, I. *J. Biol. Chem.* **1995**, *270*, 4205.
(355) Sabo, S. L.; Ikin, A. F.; Buxbaum, J. D.; Greengard, P. *J. Cell Biol.* **2001**, *153*, 1403.
(356) Vassallo, N.; Herms, J. *J. Neurochem.* **2003**, *86*, 538.
(357) Fournier, J. G.; Escaig-Haye, F.; Grigoriev, V. *Microsc. Res. Tech.* **2000**, *50*, 76.
(358) Herms, J.; Tings, T.; Gall, S.; Madlung, A.; Giese, A.; Siebert, H.; Schurmann, P.; Windl, O.; Brose, N.; Kretzschmar, H. *J. Neurosci.* **1999**, *19*, 8866.
(359) Pauly, P. C.; Harris, D. A. *J. Biol. Chem.* **1998**, *273*, 33107.
(360) Calderone, V.; Dolderer, B.; Hartmann, H.-J.; Echner, H.; Luchinat, C.; Del Bianco, C.; Mangani, S.; Weser, U. *Proc. Natl. Acad. Sci. U.S.A.* **2005**, *102*, 51.
(361) Lin, S.; Culotta, V. C. *Proc. Natl. Acad. Sci. U.S.A.* **1995**, *92*, 3784.
(362) Lin, S.-J.; Pufahl, R. A.; Dancis, A.; O'Halloran, T. V.; Culotta, V. C. *J. Biol. Chem.* **1997**, *272*, 9215.
(363) Hamza, I.; Prohaska, J.; Gitlin, J. D. *Proc. Natl. Acad. Sci. U.S.A.* **2003**, *100*, 1215.
(364) Hamza, I.; Schaefer, M.; Klomp, L. W. J.; Gitlin, J. D. *Proc. Natl. Acad. Sci. U.S.A.* **1999**, *96*, 13363.
(365) Wernimont, A. K.; Huffman, D. L.; Lamb, A. L.; O'Halloran, T. V.; Rosenzweig, A. C. *Nat. Struct. Biol.* **2000**, *7*, 766.
(366) Tanchou, V.; Gas, F.; Urvoas, A.; Cougouluegne, F.; Ruat, S.; Averseng, O.; Quemeneur, E. *Biochem. Biophys. Res. Commun.* **2004**, *325*, 388.
(367) Culotta, V. C.; Klomp, L. W. J.; Strain, J.; Casareno, R. L. B.; Krems, B.; Gitlin, J. D. *J. Biol. Chem.* **1997**, *272*, 23469.
(368) Casareno, R. L. B.; Waggoner, D.; Gitlin, J. D. *J. Biol. Chem.* **1998**, *273*, 23625.
(369) Schmidt, P. J.; Rae, T. D.; Pufahl, R. A.; Hamma, T.; Strain, J.; O'Halloran, T. V.; Culotta, V. C. *J. Biol. Chem.* **1999**, *274*, 23719.
(370) Glerum, D. M.; Shtanko, A.; Tzagoloff, A. *J. Biol. Chem.* **1996**, *271*, 14504.
(371) Carr, H. S.; Winge, D. R. *Acc. Chem. Res.* **2003**, *36*, 309.
(372) Hamza, I.; Gitlin, J. D. *J. Bioenerg. Biomembr.* **2002**, *34*, 381.
(373) Cobine, P. A.; Pierrel, F.; Winge, D. R. *Biochim. Biophys. Acta-Mol. Cell Res.* **2006**, *1763*, 759.
(374) Glerum, D. M.; Shtanko, A.; Tzagoloff, A. *J. Biol. Chem.* **1996**, *271*, 20531.
(375) Horng, Y.-C.; Cobine, P. A.; Maxfield, A. B.; Carr, H. S.; Winge, D. R. *J. Biol. Chem.* **2004**, *279*, 35334.
(376) Arnesano, F.; Balatri, E.; Banci, L.; Bertini, I.; Winge, D. R. *Structure* **2005**, *13*, 713.
(377) Voskoboinik, I.; Camakaris, J. *J. Bioenerg. Biomembr.* **2002**, *34*, 363.
(378) Forbes, J. R.; Hsi, G.; Cox, D. W. *J. Biol. Chem.* **1999**, *274*, 12408.
(379) Jensen, P. Y.; Bonander, N.; Moller, L. B.; Farver, O. *Biochim. Biophys. Acta* **1999**, *1434*, 103.
(380) Barnes, N.; Tsivkovskii, R.; Tsivkovskaia, N.; Lutsenko, S. *J. Biol. Chem.* **2005**, *280*, 9640.
(381) Hopt, A.; Korte, S.; Fink, H.; Panne, U.; Niessner, R.; Jahn, R.; Kretzschmar, H.; Herms, J. *J. Neurosci. Methods* **2003**, *128*, 159.
(382) Fu, D. D.; Beeler, T. J.; Dunn, T. M. *Yeast* **1995**, *11*, 283.
(383) Schlief, M. L.; Craig, A. M.; Gitlin, J. D. *J. Neurosci.* **2005**, *25*, 239.
(384) Miura, T.; Hori-i, A.; Mototani, H.; Takeuchi, H. *Biochemistry* **1999**, *38*, 11560.
(385) Kramer, M. L.; Kratzin, H. D.; Schmidt, B.; Romer, A.; Windl, O.; Liemann, S.; Hornemann, S.; Kretzschmar, H. *J. Biol. Chem.* **2001**, *276*, 16711.
(386) Hornshaw, M. P.; McDermott, J. R.; Candy, J. M.; Lakey, J. H. *Biochem. Biophys. Res. Commun.* **1995**, *214*, 993.
(387) Garnett, A. P.; Viles, J. H. *J. Biol. Chem.* **2003**, *278*, 6795.
(388) Viles, J. H.; Cohen, F. E.; Prusiner, S. B.; Goodin, D. B.; Wright, P. E.; Dyson, H. J. *Proc. Natl. Acad. Sci. U.S.A.* **1999**, *96*, 2042.
(389) Lee, K. S.; Magalhaes, A. C.; Zanata, S. M.; Brentani, R. R.; Martins, V. R.; Prado, M. A. M. *J. Neurochem.* **2001**, *79*, 79.
(390) Sumudhu, W.; Perera, S.; Hooper, N. M. *Curr. Biol.* **2001**, *11*, 519.
(391) Waggoner, D. J.; Drisaldi, B.; Bartnikas, T. B.; Casareno, R. L. B.; Prohaska, J. R.; Gitlin, J. D.; Harris, D. A. *J. Biol. Chem.* **2000**, *275*, 7455.
(392) Kretzschmar, H. A.; Tings, T.; Madlung, A.; Giese, A.; Herms, J *Arch. Virol.* **2000**, *16*, 239.
(393) Trombley, P. Q.; Shepherd, G. M. *J. Neurophysiol.* **1996**, *76*, 2536.
(394) Doreulee, N.; Yanovsky, Y.; Haas, H. L. *Hippocampus* **1997**, *7*, 666.
(395) Leiva, J.; Gaete, P.; Palestini, M. *Arch. Ital. Biol.* **2003**, *141*, 149.
(396) Horning, M. S.; Trombley, P. Q. *J. Neurophysiol.* **2001**, *86*, 1652.
(397) Franks, N. P.; Honore, E. *Trends Pharmacol. Sci.* **2004**, *25*, 601.
(398) Strausak, D.; Mercer, J. F. B.; Dieter, H. H.; Stremmel, W.; Multhaup, G. *Brain Res. Bull.* **2001**, *55*, 175.
(399) Waggoner, D. J.; Bartnikas, T. B.; Gitlin, J. D. *Neurobiol. Dis.* **1999**, *6*, 221.
(400) Brown, D. R.; Kozlowski, H. *Dalton Trans* **2004**, *2004*, 1907.
(401) Donnelly, P. S.; Xiao, Z.; Wedd, A. G. *Curr. Opin. Chem. Biol.* **2007**, *11*, 128.
(402) Millhauser, G. L. *Acc. Chem. Res.* **2004**, *37*, 79.
(403) Multhaup, G.; Schlicksupp, A.; Hesse, L.; Beher, D.; Ruppert, T.; Masters, C. L.; Beyreuther, K. *Science* **1996**, *271*, 1406.
(404) Ruiz, F. H.; Gonzalez, Y.; Bodini, M.; Opazo, C.; Inestrosa, N. C. *J. Neurochem.* **1999**, *73*, 1288.
(405) Ruiz, F. H.; Silva, E.; Inestrosa, N. C. *Biochem. Biophys. Res. Commun.* **2000**, *269*, 491.
(406) Barnham, K. J.; McKinstry, W. J.; Multhaup, G.; Galatis, D.; Morton, C. J.; Curtain, C. C.; Williamson, N. A.; White, A. R.; Hinds, M. G.;

Norton, R. S.; Beyreuther, K.; Masters, C. L.; Parker, M. W.; Cappai, R. *J. Biol. Chem.* **2003**, *278*, 17401.
(407) Multhaup, G.; Ruppert, T.; Schlicksupp, A.; Hesse, L.; Bill, E.; Pipkorn, R.; Masters, C. L.; Beyreuther, K. *Biochemistry* **1998**, *37*, 7224.
(408) Opazo, C.; Huang, X. D.; Cherny, R. A.; Moir, R. D.; Roher, A. E.; White, A. R.; Cappai, R.; Masters, C. L.; Tanzi, R. E.; Inestrosa, N. C.; Bush, A. I. *J. Biol. Chem.* **2002**, *277*, 40302.
(409) White, A. R.; Multhaup, G.; Maher, F.; Bellingham, S.; Camakaris, J.; Zheng, H.; Bush, A. I.; Beyreuther, K.; Masters, C. L.; Cappai, R. *J. Neurosci.* **1999**, *19*, 9170.
(410) Dong, J.; Atwood, C. S.; Anderson, V. E.; Siedlak, S. L.; Smith, M. A.; Perry, G.; Carey, P. R. *Biochemistry* **2003**, *42*, 2768.
(411) Miura, T.; Mitani, S.; Takanashi, C.; Mochizuki, N. *J. Inorg. Biochem.* **2004**, *98*, 10.
(412) Cherny, R. A.; Legg, J. T.; McLean, C. A.; Fairlie, D. P.; Huang, X. D.; Atwood, C. S.; Beyreuther, K.; Tanzi, R. E.; Masters, C. L.; Bush, A. I. *J. Biol. Chem.* **1999**, *274*, 23223.
(413) Borchardt, T.; Camakaris, J.; Cappai, R.; Masters, C. L.; Beyreuther, K.; Multhaup, G. *Biochem. J.* **1999**, *344*, 461.
(414) Brown, D. R. *Biochem. Soc. Symp.* **2004**, *71*, 193.
(415) Brown, D. R.; Clive, C.; Haswell, S. J. *J. Neurochem.* **2001**, *76*, 69.
(416) Burns, C. S.; Aronoff-Spencer, E.; Dunham, C. M.; Lario, P.; Avdievich, N. I.; Antholine, W. E.; Olmstead, M. M.; Vrielink, A.; Gerfen, G. J.; Peisach, J.; Scott, W. G.; Millhauser, G. L. *Biochemistry* **2002**, *41*, 3991.
(417) Hasnain, S. S.; Murphy, L. M.; Strange, R. W.; Grossmann, J. G.; Clarke, A. R.; Jackson, G. S.; Collinge, J. *J. Mol. Biol.* **2001**, *311*, 467.
(418) Jackson, G. S.; Murray, I.; Hosszu, L. L. P.; Gibbs, N.; Waltho, J. P.; Clarke, A. R.; Collinge, J. *Proc. Natl. Acad. Sci. U.S.A.* **2001**, *98*, 8531.
(419) Qin, K. F.; Yang, Y.; Mastrangelo, P.; Westaway, D *J. Biol. Chem.* **2002**, *277*, 1981.
(420) Whittal, R. M.; Ball, H. L.; Cohen, F. E.; Burlingame, A. L.; Prusiner, S. B.; Baldwin, M. A. *Protein Sci.* **2000**, *9*, 332.
(421) Brown, D. R.; Nicholas, R. S. J.; Canevari, L. *J. Neurosci. Res.* **2002**, *67*, 211.
(422) Brown, D. R.; Wong, B. S.; Hafiz, F.; Clive, C.; Haswell, S. J.; Jones, I. M. *Biochem. J.* **1999**, *344*, 1.
(423) Nishimura, T.; Sakudo, A.; Nakamura, I.; Lee, D. C.; Taniuchi, Y.; Saeki, K.; Matsumoto, Y.; Ogawa, M.; Sakaguchi, S.; Itohara, S.; Onodera, T. *Biochem. Biophys. Res. Commun.* **2004**, *323*, 218.
(424) Hutter, G.; Heppner, F. L.; Aguzzi, A. *Biol. Chem.* **2003**, *384*, 1279.
(425) Jones, S.; Batchelor, M.; Bhelt, D.; Clarke, A. R.; Collinge, J.; Jackson, G. S. *Biochem. J.* **2005**, *392*, 309.
(426) Nishina, K.; Jenks, S.; Supattapone, S. *J. Biol. Chem.* **2004**, *279*, 40788.
(427) George, J. M. *Genome Biol.* **2002**, *3*, REVIEWS3002.
(428) Betarbet, R.; Sherer, T. B.; MacKenzie, G.; Garcia-Osuna, M.; Panov, A. V.; Greenamyre, J. T. *Nat. Neurosci.* **2000**, *3*, 1301.
(429) Giasson, B. I.; Duda, J. E.; Murray, I. V. J.; Chen, Q. P.; Souza, J. M.; Hurtig, H. I.; Ischiropoulos, H.; Trojanowski, J. Q.; Lee, V. M. Y. *Science* **2000**, *290*, 985.
(430) Manning-Bog, A. B.; McCormack, A. L.; Li, J.; Uversky, V. N.; Fink, A. L.; Di Monte, D. A. *J. Biol. Chem.* **2002**, *277*, 1641.
(431) Kim, Y. S.; Lee, D.; Lee, E. K.; Sung, J. Y.; Chung, K. C.; Kim, J.; Paik, S. R. *Brain Res.* **2001**, *908*, 93.
(432) Paik, S. R.; Shin, H. J.; Lee, J. H.; Chang, C. S.; Kim, J. *Biochem. J.* **1999**, *340*, 821.
(433) Yamin, G.; Glaser, C. B.; Uversky, V. N.; Fink, A. L. *J. Biol. Chem.* **2003**, *278*, 27630.
(434) Uversky, V. N.; Li, J.; Fink, A. L. *J. Biol. Chem.* **2001**, *276*, 44284.
(435) Rasia, R. M.; Bertoncini, C. W.; Marsh, D.; Hoyer, W.; Cherny, D.; Zweckstetter, M.; Griesinger, C.; Jovin, T. M.; Fernandez, C. O. *Proc. Natl. Acad. Sci. U.S.A.* **2005**, *102*, 4294.
(436) Sung, Y.-H.; Rospigliosi, C.; Eliezer, D. *Biochim. Biophys. Acta-Proteins Proteomics* **2006**, *1764*, 5.
(437) Valentine, J. S.; Doucette, P. A.; Potter, S. Z. *Annu. Rev. Biochem.* **2005**, *74*, 563.
(438) Estevez, A. G.; Crow, J. P.; Sampson, J. B.; Reiter, C.; Zhuang, Y. X.; Richardson, G. J.; Tarpey, M. M.; Barbeito, L.; Beckman, J. S. *Science* **1999**, *286*, 2498.
(439) Wiedau-Pazos, M.; Goto, J. J.; Rabizadeh, S.; Gralla, E. B.; Roe, J. A.; Lee, M. K.; Valentine, J. S.; Bredesen, D. E. *Science* **1996**, *271*, 515.
(440) Wang, J.; Slunt, H.; Gonzales, V.; Fromholt, D.; Coonfield, M.; Copeland, N. G.; Jenkins, N. A.; Borchelt, D. R. *Hum. Mol. Genet.* **2003**, *12*, 2753.
(441) Hartmann, H. A.; Evenson, M. A. *Med. Hypotheses* **1992**, *38*, 75.
(442) Menkes, J. H. *Brain Dev.* **1988**, *10*, 77.
(443) Sparaco, M.; Hirano, A.; Hirano, M.; Dimauro, S.; Bonilla, E. *Brain Pathol.* **1993**, *3*, 349.
(444) Buckley, W. T. *Can. J. Anim. Sci.* **1991**, *71*, 155.
(445) Levenson, C. W.; Janghorbani, M. *Anal. Biochem.* **1994**, *221*, 243.
(446) Turnlund, J. R. *Am. J. Clin. Nutr.* **1998**, *67*, 960S.
(447) Turnlund, J. R.; Keyes, W. R.; Peiffer, G. L.; Scott, K. C. *Am. J. Clin. Nutr.* **1998**, *67*, 1219.
(448) Green, C. L. *Am. J. Pathol.* **1955**, *31*, 545.
(449) Mallory, F. B.; Parker, F. *Am. J. Pathol.* **1939**, *15*, 517.
(450) Mallory, F. B.; Parker, F.; Nye, R. N. *J. Med. Res.* **1921**, *42*, 461.
(451) Uzman, L. L. *Lab. Invest.* **1956**, *5*, 299.
(452) Uzman, L. L. *Arch. Pathol.* **1957**, *64*, 464.
(453) Howell, J. S. *J. Pathol. Bacteriol.* **1959**, *77*, 473.
(454) McNary, W. F. *J. Histochem. Cytochem.* **1960**, *8*, 124.
(455) Goldfischer, S.; Sternlieb, I. *Am. J. Pathol.* **1968**, *53*, 883.
(456) Timm, F. *Histochemie* **1961**, *2*, 332.
(457) Shikata, T.; Uzawa, T.; Yoshiwar, N; Akatsuka, T.; Yamazaki, S. *Jpn. J. Exp. Med.* **1974**, *44*, 25.
(458) Sipponen, P. *Scand. J. Gastroenterol.* **1976**, *11*, 545.
(459) Smith, G. F.; Wilkins, D. H. *Anal. Chem.* **1953**, *25*, 510.
(460) Kozma, M.; Szerdahelyi, P.; Kasa, P. *Acta Histochem.* **1981**, *69*, 12.
(461) Rapisarda, V. A.; Volentini, S. I.; Farias, R. N.; Massa, E. M. *Anal. Biochem.* **2002**, *307*, 105.
(462) Yang, L. C.; McRae, R.; Henary, M. M.; Patel, R.; Lai, B.; Vogt, S.; Fahrni, C. J. *Proc. Natl. Acad. Sci. U.S.A.* **2005**, *102*, 11179.
(463) Zeng, L.; Miller, E. W.; Pralle, A.; Isacoff, E. Y.; Chang, C. J. *J. Am. Chem. Soc.* **2006**, *128*, 10.
(464) Miller, E. W.; Zeng, L.; Domaille, D. W.; Chang, C. J. *Nat. Protoc.* **2006**, *1*, 824.
(465) Rostovtsev, V. V.; Green, L. G.; Fokin, V. V.; Sharpless, K. B. *Angew. Chem., Int. Ed.* **2002**, *41*, 2596.
(466) Moses, J. E.; Moorhouse, A. D. *Chem. Soc. Rev.* **2007**, *36*, 1249.
(467) Prescher, J. A.; Bertozzi, C. R. *Nat. Chem. Biol.* **2005**, *1*, 13.
(468) Zhou, Z.; Fahrni, C. J. *J. Am. Chem. Soc.* **2004**, *126*, 8862.
(469) Viguier, R. F. H.; Hulme, A. N. *J. Am. Chem. Soc.* **2006**, *128*, 11370.
(470) Kramer, R. *Angew. Chem., Int. Ed.* **1998**, *37*, 772.
(471) Gunnlaugsson, T.; Leonard, J. P.; Senechal, K.; Harte, A. J. *Chem. Commun.* **2004**, 782.
(472) Jiang, L.-J.; Luo, Q.-H.; Li, Q.-X.; Shen, M.-C.; Hu, H.-W. *Eur. J. Inorg. Chem.* **2002**, 664.
(473) Mayr, T.; Wencel, D.; Werner, T. *Fresenius' J. Anal. Chem.* **2001**, *371*, 44.
(474) Fabbrizzi, L.; Licchelli, M.; Pallavicini, P.; Perotti, A.; Taglietti, A.; Sacchi, D. *Chem.—Eur. J.* **1996**, *2*, 75.
(475) Fabbrizzi, L.; Licchelli, M.; Pallavicini, P.; Perotti, A.; Sacchi, D. *Angew. Chem., Int. Ed. Engl.* **1994**, *33*, 1975.
(476) Rurack, K.; Kollmannsberger, M.; Resch-Genger, U.; Daub, J. *J. Am. Chem. Soc.* **2000**, *122*, 968.
(477) Xu, Z. C.; Xiao, Y.; Qian, X. H.; Cui, J. N.; Cui, D. W. *Org. Lett.* **2005**, *7*, 889.
(478) Xu, Z. C.; Qian, X. H.; Cui, J. N. *Org. Lett.* **2005**, *7*, 3029.
(479) Bender, M. L.; Turnquest, B. W. *J. Am. Chem. Soc.* **1957**, *79*, 1889.
(480) Kroll, H. *J. Am. Chem. Soc.* **1952**, *74*, 2036.
(481) Kroll, H. *J. Am. Chem. Soc.* **1952**, *74*, 2034.
(482) Dujols, V.; Ford, F.; Czarnik, A. W. *J. Am. Chem. Soc.* **1997**, *119*, 7386.
(483) Chen, X.; Ma, H. *Anal. Chim. Acta* **2006**, *575*, 217.
(484) Kierat, R. M.; Kramer, R. *Bioorg. Med. Chem. Lett.* **2005**, *15*, 4824.
(485) Que, E. L.; Chang, C. J. *J. Am. Chem. Soc.* **2006**, *128*, 15942.
(486) He, Q.; Miller, E. W.; Wong, A. P.; Chang, C. J. *J. Am. Chem. Soc.* **2006**, *128*, 9316.
(487) Ko, S. K.; Yang, Y. K.; Tae, J.; Shin, I. *J. Am. Chem. Soc.* **2006**, *128*, 14150.
(488) Peng, X.; Du, J.; Fan, F.; Wang, J.; Wu, Y.; Zhao, J.; Sun, S.; Xu, T. *J. Am. Chem. Soc.* **2007**, *129*, 1500.
(489) Yoon, S.; Miller, E. W.; He, Q.; Do, P. H.; Chang, C. J. *Angew. Chem., Int. Ed.* **2007**, *46*, 6658.

CR078203U